INAUGURAL-DISSERTATION

zur
Erlangung der Doktorwürde
der
Naturwissenschaftlichen-Mathematischen Gesamtfakultät
der
Ruprecht-Karls Universität
Heidelberg

vorgelegt von

Verena Bosch
Giessen

Tag der mündlichen Prüfung:

Genetic interference to study amygdala function in mice

Gutachter: Prof. Dr. Peter H. Seeburg
Prof. Dr. Peter Gass

Erklärung gemäß § 7 (3) b) und c) der Promotionsordnung:

Hiermit erkläre ich, dass ich die vorliegende Dissertation selbst verfasst und mich dabei keiner anderen Mitteln, als der von mir ausdrücklich bezeichneten Quellen und Hilfen bedient habe. Des Weiteren erkläre ich, dass ich an keiner anderen Stelle ein Prüfungsverfahren beantragt oder die Dissertation in dieser oder einer anderen Form bereits anderweitig als Prüfungsarbeit verwendet oder einer anderen Fakultät als Dissertation vorgelegt habe.

Heidelberg, den 2. Februar 2008 Verena Bosch

Für meine Eltern

Table of contents

Summary

In this PhD thesis some molecular mechanisms underlying fear conditioning are addressed by genetic manipulation of a key determinant of synaptic plasticity, namely the AMPA receptor subunit GluR-A. GluR-A is critically involved in long-term potentiation at hippocampal CA3-to-CA1 synapses and is necessary for the formation of spatial working memory. To elucidate whether GluR-A, within the lateral nucleus of the amygdala (LA), is required for the acquisition of fear memories, procedures to generate LA-specific GluR-A depletion, either by generating amygdala-specific transgenic mice, or by employing stereotactic virus delivery, were implemented.

First, transgenic mouse lines were generated by expressing *enhanced green fluorescent protein* (EGFP) under control of the promoter for the *Lypdc1* gene, for which *in situ* hybridization studies showed specific activity in the basolateral amygdala. Unfortunately, in all transgenic lines the *Lypdc1*-promoter driven EGFP expression was not restricted to the amygdala but was also detected in additional brain regions. Therefore, the *Lypdc1*-promoter is not useful for manipulating the GluR-A gene specifically in the amygdala.

As an alternative strategy, recombinant adeno-associated-Cre virus (rAAV-hSyn-Cre/IRESven) was stereotactically delivered into the LA of mice with loxP-flanked exon 11 of the *Gria1* gene (*GluR-A*$^{2lox/2lox}$) prior to fear conditioning. In two-thirds of the injected animals, Cre recombinase expression, which was accompanied by loss of GluR-A signal, could be detected in 10-30% of the LA-neurons. This level of ablation had been previously shown by others to be sufficient to evoke a phenotype in fear conditioning.

As an essential step, different paradigms for fear behavior in wildtype (WT) and global GluR-A knockout (KO) mice were established. The GluR-A KO mice showed a prominent impairment during the acquisition of conditioned fear, demonstrated by the absence of tone-shock induced freezing behavior. Since the sensory systems of GluR-A KO mice were not impaired, this observation suggested that the short-term association of tone and shock is GluR-A dependent. When challenged 24 hours later, the GluR-A KO mice exhibited reduced, although still detectable, memory of the conditioned tone. Thus, it is possible that efficient short-term association of tone and shock is not necessary for the formation of long-term memory of the aversive stimulus. It seems that GluR-A dependent plasticity mechanisms are operative during the acquisition phase and that GluR-A independent mechanisms can be used for long-term fear memory formation.

GluR-A in the LA might be necessary for the immediate tone-shock association during fear acquisition, since the rAAV-Cre mediated LA-specific GluR-A KO mice showed a trend to exhibit less freezing during the acquisition phase than uninjected control animals. However, in order to substantiate this finding it would be necessary to optimize virus injection to achieve more efficient Cre targeting within the LA.

Zusammenfassung

Ziel der Doktorarbeit war es die molekularen Mechanismen der Angstkonditionierung zu untersuchen. Dies sollte mittels genetischer Beeinflussung einer Schlüsselkomponente synaptischer Plastizität, nämlich durch Manipulation der AMPA-Rezeptoruntereinheit GluR-A, erreicht werden. GluR-A spielt eine entscheidende Rolle bei der Etablierung der Langzeitpotenzierung an CA3 zu CA1 Synapsen und ist erforderlich für die Ausbildung des räumlichen Arbeitsgedächtnisses. Um herauszufinden, ob die Expression von GluR-A innerhalb des lateralen Amygdalakerns (LA) für die Induktion von Angsterinnerungen benötigt wird, habe ich versucht, durch Herstellung von Amygdala-spezifischen transgenen Mäusen bzw. durch stereotaktischen Virustransfer, einen LA spezifischen GluR-A Verlust zu erzeugen.

Es wurden transgene Mäuse generiert, die das Reportergen „*enhanced green fluorescent protein*“ (EGFP) in dem *Lypdc1*-Genlokus enthalten, welcher nur in der basolateralen Amygdala exprimiert zu werden schien. In den transgenen Mäusen war jedoch die durch den *Lypdc1*-Promoter getriebene EGFP Expression nicht nur auf die Amygdala begrenzt, sondern wurde darüber hinaus auch in weiteren Gehirnregionen gefunden. Somit ist der *Lypdc1*-Promoter zur gezielten GluR-A Manipulation in Neuronen der Amygdala nicht geeignet.

Es wurden als alternative Strategie rekombinante Cre exprimierende adeno-assoziierte Viren (rAAV-hSyn-Cre/IRESven) in die LA von Mäusen mit loxP-flankiertem Exon 11 des *Gria1* Gens (*GluR-A*$^{2lox/2lox}$) stereotaktisch injiziert und anschließend an diesen Mäusen Angstkonditionierungsversuche durchgeführt.

An Wildtyp (WT) und GluR-A knockout (KO) Mäusen wurden zunächst unterschiedliche Konditionierungsprotokolle getestet und etabliert. Die GluR-A KO Mäuse wiesen in allen Experimenten eine markante Beeinträchtigung in der Akquisition konditionierter Angst auf, welches sich in einem fehlenden Ton-Schock induzierten „Freezing“-Verhalten widerspiegelte. Da die Sensorik der GluR-A KO Tiere nicht beeinträchtigt war, ist anzunehmen, dass die kurzzeitige Assoziation zwischen Ton und Schock GluR-A abhängig ist. Wurden die Mäuse 24 Stunden später erneut getestet, so war ein reduziertes, aber trotzdem detektierbares Gedächtnis für den Konditionierungston nachweisbar. Deshalb scheint die kurzzeitige Assoziation zwischen Ton und Schock zur Ausbildung eines Langzeitgedächtnisses für den aversiven Reiz nicht notwendig zu sein. Möglicherweise ist, wie schon beim räumlichen Gedächtnis beobachtet, die schnelle Assoziation zweier Ereignisse GluR-A abhängig, wohingegen die Ausbildung eines Langzeitgedächtnisses ohne GluR-A auskommt.

Die Expression von GluR-A innerhalb der LA könnte notwendig sein für die kurzzeitige Assoziation zwischen Ton und Schock, da die rAAV-Cre vermittelten LA spezifischen GluR-A KO Mäuse im Vergleich zu den uninjizierten Kontrollmäusen eine Tendenz zu weniger „Freezing“ während der Akquisitionsphase zeigten. Um diese Beobachtung zu konkretisieren muss die Virusinjektion verbessert werden, damit ein effizienteres Cre Targeting innerhalb der LA erreicht wird.

Acknowledgments

First of all I would like to thank Prof. Dr. Peter H. Seeburg for providing me the opportunity of placement in his laboratory, the financial support for this dissertation, and that he made it possible for me to perform this project under his invaluable guidance and for teaching me important lessons in molecular neuroscience.

Furthermore, I want to thank my supervisor Dr. Rolf Sprengel for his thorough introduction into this project, his invaluable help and that he was always cooperative and at any time available for discussions.

Additional, I would like to thank Prof. Dr. Peter Gass for his willingness to evaluate my thesis.

I want to address special thanks to Tansu Celikel with whom I had many discussions that were always aimed to benefit this project.

I especially wish to express my unending gratitude to Cornelia Strobel who did many behavioral experiments with me during her HiWi time. She was always there when I needed help and she always made me smile in times when nothing seemed to work out.

And finally, I want to express my special thanks to all the people in the lab for being always willing to help and for the moral support during my work. Particularly I would like to thank Stephan Meyer, Thorsten Bus, Jan Herb, Sven Berberich, Simone Giese, Martin Schwarz, Simone Astori, Claudia Rauner, Wannan Tang, Sabine Grünewald, Annette Herold, Simone Hundemer and all other members from the lab for their help without which this project would not have been completed!!
Thanks to all of you!!

1. Introduction

1.1 Amygdala and Emotions

Research over the last decades has made great advances in the understanding of the neural and physiological mechanisms of emotions, with the amygdala, as part of the limbic system, playing an exceptional role in emotional processing.

The term emotion is in fact a complicated concept for which there is no universally accepted definition. Emotions are subjective experiences and feelings such as pain, fear, desire, love and hope. In the past emotions were thought to be exclusively human and distinct from other aspects of brain function such as cognition and perception. In 1872, Charles Darwin made an important claim in his publication the “Expression of emotions in man and animals” by stating that some aspects of emotion show similarities in the behaviors of both man and animals. Roughly at the same time, the “James-Lange theory” of emotions emerged, which proposed that emotions are the cognitive processes that accompany our physiological responses to sensory stimuli. This, together with Darwin’s proposal, was the first indication that it might be possible to draw conclusions about human emotions by investigating physiological responses to sensory stimuli in animal behavior. Later these theories were extended by the first neurophysiologic hypothesis, which suggested that specific brain regions, such as the hypothalamus and its connections to the cortex and brainstem, were central elements in emotional processing (Cannan and Bard, 1920). Over time, additional medial temporal lobe structures, including the amygdala, were added to the emotional circuitry. The notion that the amygdala plays a key role in emotional processing came from studies performed by Klüver and Bucy (1937). Klüver and Bucy examined the behavioral defects of bilateral medial temporal lobe lesions in monkeys. The temporal-lobectomized monkeys developed emotional alterations, visual agnosia and altered sexual behavior. Although the monkeys had intact vision, they were incapable of recognizing formerly familiar objects, or their use. The sexual behavior of the monkeys increased considerably and they displayed “oral tendencies” meaning that they examined their world with their mouths instead of their eyes. In addition, the facial expression and vocalization of the monkeys became far less expressive. The monkeys also

became less anxious of things, such as snakes, that would have instinctively evoked a state of panic and fear in their natural environment. They would willingly approach a snake again even after having been attacked by it. These striking emotional deficits were described by Klüver and Bucy as “psychic blindness” and are nowadays known as the Klüver Bucy syndrome. The lesions made by Klüver and Bucy were quite large and included many medial temporal lobe structures, like the hippocampus, the amygdala and surrounding cortical areas. However, it was shown afterwards by Weiskrantz and others (Weiskrantz, 1956; Zola Morgan et al., 1991) that more restricted bilateral amygdala lesions could reproduce most aspects of the Klüver Bucy syndrome. This pointed to a fundamental role of the amygdala in allocating significance to sensory information and in generating the appropriate responses to such stimuli. In particular, it was demonstrated that the amygdala is a core component of the circuitry essential for fear-related responses (for review see LeDoux, 2003; Misslin, 2003; Lang, Davis and Ohman, 2000). This makes the amygdala an attractive target to investigate the underlying physiological and molecular mechanisms contributing to fear learning and memory formation.

Today it is known that amygdala dysfunction is related to behavioral abnormalities in many psychopathologies like autism, depression, schizophrenia, narcolepsy, posttraumatic stress syndromes and phobias in general. Therefore investigation of amygdala function, even if performed in other vertebrate brains, should have implications for the treatment of these human disorders.

1.2 Anatomy

The anatomist Burdach originally described the human amygdala in the early 19th century as an almond-shaped structure located deep within the temporal lobe. Burdach actually described a group of cells, which are now known as the basolateral (BLA) complex of the amygdala. Subsequent studies, in many species, identified several other structures surrounding the BLA and completed the description of what is known as the amygdala complex.

The amygdala complex is a group of at least 10 different nuclei located within the medial temporal lobe. Most of the studies investigating amygdala function have been carried out in rodents, although its role has also been intensively studied in monkeys, cats, dogs and other species, including humans. From these studies, it became clear that despite differences, there are many similarities between diverse species in the organization of the amygdala complex. The following description of the organization and function of the amygdala is focused mainly on results obtained with rodents.

The amygdala can be divided into three anatomically separated regions: 1) the basolateral (BLA) group or BLA complex (Fig. 1), which includes the lateral nucleus, the basal nucleus and the accessory basal nucleus; 2) the cortical group, that includes cortical nuclei and the lateral olfactory tract; and 3) the centromedial group composed of the central and the medial nuclei as well as the amygdaloid part of the bed nucleus of stria terminalis (BNST). And lastly, the intercalated cell mass (ICM) and the amygdalo-hippocampal area comprise another group of nuclei, that belongs to the amygdala complex (for review see Sah et al., 2003).

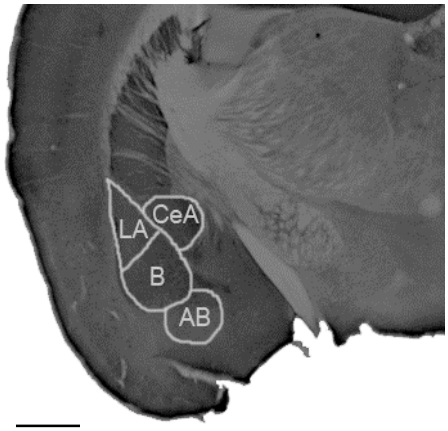

Fig. 1: Location of amygdala.
Low magnification brightfield image of a coronal section from the left brain hemisphere with parts of the amygdala outlined. LA: lateral nucleus; B: basal nucleus; AB: accessory basal nucleus; CeA: central amygdala. Scalebar: 1mm.

1.3 Amygdala connections

Within the amygdala the different nuclei are highly interconnected. The main efferent and afferent connections, which are important during fear conditioning, are schematically depicted in Fig. 2. Afferents from subcortical and cortical sensory systems converge onto BLA neurons (Mc Donald, 1998; Pitkaenen, 2000; Swanson and Petrovich, 1998). It has been shown that projections either from the thalamus or auditory cortex are critical for auditory fear conditioning (Campeau and Davis, 1995; LeDoux, 1986; Romanski and

LeDoux, 1992; Nader et al., 2001), whereas projections from the hippocampus to the BLA are relevant during contextual conditioning (Maren and Fanselow, 1996).

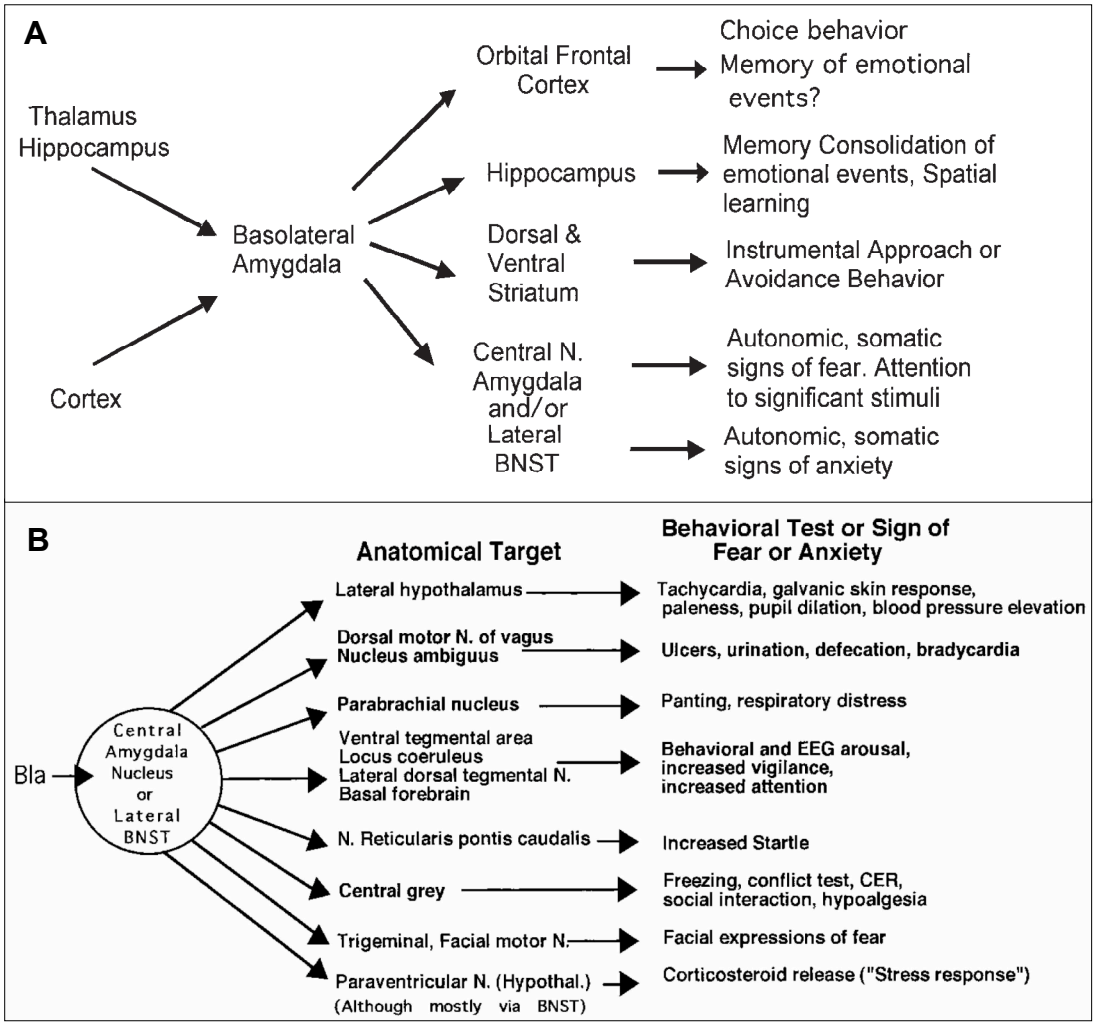

Fig. 2: Schematic representation of the main amygdala nuclei and their connections.
A: Outputs of the basolateral amygdala to various target structures and possible functions of these connections.
B: Outputs of the central nucleus or lateral BNST to various target structures and possible functions of these connections.
From Davis M. and Whalen PJ., 2001.

Parallel thalamic and cortical pathways feed the BLA with information about the aversive electric foot-shock (Shi and Davis, 1999). Indeed, neurons within the BLA have been shown to respond to visual, auditory and somatic (shock) stimuli (Romanski et al., 1993). This demonstrates that information about the conditioned stimulus (CS) and unconditioned stimulus (US) both converge within the amygdala. Furthermore, direct or indirect projections via the ICM

(for review see Pare, Quirk and LeDoux, 2004) from the BLA to the central amydgala (CeA) allow the association made in the BLA during fear conditioning (description see 1.4) to produce fear responses. Activation of the CeA, in turn, results in activation of neurons within the brainstem as well as within the hypothalamus that control and modulate the autonomic systems. The medial subdivision of the CeA has extensive projections to the brainstem (periaqueductal grey and parabrachial nucleus), hypothalamus, BNST and other nuclei in the midbrain, pons and medulla. Together, all these connections orchestrate the behavioral and autonomic effects seen during fear conditioning.

Functionally, the amygdala can be divided into two subsystems. The BLA complex, together with the cortical nuclei, forms the main sensory interface of the amygdala, which can be considered as an input station during fear conditioning. The centromedial part of the amygdala complex constitutes the interface to the fear response systems and is mainly regarded as the output station or even as a passive relay to downstream structures.

1.4 Pavlovian auditory fear conditioning and Lesion studies

In 1927 Ivan Petrovich Pavlov was the first to systematically analyze simple forms of associative learning. Over the last years one form of Pavlovian conditioning, also known as fear conditioning, has received most attention due to its easy induction protocol, long lasting memory trace and universal nature. Through Pavlovian fear conditioning, organisms learn that a certain sensory stimulus predicts subsequent aversive events. This form of learning is important to aid the survival of animals and is a vital component of many mammalian defensive systems. During fear conditioning, a neutral stimulus (CS), such as a tone, light-pulse or odor, is paired with a noxious stimulus (US), in most cases an electric foot-shock. After several of these pairings the CS, when presented alone, acquires the ability to initiate behavioral, autonomic and endocrine responses that help the organism to cope with the predicted upcoming aversive situation. Behavioral expression of these responses (i.e. freezing behavior) in the presence of the CS serves as a

measure of the emotional memory acquired during learning (i.e. conditioning). This makes fear conditioning a valuable behavioral paradigm for investigating the neural basis of emotional memory and of learning and memory in general. This form of associative learning occurs rapidly (sometimes within one trial), and the memory is exceedingly long lasting (it can persist a lifetime). As mentioned previously, there is an abundance of evidence suggesting an important role for the BLA, and especially for the LA, during acquisition of fear conditioning (Fig. 3), particularly upon an auditory CS (for review see LeDoux, 2000; Maren, 2001; Walker and Davis, 2002; Fanselow and LeDoux 1999; Blair et al., 2001).

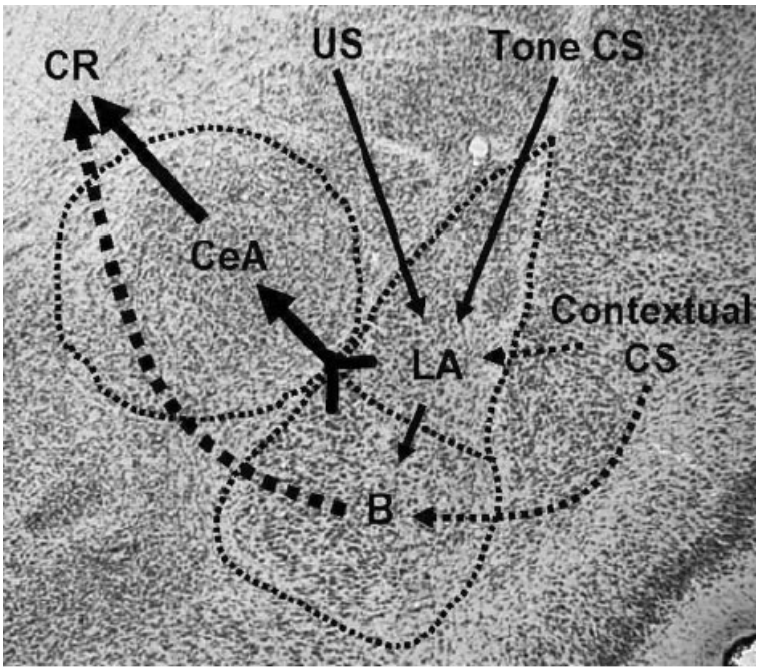

Fig. 3: Schematic model of fear conditioning circuits within the amygdala.
The auditory CS and the electric foot-shock US converge onto LA neurons, where they become associated. Indirect projections of the LA to the CeA via the basal nucleus (B) or direct projections from LA to CeA mediate the expression of conditioned responses (CR) due to the various connections of the CeA to downstream targets.
From Goosens and Maren, 2001.

Electrical stimulation of the BLA or amygdaloid seizures result in behavioral response patterns that are similar to those evoked by stress- and fear-inducing stimuli (Chapman et al., 1954; Feindel, 1954). On the contrary, selective lesions of the BLA prior to fear conditioning produce severe deficits in acquisition and expression of Pavlovian fear conditioning (LeDoux et al., 1986; LeDoux et al., 1990; Campeau et al., 1992; Davis et al., 1993; Campeau and Davis 1995; Maren et al., 1996; Amorapanth, 2000). Lesions of the central amygdaloid (CeA) nucleus also produce deficits in both acquisition and expression of conditioned fear (Roozendaal et al., 1991; Kim and Davis, 1993), as characterized by complete absence of conditioned fear responses, including

freezing behavior, during memory testing. BLA lesions, made even a month after conditioning, also destroy fear responses, suggesting that the BLA plays an important role in the long-term storage of fear memories (Kim and Davis, 1993; Lee et al., 1996; Maren et al., 1996). Lesions of the BLA do not influence foot-shock reactivity or baseline locomotor activity (LeDoux et al., 1990; Campeau and Davis 1995; Maren et al., 1996), showing that the deficits observed with BLA lesions are not due to performance problems (but see Blair et al., 2005). All these studies suggest a role for associative processes within the BLA underlying fear conditioning (Maren, 2001).

1.5 Evidence for synaptic plasticity in the LA during fear conditioning

It has been shown that neural activity within the BLA changes during fear conditioning (Quirk et al., 1995 and 1997; McKernan and Shinnick-Gallagher, 1997; Rogan et al., 1997). In particular, the LA is supposed to be the main site of plastic changes that contribute to fear learning, since the convergence of CS and US inputs to the LA (see schematic model in Fig. 3) increases the efficacy of synapses transmitting information about the CS to the LA (Maren and Quirk, 2004; LeDoux, 2000; Walker and Davis, 2002). This results in increased firing rates of LA neurons during CS alone presentation (Collins and Pare, 2000; Quirk et al., 1995 and 1997; Repa et al., 2001). Furthermore, induction of long term potentiation (LTP), which is an artificial process to increase synaptic strength and is viewed as a physiologic correlate for learning and memory (Bliss and Collingridge, 1993; Malenka and Nicoll, 1999), has been shown to occur in the CS pathways to the LA (Maren and Fanselow, 1995; Huang and Kandel, 1998; McKernan and Shinnick-Gallagher, 1997; Rogan et al., 1997).

The mechanisms underlying amygdala LTP were shown to be different at thalamic compared to cortical afferents to the LA and have been studied to a large extent in these two pathways (Sigurdsson et al., 2007). LTP at the thalamo-LA pathway seems to be expressed postsynaptically (Humeau et al., 2005). The AMPA receptor subunit GluR-A was shown to have a dominant role in the expression of synaptic plasticity in the thalamo-LA pathway, as LTP

is completely absent at these synapses in the global GluR-A KO mouse line (Humeau et al., 2007). On the contrary, in the cortico-LA pathway the expression mechanism has both pre- and postsynaptic components (McKernan and Shinnick-Gallagher, 1997; Huang and Kandel, 1998), and GluR-A as well as GluR-C subunit containing AMPA receptors contribute to LTP at these synapses (Humeau et al., 2007).

Of note, the CeA might itself be a site of plasticity during fear conditioning independent of the LA (for review see Pare and LeDoux, 2004; Wilensky et al., 2006). This is suggested by the observation that LTP can be induced in the CeA after stimulation of the posterior thalamic auditory pathways (Samson and Pare, 2005). LTP at this synapse is expressed presynaptically and was shown to depend on NMDA receptor activation. Pare suggested a model in which the intercalated GABAergic neurons within the ICM between the BLA and CeA have an impact in modulating LTP-like facilitation of excitatory transmission in the CeA. The BLA thereby regulates activity in the CeA, which in turn not only participates in the storage but also in the expression of fear memories.

Nevertheless, these studies suggest that neurons within the LA play a central role in the acquisition of fear memories, thus making the LA an attractive target for investigating the molecular basis of associative memory.

1.6 Pharmacological manipulations prevent fear learning and memory

As detailed above, fear conditioning induces alterations in the firing patterns of LA neurons, similar to those activity changes seen during LTP induction (Quirk et al., 1995 and 1997; McKernan and Shinnick-Gallagher, 1997; Rogan et al., 1997). Pharmacological tools, which block or reduce synaptic plasticity, have also been shown in most cases to prevent learning and/or memory formation during fear conditioning. Listed below is a summary of some of the findings, which implicate a role of different synaptic key molecules in the acquisition of fear conditioning.

-LA inactivation by muscimol:

Infusion of muscimol, a $GABA_A$ agonist, into the LA prior to fear conditioning blocks acquisition of fear conditioning but also disrupts shock-

reactivity. This indicates that neuronal activity within the LA is required for expression of both unconditioned and conditioned responses to aversive stimuli (Blair et al., 2005).

-Blockade of NMDA receptors:

Infusion of the NMDA receptor antagonist APV into the LA prior to or immediately after fear conditioning obstructs the acquisition of fear conditioning (Miserendino et al., 1990; Campeau et al., 1992; Fanselow and Kim, 1994; Bauer et al., 2002). APV also attenuates shock-reactivity probably by disrupting routine synaptic transmission, which suggested that impairment of fear conditioning might be confounded by impaired sensory responses. Nevertheless, results from application of ifenprodil (Rodrigues et al., 2001) or CPP (Goosens and Maren, 2004), antagonists of the NR2B-containing NMDA receptors, into the LA, prior to fear conditioning, show that independent from the role of NMDA receptors in synaptic transmission, NR2B-containing NMDA receptors are required for expression of fear conditioning and long-term synaptic potentiation in the LA.

-Blockade of AMPA receptors:

Infusion of NBQX, an AMPA/kainate receptor antagonist, not only disrupts fear-potentiated startle reflex, but also attenuates the expression of CRs. This indicates that AMPA receptor activation is not only important for the establishment of long-term memories, but is also required for the expression of fear-associated responses (Kim et al., 1993; Walker and Davis, 2002).

-Blockade of VGCC (voltage gated Ca^{2+} channels):

Infusion of a L- type VGCC antagonist into the LA prior to training prevents fear conditioning without altering shock-reactivity, demonstrating that VGCCs are needed for the consolidation of long-term memories (Weisskopf et al., 1999; Bauer et al., 2002).

-Blockade of group I metabotropic glutamate receptors (mGluRs):

Infusion of MPEP, a mGluR5 receptor antagonist, blocks the acquisition of fear conditioning, which shows that these receptors have an important role in this process (Fendt and Schmid, 2002; Rodrigues et al., 2002).

All these pharmacological studies suggest that NMDA receptors, particularly the NR2B-containing receptors, as well as AMPA receptors and

mGluR5 receptors are involved in the acquisition of fear conditioning. This supports the conclusion that synaptic plasticity may be required for the acquisition of fear memories.

1.7 GluR-A containing AMPA receptors are involved in learning and memory formation

GluR-A containing AMPA receptors are crucially involved in certain forms of memory formation. Mice lacking the GluR-A subunit do not express LTP at CA3-to-CA1 synapses, and have impaired spatial working memory (WM) – a behavioral task dependent on intact information processing within the hippocampus (Zamanillo et al., 1999; Reisel et al., 2002). These impairments (lack of LTP and impaired spatial WM) can be rescued by reintroduction of the GluR-A subunit in hippocampal pyramidal neurons by transgenic means (Mack et al., 2001; Schmitt et al., 2005). This proves the importance of this subunit for synaptic plasticity and for the performance of hippocampus-dependent tasks.

Not surprisingly, GluR-A has been shown to be important for many other activity-dependent plasticity forms (Malinow and Malenka, 2002). In the thalamo- and cortico-LA pathways, both GluR-A/-B and GluR-B/-C subunit combinations are expressed (Farb and LeDoux, 1997, 1999; Radley et al. 007). Lüthi and colleagues recently showed that in complete GluR-A KO mice, LTP is absent at the thalamic-LA synapses, and that these mice are impaired in fear conditioning, which indicated a major role for this subunit during fear learning (Humeau et al. 2007). A different study demonstrated that disrupting GluR-A trafficking blocked thalamo-LA LTP and reduced the acquisition of auditory fear conditioning (Rumpel et al., 2005).

1.8 Aim of thesis

The aim of this thesis is to address the role of GluR-A containing AMPA receptors, which are expressed, amongst others, within the LA, during auditory fear conditioning. Current findings support the view that LA-specific deletion of the GluR-A gene, prior to fear conditioning, would prevent the occurrence of LTP at the CS pathways to the LA (especially the thalamic input to the LA). This would render mice unable to associate CS-US pairing, would

prevent the acquisition of fear memories and result in their exhibiting no, or less, fear responses (e.g. freezing). Rumpel et al. (2005) have made use of a viral transduction technique to interfere with GluR-A containing AMPA receptor trafficking in LA neurons. They showed that overexpression of the C-terminal domain (81aa) of the GluR-A subunit in a subset of LA neurons (20%) was sufficient to reduce memory to a tone-shock association and to impair LTP (Rumpel et al; 2005). However, it cannot be excluded that mechanisms, other than the specific interference with GluR-A trafficking, account for the memory deficit observed. The C-terminal domain of the GluR-A subunit contains various protein interaction domains and phosphorylation sites and its overexpression may interfere with other cellular processes, not exclusively linked to GluR-A trafficking. It is, therefore, crucial to prove that a site-specific gene ablation of the GluR-A subunit within the LA does, indeed, impair synaptic plasticity at thalamo-LA synapses and hence block the associative processes underlying acquisition of fear memories.

In this thesis, two alternatives approaches were followed with the aim of achieving efficient LA-specific gene knockout. Firstly, a transgenic mouse model, exhibiting LA-specific expression of molecular tools (like Cre recombinase) to knockout key genes, potentially involved in learning and memory (e.g. the GluR-A gene), should be generated. In a second approach, LA-specific gene knockout should be achieved by stereotactic delivery of adeno-associated virus (AAV)-derived vector particles, expressing Cre recombinase, to the LA of conditional GluR-A (*GluR-A*$^{2lox/2lox}$) mice. In both approaches, successfully generated animals should be analyzed in fear conditioning experiments. Thus, a further essential step of this thesis was to establish and validate fear conditioning protocols. For this, in addition to normal wildtype (WT) mice, the complete GluR-A KO mouse line, which has been reported to be impaired in fear conditioning experiments (Humeau et al., 2007), were employed.

2. Results

2.1 Search for genes specifically expressed in the amygdala

This thesis aimed at gaining further insight into the function of the amygdala and, in particular, into its involvement during fear conditioning. As a tool for this purpose, a mouse model, permitting gene regulation specifically within the amygdala, should be generated. Such a mouse line would be beneficial for the generation of amygdala-specific ablations of molecules known to be important for learning and memory, e.g. the AMPA receptor subunit GluR-A (Zamanillo et al., 1999; Schmitt et al., 2005), which is a focus of this thesis.

Information on tissue-specific gene expression can be obtained from different online databases. These summarize expression patterns obtained by *in situ* hybridization studies (e.g. Allen Brain Atlas), microarray chips (Symatlas), or, alternatively, from BAC transgenic mouse lines with specific reporter gene expression (e.g. GENSAT). At the beginning of this thesis data from the Symatlas database was available (symatlas.gnf.org/SymAtlas; Su et al., 2004). It provides an extensive atlas of tissue-specific gene expression obtained by custom made arrays that assess known and predicted protein-coding genes ranging from mouse to human. The design process used a nonredundant set of known genes and gene predictions compiled from Refseq, Celera, Ensembl (for human), and RIKEN (for mouse). In total, the custom-designed GNF1M mouse array interrogates 36,182 probe sets. One potential gene, named *Ly6/Plaur domain 1 containing gene* (*Lypdc1*), with an apparently high and exclusive expression within the amygdala (Fig. 4A), was selected. *In situ* hybridization (ISH) experiments were performed to verify the accuracy of the expression pattern published by SymAtlas.

2.1.1 Expression of endogenous *Lypdc1* in the mouse brain

ISH for *Lypdc1* was carried out with two different oligoprobes (see Methods). Since the amygdala is best represented/visualized on coronal sections, the labeled probes were hybridized onto coronal cryostat sections of the mouse brain. Only those sections were chosen for ISH, in which the dorsal hippocampus was around 2mm wide, because on these sections the amygdala has a pronounced morphology. The observed expression pattern

(Fig. 4B) was mainly restricted to the BLA, although weak expression was also seen in the dentate gyrus (DG) and the cornu ammonis 1 (CA1) region of the hippocampus.

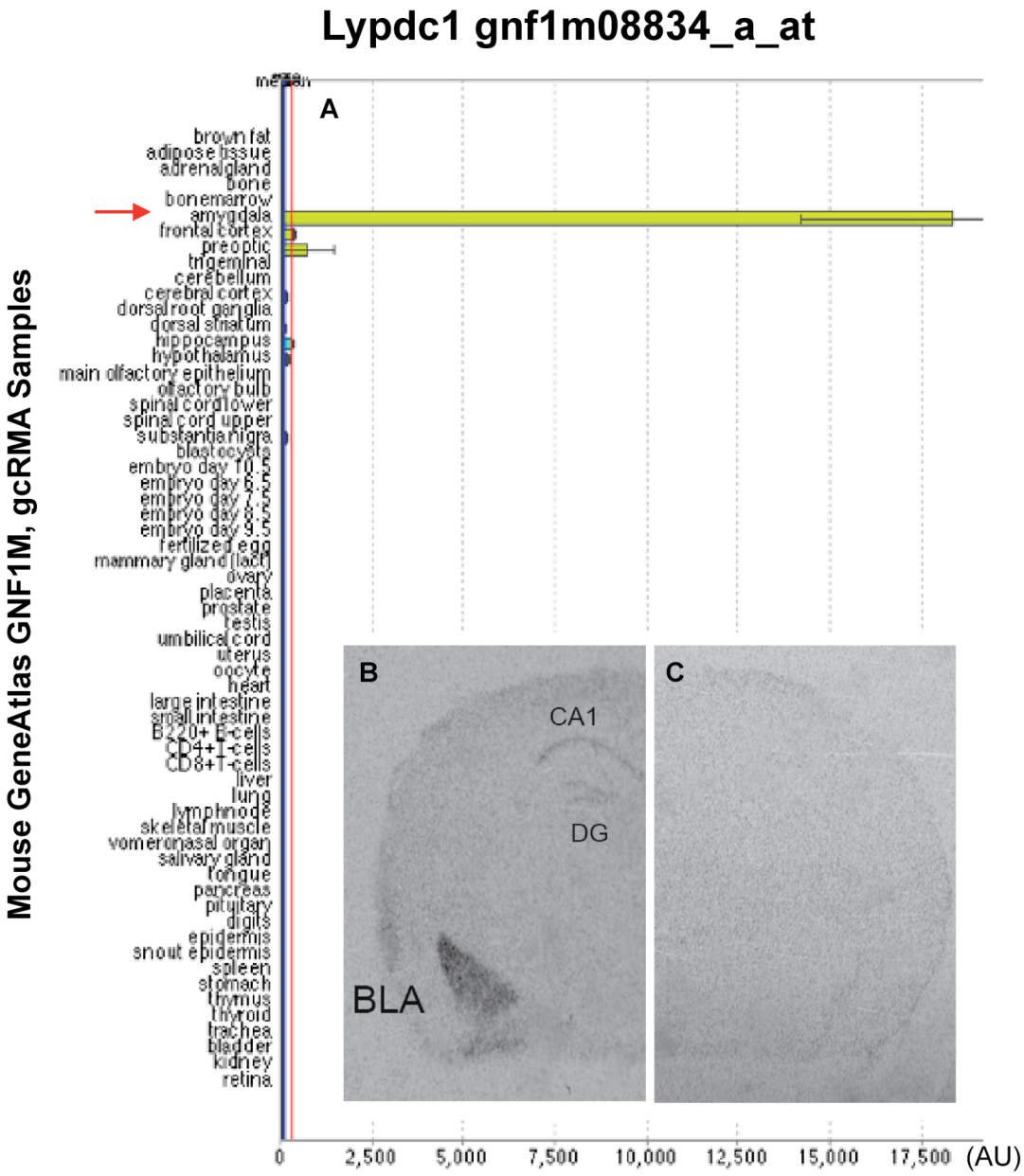

Fig. 4: SymAtlas expression diagram (A) and ISH results (B, C). *Lypdc1* was strongly expressed in the BLA with additional weak expression in DG and CA1 of the hippocampus.
A: Expression database search for *Lypdc1*. Red arrow marks expression within the amygdala. Y-axis displays analyzed tissues. X-axis displays arbitrary unit (AU) scale. B: ISH of a mouse coronal cryostat section using *Lypdc1* (ASexon2) as probe. (CA1=cornu ammonis 1, DG=dentate gyrus, BLA=basolateral amygdala). C: ISH of a mouse coronal cryostat section using a control probe.

The expression of *Lypdc1* was stronger at the tip of the BLA, namely the LA of the amygdala, which is the subnucleus of the amygdala particularly

important during the generation of fear memories (LeDoux et al., 1990). Both probes revealed the same results (here only shown for one probe). Despite the fact that weaker expression was also seen within the hippocampus, this particular gene locus was chosen to generate transgenic mice. For this purpose, the BAC transgene technology was employed. This technique is superior to the conventional transgenic approach, since the introduced long BAC transgene contains authentic regulatory elements (upstream and downstream sequences flanking the gene, introns), ideally leading to a transgene expression more comparable to the endogenous expression pattern of the modified gene (Gong et al., 2003).

A strategy was designed for homologous recombination into a BAC clone (chori.org/BACPAC/vectorframe.htm; RP23-462P13) containing the *Lypdc1* gene locus.

2.1.2 Expression of BAC-encoded *Lypdc1*

To test whether *Lypdc1* promoter-driven transgenes were indeed only expressed within the amygdala, the *Lypdc1* expression pattern using EGFP as a reporter gene instead of directly expressing Cre recombinase was assessed. After homologous recombination and removal of the selection marker (see Methods), a Southern blot experiment (Fig. 5) was performed to verify correct recombination and excision of the selection marker.

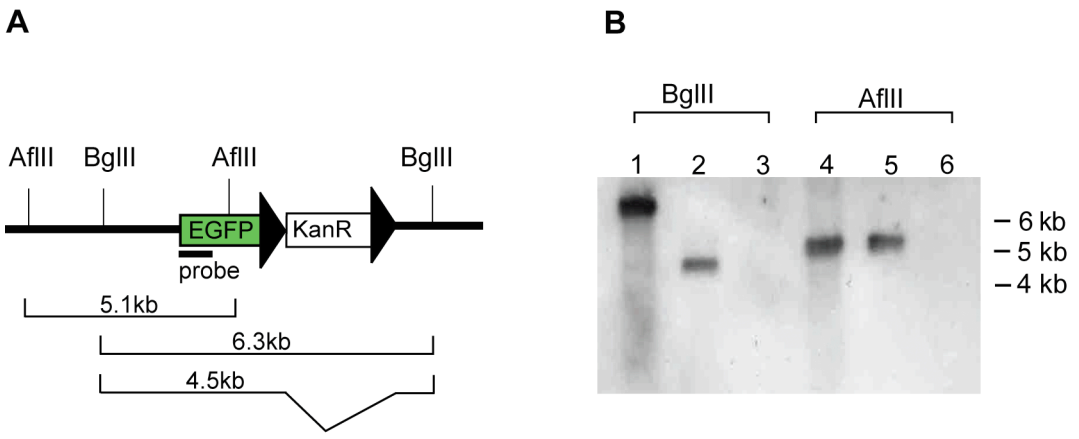

Fig. 5: Southern blot strategy (A) and results (B). Successful recombination into *Lypdc1* and excision of selection marker were confirmed.
A: Scheme of Southern strategy for screening of recombined BAC clones. B: Southern blot of two digests (BglII and AflII) of BAC clone 2, BAC clone 2-9 and original BAC. Digests were probed against EGFP. Lane 1 and 4: BAC clone 2. Lane 2 and 5: BAC clone 2-9. Lane 3 and 6: original BAC clone.

The results of the Southern blot experiment are shown in Fig. 5B. BAC clone 2 (before removing the selection marker, see Fig. 5A) showed the expected band pattern in the two digestions (BglII and AflII). BglII digestion resulted in a 6.3kb DNA fragment (Fig. 5B, lane 1) and AflII digestion resulted in a 5.1kb DNA fragment (Fig. 5B, lane 4), confirming correct recombination. BAC clone 2-9 (after removing the selection marker, see Fig. 5A) also revealed the expected band pattern in the different digestions. BglII digestion yielded a 4.5kb DNA fragment (Fig. 5B, lane 2), confirming excision of the selection marker and AflII digestion again resulted in a 5.1kb DNA fragment (Fig. 5B, lane 5). This BAC clone 2-9 was selected for pronucleus injection (performed by Frank Zimmermann at the IBF, Uni-Heidelberg). Therefore the modified BAC was retrieved from its plasmid-backbone via NotI digestion, followed by sepharose chromatography to separate the plasmid-backbone from the modified BAC sequence.

From this pronucleus injection, 151 pups were born (F0 generation), which were analyzed by tail-PCR for the integration of the modified BAC into the genome. The transgene was detected in 12 of the pups and these were crossed with C57/Bl6 mice for the establishment of transgenic lines, termed Ly1GFP. Once the founders gave rise to pups (F1 generation) they were sacrificed (at age >P40) for analysis of the expression pattern of the *Lypdc1* promoter-driven EGFP reporter by immunohistochemical (IHC) staining. From each founder, five coronal sections across the brain were stained against EGFP. An assortment of anti-EGFP stainings from the founders is shown in Fig. 6, and a detailed analysis of EGFP expression for some founders can be seen in Fig. 7. It became apparent that in contrast to the results obtained with ISH none of the transgenic mice showed a predominant amgydala expression of the reporter gene. Most founders showed strong EGFP labeling within the DG of the hippocampus and only moderate expression within the BLA and CeA of the amygdala (i.e. F31, 151, F29, F30, F59, F53). EGFP expression was also detected in the cerebellum, the olfactory bulb, striatum, and other areas (not shown). One founder (F55; Fig. 6 red arrow), for example, displayed no EGFP labeling within the hippocampus but expression within the striatum (F55; Fig. 7). Two founders (F71 and F40; Fig. 6 red arrowhead)

even had no expression within the amygdala. This indicated that multiple integrations of the modified BAC transgene might have occurred and/or that there were strong influences of the transgene´s integration site.

This lack of specific reporter gene expression within the amygdala clearly made it not worthwhile to establish a transgenic mouse line by modifying this particular gene locus (*Lypdc1*).

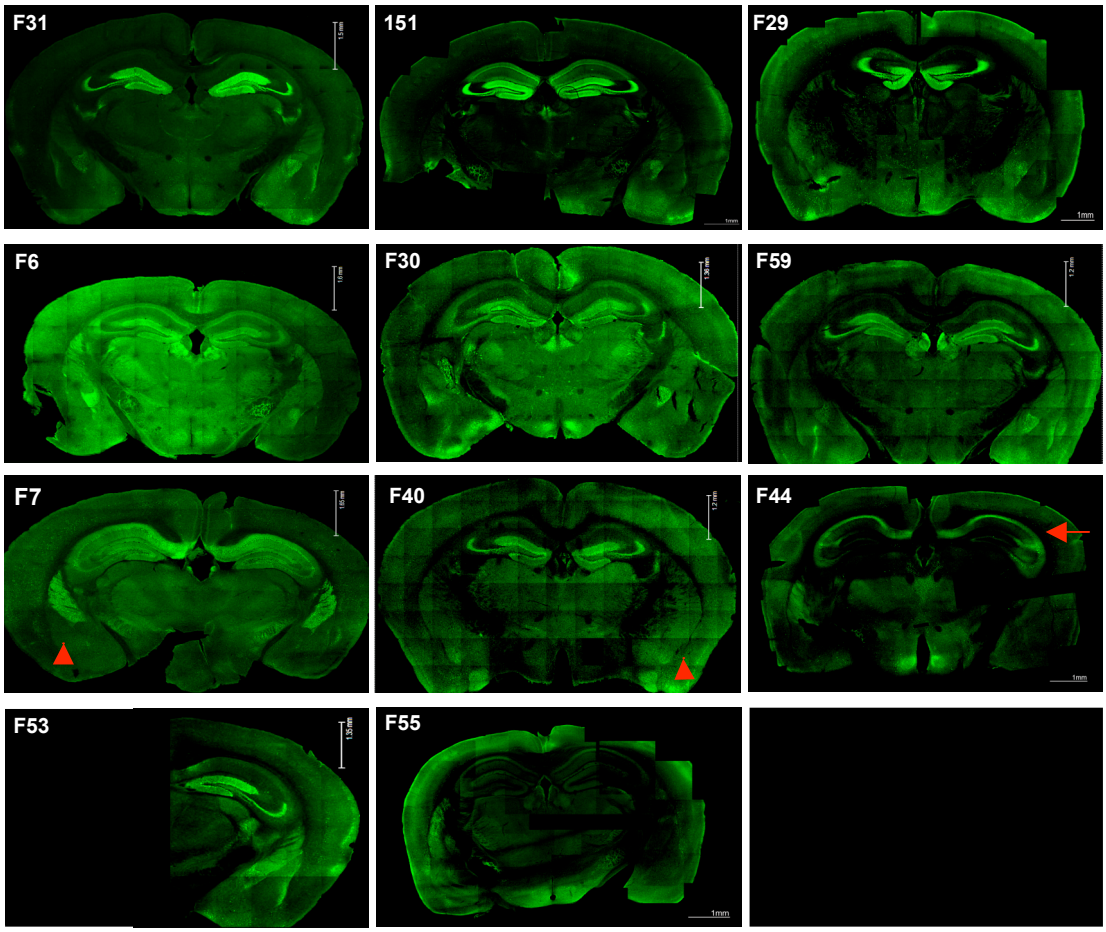

Fig. 6: *Lypdc1*-EGFP expression pattern in different founder mice. In none of the founder mice an amygdala predominant EGFP expression was observed.
Confocal overview pictures of EGFP immunostaining of one coronal section including representation of the hippocampus and the amygdala are depicted for each founder. Founder 31, 151, 29, 30, 59 and 53 showed EGFP labeling within the DG of the hippocampus as well as within the BLA and CeA of the amygdala. Founder 44, on the contrary, expressed within the CA1 region of the hippocampus (red arrow) and F55 had no detectable EGFP within the hippocampus. EGFP expression in founder 40 and 71 was not detectable within the amygdala (red arrowhead).

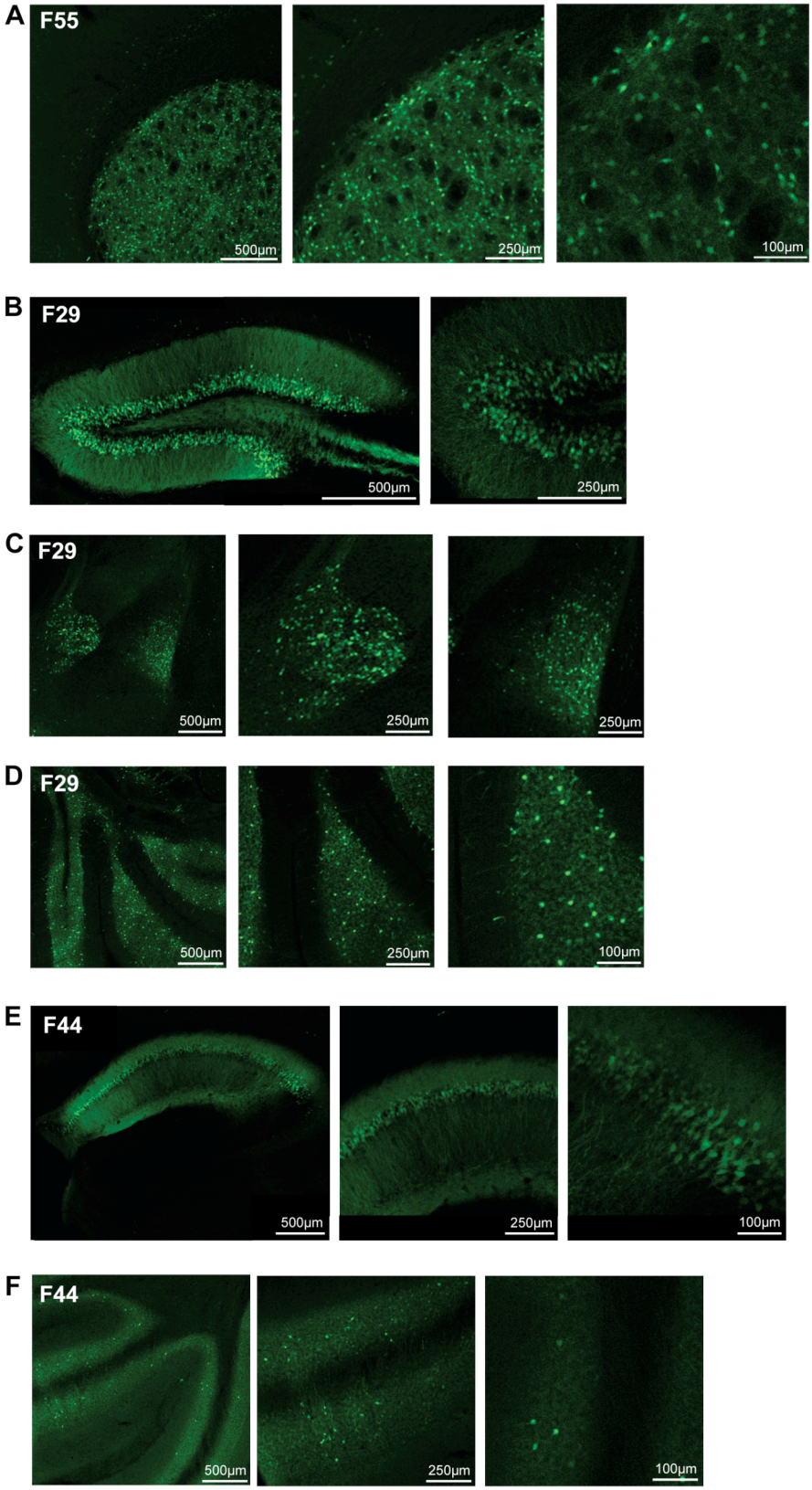

Fig. 7: Localization of *Lypdc1*-EGFP in three different founder mice. Predominant amygdala specific expression was not observed in any of the founder (F) mice.
Confocal microscopy images of A: Striatum of F55, B: Hippocampus (HC) with DG of F29, C: Amygdala (CeA+BLA) of F29, D: Cerebellum of F29, E: HC of F44 and F: Cerebellum of F44.

2.2 Virus-mediated GluR-A deletion in the amygdala

As an alternative strategy for the generation of an amygdala-specific knockout mouse line, it is possible to use virus-mediated gene delivery of Cre recombinase into conditional mice, carrying "floxed" alleles of genes of interest (e.g. *GluR-A*$^{2lox/2lox}$). For this purpose, the recombinant adeno-associated virus (rAAV) system was employed. It represents a powerful procedure for the creation of target specific infections because of its lack of toxicity (reviewed by During et al., 2003; Tenenbaum et al., 2004; Samulski R.J., 1996) and the efficient transduction of non-dividing cells, like neurons (Terwilliger E.F., 1996; Chatterjee S., 1994). Other advantages of rAAV are the long-term expression of the delivered gene without causing an immune response (Peel and Klein, 2000; Jooss et al., 1998; Hernandez et al., 1999). Furthermore, rAAV-transduced transgenes have only a low frequency of integration into the genome and therefore there should be less, if any, integration-dependent effects on transgene expression. AAV 2 vectors have the ability to integrate into host chromosomes in tissues (Terwilliger E.F., 1998), but extrachromosomal vector genomes dominate over integrated forms and are primarily responsible for persistent expression (Engelhardt, 1998; Nakai et al., 2001). The rAAV constructs used in this study expressed Cre recombinase or GFP, respectively, under the neuron-specific human synapsin promoter (Fig. 8A). After virus production and iodixanol purification (see Methods), SDS-PAGE followed by Coomassie staining revealed the purity of the prepared vector particle sample for stereotactic injection. Three specific protein bands, corresponding to the viral capsid proteins (VP1: 87kDA; VP2: 73kDa; VP3: 62kDa; Fig. 8D), and no contaminating non-viral proteins, were apparent. To reveal the genomic titer, real-time PCR was performed (by Jan Herb, MPI, Heidelberg), and a value of 5.9 x 10^{11} copies/ml, indicating high-titer virus stock, was obtained. These vectors were delivered into the LA of conditional GluR-A mice (*GluR-A*$^{2lox/2lox}$) via stereotactic injection (illustrated in Fig. 8C). Subsequent to injection, mice were allowed to recover for at least 28 days (Fig. 8D) and were then subjected to conditioning experiments. As essential first step, prior to analyzing the rAAV-Cre injected mice, the parameters for fear conditioning experiments had to be established and

validated. The characterization and phenotypical analysis of the rAAV-Cre injected mice is described later in section 2.2.2.

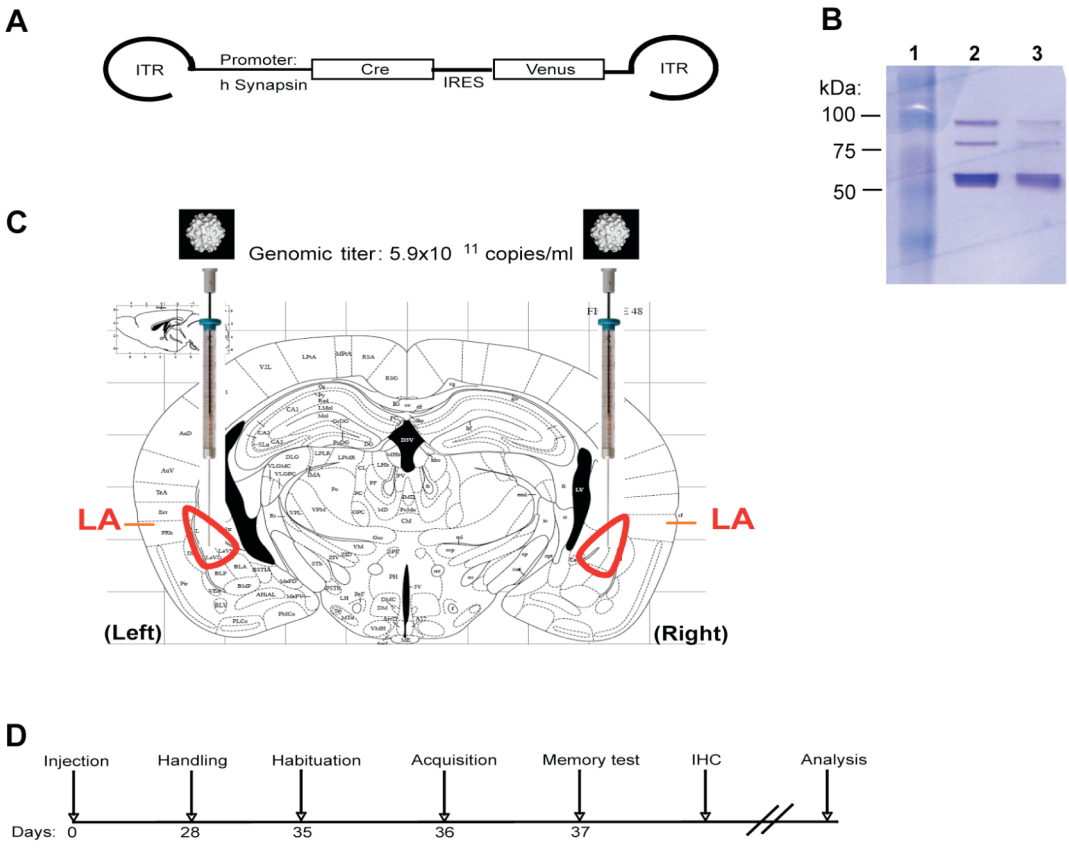

Fig. 8: Experimental design of virus-mediated GluR-A deletion in the lateral amygdala. A: Schematic diagram of rAAV vector (rAAV-hSyn-iCre/IRESven). ITR=inverted terminal repeats, IRES=internal ribosomal entry site. B: Coomassie staining of viral preperation after iodixanol gradient purification. Lane 1: Standard protein marker. Lane 2: rAAV-hSyn-iCre/IRESven (10µl). Lane 3: rAAV-hSyn-GFP (10µl). C: Overview diagram of targeting the lateral amygdala (LA). D: Time-line of experiments.

2.2.1 Fear conditioning

Two fear conditioning protocols were employed to induce fear behaviors in mice. A one-trial and a multi-trial protocol were performed, which differed in the number of tone-shock pairings (one versus three pairings), the duration of the tone (one pairing: 20 sec tone; three pairings: 30 sec tone) and the intensity of the foot shock (one pairing: 1 sec at 0.5mA; three pairings: 2 sec at 0.4mA; see Methods). In addition to wildtype mice (WT), global GluR-A knockout (KO) mice were used for the establishment and validation of these two protocols. This mouse line lacks a functional gene for the AMPA receptor

subunit GluR-A in all cells and it has been previously reported that these mice are impaired in fear conditioning experiments (Humeau et al. 2007). This observation fits into the fact that the GluR-A subunit appears to be important in a plethora of behavioral learning paradigms (Mack et al., 2001; Schmitt et al., 2005). This line therefore appeared to be ideal to serve as a positive control for the behavioral read-out before testing the rAAV-Cre injected mice. Experiments were performed with four cohorts of GluR-A KO mice. One cohort was used to test the one-trial protocol and the other three cohorts of mice were used in the multi-trial paradigm with different experimental modifications (see Table 1).

Animal cohorts	Training protocol	Age (in months)	Number of mice	Handling	Habituation
1	1 pairing (0.5mA/1sec)	WT: 2 - 3 KO: 2 - 4.5	WT: 6 KO: 5	√	√
2	3 pairing (0.4mA/2sec)	WT: 1.5 - 2.5 KO: 2 - 12	WT: 12 KO: 21	√	√
3	3 pairing (0.4mA/2sec)	Both: 2.5	WT: 6 KO: 6	√	No
4	3 pairing (0.4mA/2sec)	WT: 1.5 - 5.5 KO: 5.5 - 7.5	WT: 9 KO: 9	No	No

Table 1: Summary of the behavioral experiments performed with the complete GluR-A KO mouse line. One cohort (1) was tested in the one-trial fear conditioning experiment and three cohorts of mice were tested in the multi-trial fear conditioning paradigm with different experimental alterations (with or without handling and habituation).

2.2.1.1 One-trial fear conditioning paradigm

To address the role of GluR-A containing AMPA receptors in fear learning, the GluR-A KO mice were first tested in the one-trial pairing fear conditioning paradigm.

2.2.1.1.1 Habituation phase

On the first day of training, mice (n=6 WT, n=5 KO) were subjected to a habituation session, during which they were allowed to freely explore the conditioning chamber (Context A) for a period of 6 min (Fig. 9A a, depicts the mobility traces during habituation). A statistical comparison of mean mobility in the first and the last min during habituation (Fig. 9A b, Phases 1+2) did not

reveal significant differences between groups (Mean ± SEM; first 60 sec: KO=93 ± 4.2%, first 60 sec: WT=99.7 ± 0.3%, p>0.05; last 60 sec: KO=98.7 ± 0.6%, last 60 sec: WT=89.2 ± 4.5%, p>0.05), although WT mice showed a tendency to habituate to the chamber, i.e. had become slightly less mobile (first 60 sec: WT=99.7 ± 0.3%, last 60 sec: WT=89.2 ± 4.5%, p>0.05). GluR-A KO mice, on the contrary, increased their mobility, albeit not significantly (first 60 sec: KO=93 ± 4.2%, last 60 sec: KO=98.7 ± 0.6%, p>0.05). A general observation seen in this experiment and, as a trend in all following fear conditioning experiments is that GluR-A KO mice often exhibited higher baseline mobility in comparison to WT mice.

2.2.1.1.2 Acquisition phase

One day after the habituation phase, mice were placed in the conditioning chamber (Context A) once again and received an acclimatization period of 6 min. This was followed by one tone-shock pairing (CS+US = CS1) whereby the tone was present for 20 sec and was co-terminated with a 1 sec, 0.5mA foot shock. The behavior of the mice was recorded for a further two and a half min after CS+US presentation, a period designated as intertrial interval (ITI). In summary, the resultant mobility traces (Fig. 9B a) revealed that, in contrast to WT mice, GluR-A KO mice did not exhibit a CS+US induced mobility reduction. They showed similarly high mobility levels after CS+US presentation as before conditioning, indicating impaired acquisition of fear behavior in absence of GluR-A.

Baseline analysis: Changes in mobility during the acclimatization period were assessed by averaging the mobility in the first min before conditioning and by statistically comparing this to the mean mobility in the last min before conditioning (Fig. 9B b, Phases 1+2). In this case, for both groups, this did not reveal a significant change in mobility (first 60 sec: WT=83.6 ± 5.7%, last 60 sec: WT=90.3 ± 3.7%, p>0.05; first 60 sec: KO=93 ± 2.2%, last 60 sec: KO=99 ± 0.6%, p>0.05). Furthermore, there were no significant differences between groups immediately prior to CS+US onset (last 60 sec: KO vs control, p>0.05).

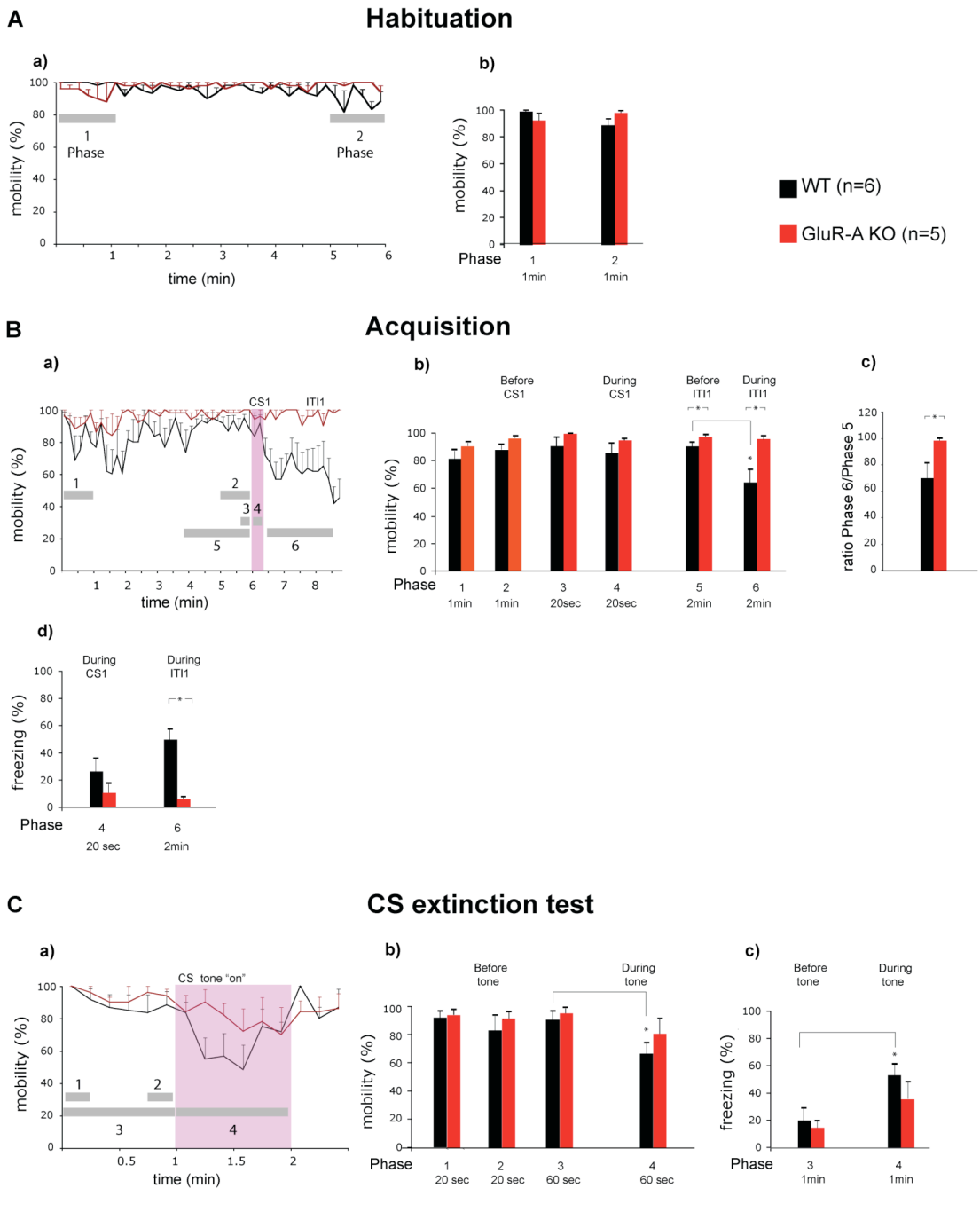

Fig. 9: Summary of the behavioral analysis in the one-trial fear conditioning paradigm (Cohort 1). GluR-A KO mice showed a strong impairment during acquisition of fear conditioning but displayed similar behavior as WT mice when memory was assessed 24 hrs after conditioning.
A: a) Mobility pattern for the habituation session and b) statistical comparison of first min versus last min during the habituation phase. B: a) Activity traces for the acquisition session, b) statistical analysis of mobility before, during (CS) and after (ITI) conditioning, c) statistical analysis of normalized mobilty during ITI (ratio during ITI1/before ITI1) and d) statistical analysis of freezing levels during (CS) and after (ITI) conditioning. C: a) Mobility graph for the memory test session (CS extinction phase), b) statistical analysis of mobility before and during tone presentation and c) statisical comparison of freezing responses before and during tone presentation. WT mice (n=6) are shown in black. GluR-A KO mice (n=5) are shown in red. Mean ± SEM. Grey bars in the mobility graphs delineates different Phases.

CS1 analysis: Analysis of the average mobility of 20 sec before conditioning compared to the average activity of 20 sec during CS1 revealed no significant changes within group (Fig. 9B b, Phases 3+4; before CS1: WT= 91.7 ± 6.4%, CS1: WT=87.5 ± 8.7%, $p>0.05$; before CS1: KO=100 ± 0%, CS1: KO=95 ± 3.9%, $p>0.05$), nor any significant differences between groups (before CS1: KO vs control, $p>0.05$; CS1: KO vs control, $p>0.05$). This also held true for the freezing responses (Fig. 9B d, Phase 4; CS1: WT=26.7 ± 9.5%, KO= 11 ± 6%, $p>0.05$).

ITI1 analysis: However, the aforementioned impairment of GluR-A KO mice in fear conditioning is clearly revealed in the analysis of the ITI period. A comparison of mean mobility before ITI1 (Fig. 9B b, Phase 5) to average mobility during ITI1 (Fig. 9B b, Phase 6) revealed a significant decrease for WT mice (before ITI1: WT=91 ± 2.2%, ITI1: WT= 63.75 ± 9.3%, $p<0.05$), whereas GluR-A KO mice did not show a significant mobility reduction (before ITI1: KO=97.5 ± 1.1%, ITI1: KO=96.5 ± 1.2%, $p>0.05$). However, the comparison of mobility in the two min time frame period before conditioning (as opposed to the one min comparison in the baseline analysis) revealed a significant difference between groups (before ITI1: WT=91 ± 2.2%, before ITI1: KO=97.5 ± 1.1%, $p<0.05$). Thus, in order to compare the percentage mobility reduction between groups, the data were normalized to the average mobility of two min before conditioning (ratio: Phase 6/Phase 5). After normalization (Fig. 9B c), the mobility levels were still significantly different between groups (WT=70.3 ± 10.7%, KO=99 ± 1%, $p<0.05$), demonstrating that only WT mice displayed significant conditioning-induced mobility reduction. The freezing analysis during ITI1 (Fig. 9B d, Phase 6) yielded results similar to those of the mobility analysis. The percentage freezing during ITI1 differed significantly between groups (ITI1: WT=51.5 ± 7.4%, KO=6.2 ± 1.2%, $p<0.05$), with only WT mice displaying increased freezing during ITI1. These results revealed a complete lack of a single CS+US pairing-induced fear response in GluR-A KO mice, pointing to an important role of GluR-A containing AMPA receptors during the acquisition phase of fear conditioning.

2.2.1.1.3 CS extinction phase

Fear memory - the retention of fear responses upon CS presentation - was tested 24 hrs after conditioning. This session is termed the CS extinction test. Mice were placed in an altered context (Context B, see Methods) and presented with the tone (CS) alone after an initial 1 min acclimatization period, during which baseline activity was assessed. The tone lasted for another min and recording ended thirty seconds after the tone. The activity pattern during CS extinction testing is depicted in Fig. 9C a. The activity of both groups prior to tone onset tone onset (Fig. 9C b, Phases 1+2) did not change significantly (first 20 sec: WT=95.8 ± 3.3%, last 20 sec: WT=85.8 ± 9.3%, $p>0.05$; first 20 sec: KO=98 ± 2%, last 20 sec: KO=95 ± 3.2%, $p>0.05$) nor was there a difference of mobility between groups (first 20 sec: KO vs control, $p>0.05$; last 20 sec: KO vs control, $p>0.05$). This demonstrated similar baseline activity before tone presentation. Following tone onset, mobility decreased significantly in WT mice (Fig. 9C b, Phases 3+4; before tone onset: WT=89.2 ± 5.4%; after tone onset: WT=65 ± 7%, $p<0.05$), indicating that WT mice had formed a memory of the CS. The GluR-A KO mice did not display significant mobility reduction upon tone presentation (before tone onset: KO=94.3 ± 2.4%; after tone onset: KO=79.3 ± 9.1%, $p>0.05$). However, when comparing the two groups, perhaps due to high error bars, mobility of GluR-A KO mice was not statistically significantly different to WT mice (before tone onset: KO= vs control, $p>0.05$; after tone onset: KO vs control, $p>0.05$). This means that, although GluR-A KO mice did not exhibit significant mobility reduction during tone presentation, the fact that their mobility was comparable to WT mice indicated successful memory retrieval in both groups. Complementary results to the mobility analyses were obtained when freezing responses were analyzed before and after the tone onset (Fig. 9C c, Phases 3+4). Freezing increased significantly for WT mice after tone onset (before tone: WT=20.6 ± 9%; with tone: WT=54.2 ± 10%, $p<0.05$), whereas freezing in GluR-A KO mice did not increase significantly (before tone: KO=15.3 ± 4.6%; with tone: KO=36.6 ± 11.9%, $p>0.05$). However, there were no significant differences between groups (before tone: KO vs control, $p>0.05$; with tone: KO vs control, $p>0.05$), as was seen in the mobility analysis. Despite these complications,

the results show a trend that GluR-A KO mice exhibited less freezing than WT mice.

The results obtained with the one-trial fear conditioning paradigm showed a clear impairment of GluR-A KO mice in acquiring fear responses during conditioning. Furthermore, in the memory test session, GluR-A KO mice displayed less mobility reduction and less freezing levels upon tone presentation than WT mice, indicating weaker memory of the tone-shock experience. This phenotype might be explained if the experience during induction of fear conditioning by the one-trial pairing paradigm was too subtle to induce a strong fear memory in GluR-A KO mice.

2.2.1.2 Multi-trial fear conditioning paradigm

Within the one-trial fear conditioning paradigm, GluR-A KO mice showed weaker fear memory than WT mice. To test whether increasing numbers of tone-shock pairings have an impact on the phenotype observed during the acquisition of fear memories, groups of 21 GluR-A KO mice and 12 WT mice were tested in the multi-trial fear conditioning paradigm.

2.2.1.2.1 Habituation phase

A habituation session was performed one day before conditioning. As can be seen in the activity traces (Fig. 10A a), there was a difference between genotypes at the end of this session. The statistical comparison of the average mobility during the first min to the average mobility during the last min in the habituation phase (Fig. 10A b, Phases 1+2) revealed that WT decreased (first 60 sec: WT=98.5 ± 0.6%; last 60 sec: WT=95.1 ± 1.4%, $p<0.05$) and GluR-A KO mice increased their mobility significantly (first 60 sec: KO=97.6 ± 0.8%; last 60 sec: KO=98.8 ± 0.5%, $p<0.05$). Activity between groups was therefore significantly different at the end of this phase (first 60 sec: KO vs control, $p>0.05$; last 60 sec: KO vs control, $p<0.05$). Thus, GluR-A KO mice had not habituated to the chamber, whereas WT mice had.

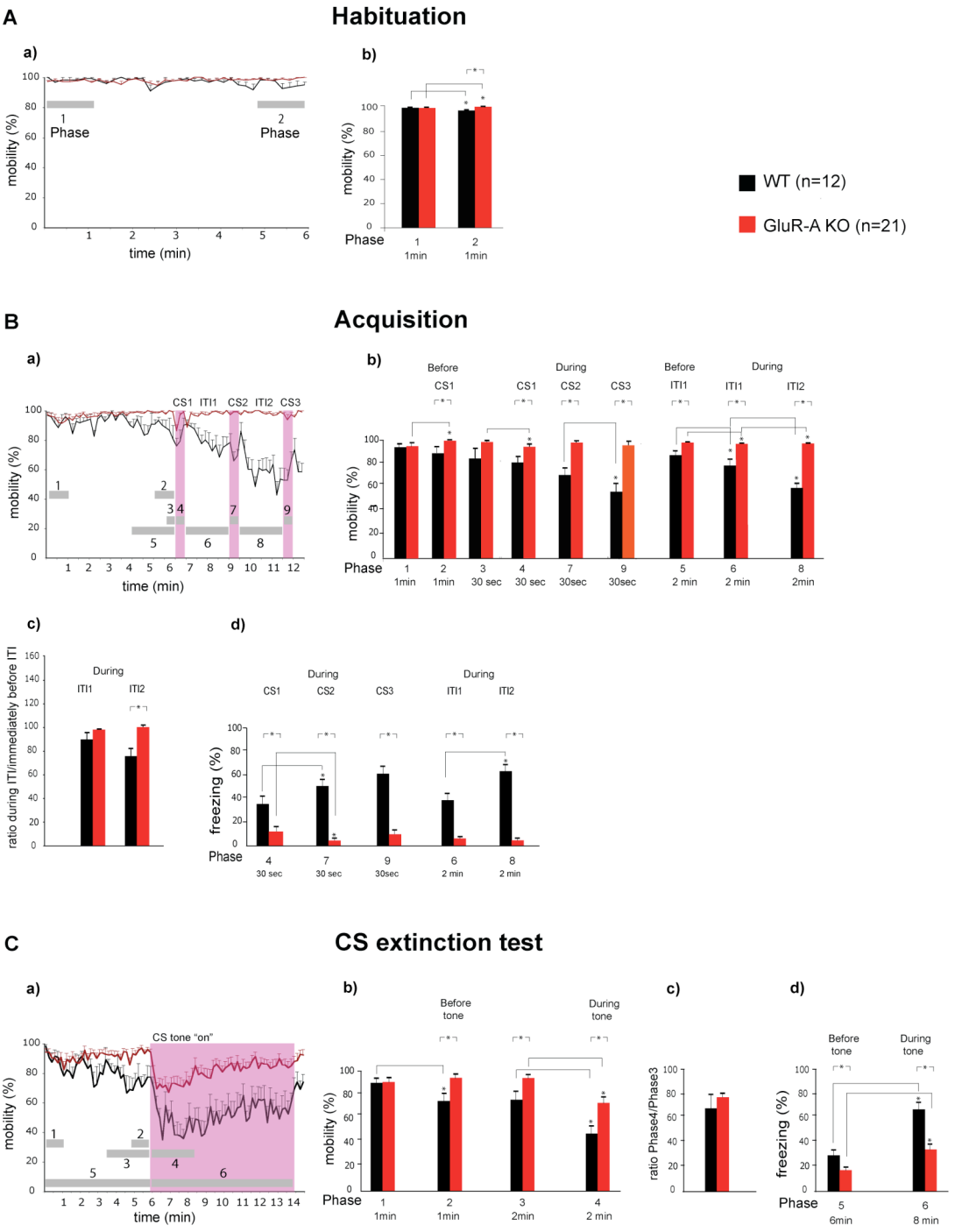

Fig. 10: Summary of the behavioral analysis in the multi-trial fear conditioning paradigm (Cohort 2). GluR-A KO mice showed a strong impairment during acquisition of fear conditioning even after three tone-shock pairings but displayed successful memory retrieval like WT mice when tested 24 hrs after conditioning.
A: a) Mobility pattern for the habituation session and b) statistical comparison of first min versus last min during the habituation phase. B: a) Activity traces for the acquisition session, b) statistical analysis of mobility before, during (CS) and after (ITI) conditioning, c) statistical analysis of normalized mobility during ITI (ratio during ITI/immediately before) and d) statistical analysis of freezing levels during (CS) and after (ITI) conditioning. C: a) Mobility graph for the memory test session, b) statistical analysis of mobility before and during tone presentation, c) statistical analysis of normalized mobility (ratio Phase 4/Phase 3) and d) statisical comparison of freezing responses before and during tone presentation. WT mice (n=12) are shown in black. GluR-A KO mice (n=21) are shown in red. Mean ± SEM. Grey bars in the mobility graphs delineates different Phases.

2.2.1.2.2 Acquisition phase

One day after habituation the conditioning session was performed. The mice were placed in the conditioning chamber (Context A) and received an acclimatization period of 6 min followed by three tone-shock pairings (CS1-CS3). The tone was present for 30 sec, and termination coincided with a 2 sec, 0.4mA foot shock. Pairings were separated (ITI) by 2 min. The recording ended thirty seconds after the last tone-shock pairing (CS3). Observed activity patterns during acquisition were similar to the ones reported during single tone-shock pairing (Fig. 10B a). WT mice decreased mobility gradually after each CS+US pairing, reflecting successful conditioning as well as the ability of these mice to acquire a fearful experience and to react in a species typical manner. In contrast, GluR-A KO failed to show any conditioning-induced mobility reduction, even after three tone-shock pairings.

Baseline analysis: Average mobility before conditioning (Fig. 10B b, Phases 1+2) differed significantly between groups (first 60 sec: WT=93.5 ± 1.5%, KO=94.2 ± 2.1% $p>0.05$; last 60 sec: WT=88.3 ± 4.2%, KO=98.9 ± 0.3%, $p<0.05$). WT mice did not significantly change mobility (WT: first 60 sec vs last 60 sec, $p>0.05$), whereas GluR-A KO mice had significantly increased their mobility before conditioning (KO: first 60 sec vs last 60 sec, $p<0.05$), similar to the reported mobility pattern in the habituation phase of training.

CS analyses: Mean mobility during CS1 to CS3 (Fig. 10B b, Phases 3, 4, 7, 9) differed significantly between groups (before CS1: WT=85.3 ± 6.9%, KO=98.9 ± 0.4%, $p>0.05$; CS1: WT=81.7 ± 5%, KO=94.1 ± 1.9%, $p<0.05$; CS2: WT=71.1 ± 4.8%, KO=98.4 ± 0.7%, $p<0.05$; CS3: WT=56.9 ± 6.4%, KO=96.2 ± 2%, $p<0.05$). Within group, WT mice decreased mobility significantly during CS3 (WT: before CS1 vs CS1, $p>0.05$; CS1 vs CS2, $p>0.05$; CS2 vs CS3, $p<0.05$), whereas GluR-A KO mice did not show such mobility reduction. Even though GluR-A KO mice reduced their mobility significantly during CS1 (due to the low SEM values), the mean values of activity remained at high levels throughout CS1 to CS3 (before CS1: KO=98.9 ± 0.4%, CS1: KO=94.1 ± 1.9%, $p<0.05$; CS1 vs CS2: KO=98.4 ± 0.7%, $p>0.05$; CS2 vs CS3: KO=96.2 ± 2%, $p>0.05$), revealing that these mice did not decrease activity due to conditioning. The freezing analysis during CS+US pairings (Fig. 10B d,

Phases 4, 7, 9) resulted in a similar outcome. There were significant differences in freezing responses between groups during CS1 to CS3 (CS1: WT=31.1 ± 6%, KO= 12.5 ± 3.4%, $p<0.05$; CS2: WT=51.4 ± 5.3%, KO=4.9 ± 1.2%, $p<0.05$; CS3: WT=64.7 ± 4.4%, KO=10.3 ± 3.5%, $p<0.05$). Within group, WT mice showed a significant increase in freezing responses during CS2 (CS1 vs CS2, $p<0.05$; CS2 vs CS3, $p>0.05$), whereas GluR-A KO mice showed low levels of freezing responses throughout the CS+US presentations. In fact, they exhibited a significant decrease in freezing during CS2 (KO: CS1 vs CS2, $p<0.05$; CS2 vs CS3, $p>0.05$).

ITI analyses: The comparison of average mobility before and during ITIs (Fig. 10B b, Phases 5, 6, 8) revealed significant differences between groups (before ITI1: WT=88.3 ± 3.7%, KO=98.9 ± 0.3%, $p<0.05$; ITI1: WT= 79.5 ± 4.4%, KO=97.3 ± 0.6%, $p<0.05$; ITI2: WT=60.3 ± 4.6%, KO=98.5 ± 0.3%, $p<0.05$). Since mobility before conditioning (see also baseline analysis; Fig. 10B b, Phases 1+2) differed significantly between groups, normalization was required. Normalization was with respect to mobility of two min before conditioning (ratio: during ITI/immediately before ITI). After normalization (Fig. 10B c), there was a significant difference between groups during ITI2 (ITI1: WT=90.8 ± 4.5%, KO=98.4 ± 0.7%, $p>0.05$; ITI2: WT=76.6 ± 4.9%, KO=101.3 ± 0.6%, $p<0.05$), which specified that only WT mice displayed significant conditioning-induced mobility reduction. The freezing analysis during ITIs (Fig. 10B d, Phases 6+8) yielded results similar to the mobility analysis. Freezing increased significantly for WT mice during ITI2 (ITI1: WT=39.4 ± 5.3%, ITI2: WT=64.7 ± 4.4%, $p<0.05$), while GluR-A KO mice did not show any increased freezing responses during ITIs (ITI1: KO=6.3 ± 1%, ITI2: KO=5 ± 1%, $p>0.05$). Freezing responses differed therefore significantly between groups during all ITIs (ITI1: KO vs control, $p<0.05$; ITI2: KO vs control, $p<0.05$). Across all ITIs, GluR-A KO mice did not display increased freezing responses, suggesting that, independent of the number of tone-shock pairings, they failed to acquire the conditioning task.

2.2.1.2.3 CS extinction phase

Fear memory was tested 24 hours after conditioning. The mice were placed in a changed context (Context B), and the tone was presented alone after an initial 6 min acclimatization period during which baseline activity was assessed. The tone lasted for 8 min. Recordings ended thirty seconds after the tone ended. The activity traces for this session are depicted in Fig. 10C a. Baseline activity before tone onset (Fig. 10C b) differed significantly between groups (Phase 2; last 60 sec: WT=75.1 ± 5%; KO=94.8 ± 2%, $p<0.05$), since WT mice decreased their mobility significantly during the pre-tone phase (Phases 1+2; first 60 sec: WT=90.4 ± 2.4%; last 60 sec: WT=75.1 ± 5%, $p<0.05$), while GluR-A KO mice showed no significant change in mobility (first 60 sec: KO=91.2 ± 2.6%; last 60 sec: KO=94.8 ± 2%, $p>0.05$). This indicated that WT mice had habituated to the environment prior to the CS presentation, similar to the reported mobility pattern in the habituation phase of training. Upon tone presentation, mobility decreased significantly for both groups (Fig. 10C b, Phases 3+4; before tone onset: WT=74.7 ± 5.6%; after tone onset: WT=46.8 ± 4.5%, $p<0.05$; before tone onset: KO=93.3 ± 1.6%; after tone onset: KO=72.5 ± 3%, $p<0.05$). However, there were significant differences between groups before tone onset (before tone onset: KO vs control, $p<0.05$) and thus, normalization was required. Following normalization (ratio: Phase 4/Phase 3; Fig.10C c), there was no significant difference between groups (WT=68.4 ± 11.8, KO=77.7 ± 2.8, $p>0.05$) but the mobility reduction in GluR-A KO mice was smaller than in WT mice. The freezing analysis before and after tone onset (Fig. 10C d; Phases 5+6) revealed similar results as the mobility analysis. Freezing responses increased significantly for both groups (before tone: WT=30.2 ± 4.2%; with tone: WT=69.3 ± 4.1%, $p<0.05$; before tone: KO=18 ± 2.6%; with tone: KO=34.7 ± 3.6%, $p<0.05$). However, also freezing differed significantly between groups before tone onset (before tone: KO vs control, $p<0.05$). The average freezing responses of 6 min before tone (Phase 5) were therefore subtracted from the average freezing responses of 8 min after tone onset (Phase 6), to reveal an increase in freezing levels only during CS presentation. This revealed 39.1% increased freezing levels for WT and 16.7% increased freezing levels for GluR-A KO mice. This demonstrated

again that during memory testing GluR-A KO mice showed less freezing behavior than WT mice.

The results obtained with the multi-trial fear conditioning paradigm revealed a clear impairment of GluR-A KO mice in acquiring fear responses during conditioning, as was already observed when mice were trained with a single CS-US pairing protocol. Furthermore, GluR-A KO mice froze upon tone presentation less than WT mice. The learning deficit observed in GluR-A KO mice was not due to the number of tone-shock pairings used to induce the fear memory.

2.2.1.3 The multi-trial fear conditioning paradigm without prior habituation

So far the mice received a habituation session prior to conditioning to familiarize them to the new environment where conditioning afterwards will take place and to assess basic locomotor activity. However, habituating the mice to the new environment for too long before conditioning might cause the mice to freeze less during conditioning (Perez-Villalba et al., 2005; Perez-Villalba et al., 2007). To test this hypothesis, a fear conditioning experiment was performed without prior habituation session. Cohorts of six GluR-A KO and six WT mice were selected to perform the multi-trial paradigm without habituation to the conditioning chamber before the acquisition session.

2.2.1.3.1 Acquisition phase

As can be seen from the activity graph (Fig. 11A a), WT mice reduced mobility following the tone-shock pairings, whereas GluR-A KO mice showed high mobility before as well as after conditioning.

Baseline analysis: Baseline activity was similar between groups, since there were no significant differences within group as well as between groups prior CS+US presentations (not shown).

CS analyses: Comparison of mobility during CS+US presentations (Fig. 11A b, Phases 1, 2, 5, 7) revealed significant differences between groups during CS2 and CS3 (before CS1: WT=99.4 ± 0.6%, KO=99.4 ± 0.6%, $p>0.05$; CS1: WT=94.4 ± 2%, KO=98.3 ± 1.1%, $p>0.05$; CS2: WT=80.6 ± 5.7%, KO=97.2 ±

1.3%, p<0.05; CS3: WT=62.2 ± 9.9%, KO=99.4 ± 0.6%, p<0.05), demonstrating that only WT mice but not GluR-A KO mice decreased mobility significantly after CS presentation. Within group, GluR-A KO mice did not show any significant mobility reduction during CS+US pairings (before CS1 vs CS1, p>0.05; CS1 vs CS2, p>0.05; CS2 vs CS3, p>0.05), whereas WT mice showed significantly decreased mobility during CS3 (before CS1 vs CS1, p>0.05; CS1 vs CS2, p>0.05; CS2 vs CS3, p<0.05). The freezing analysis during CS1 to CS3 (Fig. 11A c, Phases 2, 5, 7) yielded similar results. There were significant differences between groups across all CS+US presentations (CS1: WT=18.9 ± 3.3%, KO= 6.1 ± 2.4%, p<0.05; CS2: WT=41.1 ± 6.4%, KO=8.3 ± 3.3%, p<0.05; CS3: WT=61.1 ± 10.3%, KO=3.8 ± 1.3%, p<0.05), demonstrating that GluR-A KO mice exhibited no conditioning-induced freezing responses. Freezing increased significantly for WT mice during CS2 and CS3 (CS1 vs CS2, p<0.05; CS2 vs CS3, p<0.05), whereas GluR-A KO mice did not show any significantly increased freezing responses (CS1 vs CS2, p>0.05; CS2 vs CS3, p>0.05).

ITI analyses: Comparison of mobility during ITIs (Fig. 11A b, Phases 3, 4, 6, 8) revealed significant differences between groups during ITI2 and ITI3 (before ITI1: WT=97.5 ± 1%, KO=99.3 ± 0.4%, p>0.05; ITI1: WT= 89.6 ± 4.1%, KO=96.9 ± 1%, p>0.05; ITI2: WT=78.6 ± 7.1%, KO=99.6 ± 0.2%, p<0.05; ITI3: WT=79.6 ± 5.6%, KO=99 ± 0.5%, p<0.05), demonstrating that GluR-A KO mice did not reduce mobility during conditioning. Within both groups mobility did not decrease significantly after each ITI compared to the preceding pre-CS duration (WT: before ITI1 vs ITI1, p>0.05; ITI1 vs ITI2, p>0.05; ITI2 vs ITI3, p>0.05; KO: before ITI1 vs ITI1, p>0.05; ITI1 vs ITI2, p>0.05; ITI2 vs ITI3, p>0.05). But compared to WT mice, the average mobility values of GluR-A KO mice remained at high levels throughout the preceding CS duration. In contrast to the mobility analysis, freezing levels (Fig. 11A c, Phases 4, 6, 8) showed a significant increase during ITI2 for WT mice (ITI1: WT=22.4 ± 6.5%, ITI2: WT=41.8 ± 10%, p>0.05; ITI3: WT=43.5 ± 7.7%; p<0.05 vs ITI2). GluR-A KO mice did not display any increased freezing responses throughout the ITIs (ITI1: KO=5.3 ± 0.9%, ITI2: KO=2.7 ± 1%, p>0.05; ITI3: KO=3.6 ± 0.9%; p>0.05 vs ITI2) and freezing between groups

differed significantly throughout the intervals between CS+US pairings (ITI1: KO vs control, $p<0.05$; ITI2: KO vs control, $p<0.05$; ITI3: KO vs control, $p<0.05$), demonstrating yet again the complete absence of conditioning-induced fear responses in GluR-A KO mice during the acquisition phase of fear conditioning.

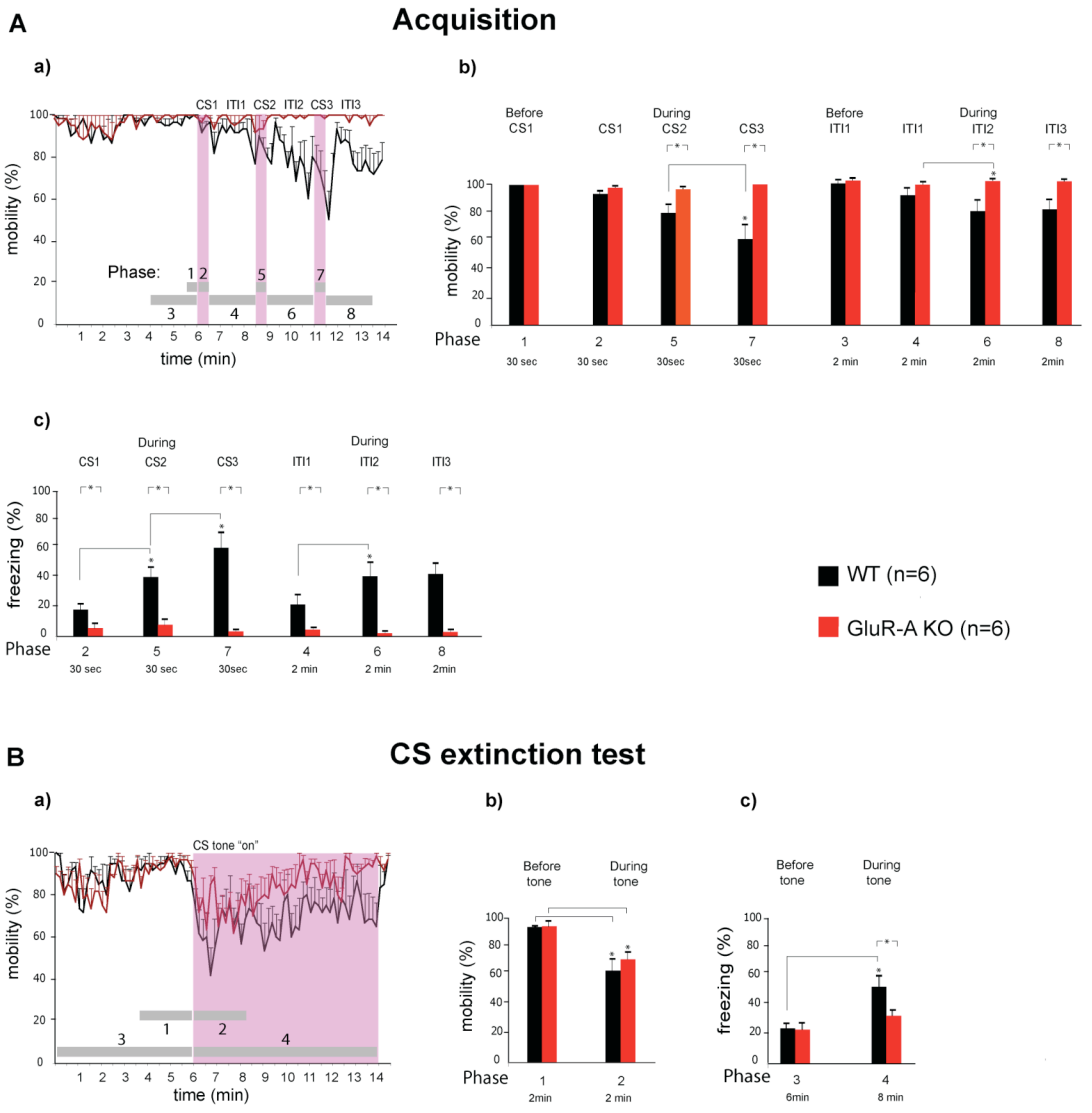

Fig. 11: Summary of the behavioral analysis in the multi-trial fear conditioning paradigm without prior habituation (Cohort 3). GluR-A KO mice showed a strong impairment during acquisition of fear conditioning and displayed no freezing responses upon CS presentation when tested 24 hrs after conditioning.
A: a) Activity traces for the acquisition session, b) statistical analysis of mobility before, during (CS) and after (ITI) conditioning and c) statistical analysis of freezing levels during (CS) and after (ITI) conditioning. B: a) Mobility graph for the memory test session, b) statistical analysis of mobility before and during tone presentation and c) statisical comparison of freezing responses before and during tone presentation. WT mice (n=6) are shown in black. GluR-A KO mice (n=6) are shown in red. Mean ± SEM. Grey bars in the mobility graphs delineates different Phases.

2.2.1.3.2 CS extinction phase

Mice were tested 24 hours after conditioning whether they were able to show successful memory retrieval of the CS. The mobility graph for this test session is depicted in Fig. 11B a. There were no significant differences between groups before tone onset (not shown). Mean mobility within both groups (Fig. 11B b, Phases 1+2) was significantly reduced upon tone presentation (before tone onset: WT=93.1 ± 1%, after tone onset: WT=64 ± 6.8%, $p<0.05$; before tone onset: KO=94.6 ± 1.7%, after tone onset: KO=73.9 ± 3.3%, $p<0.05$) and there were no significant differences between groups (before tone onset: KO vs control, $p>0.05$; after tone onset: KO vs control, $p>0.05$). This illustrated that both groups showed memory retention of the CS. However, when freezing responses before and after tone onset (Fig. 11B c, Phases 3+4) were analyzed, different results were obtained compared to the mobility analysis. There was no significantly increased freezing observed in GluR-A KO mice (before tone: KO=23.6 ± 3.6%, with tone: KO=32.6 ± 3%, $p>0.05$), whereas WT mice showed significantly increased freezing responses upon tone presentation (before tone: WT=23.9 ± 2.8%, with tone: WT=52.7 ± 7.2%, $p<0.05$). Furthermore, there was a significant difference in freezing levels between groups after tone onset (with tone: WT=52.7 ± 7.2%; with tone: KO=32.6 ± 3%, $p<0.05$) with no differences in baseline freezing before tone onset (before tone: KO vs control, $p>0.05$; with tone: KO vs control, $p<0.05$), demonstrating successful memory retrieval in WT but not in GluR-A KO mice.

Collectively, these results show that the habituation to the environment prior to fear conditioning had not changed the freezing behavior of both genotypes during the acquisition phase of fear conditioning. GluR-A KO mice completely lacked fear responses during acquisition independent from the number of CS-US pairings or the prior habituation to the context in which conditioning was performed. But, GluR-A KO mice showed no successful memory retrieval when tested 24 hrs after conditioning, which, however, became only apparent in the freezing analysis. This supports the conclusion that prior exposure to the fear conditioning context could alter the role of GluR-A containing AMPA receptors in the retrieval of fear memories.

2.2.1.4 The multi-trial fear conditioning paradigm without prior handling and habituation

Experimental protocols applied so far included a familiarization session during which mice were accustomed to the experimenter. This prior experience to the experimenter might also diminish the fear responses in these mice. Therefore a final set of experiments was performed to address this possible influence of pre-handling mice on the acquisition of fear memories. The group of mice tested did not receive any handling nor did they receive a habituation phase prior to the acquisition session. Cohorts of nine WT and nine GluR-A KO mice were included in this experiment.

2.2.1.4.1 Acquisition phase

The mobility graph for this phase is shown in Fig. 12A a. As in the previous paradigms, WT mice showed CS-induced reduction in mobility, and GluR-A KO mice remained at high mobility levels before as well as after conditioning. CS analyses: Comparison of mobility between groups (Fig. 12A b, Phases 1, 2, 5, 7) revealed significant differences before conditioning as well as during CSs presentations (before CS1: WT=94.4 ± 2.1%, before CS1: KO=100 ± 0%, $p<0.05$; CS1: WT=90.4 ± 3.3%, CS1: KO=98.9 ± 0.6%, $p<0.05$; CS2: WT=65.2 ± 6.6%; CS2: KO=99.6 ± 0.4%, $p<0.05$; CS3: WT=49.6 ± 5.3% CS3: KO=97.8 ± 1%; $p<0.05$) and therefore normalization of the mobility during CS with respect to mobility prior to the CS onset (ratio: during CS/immediately before CS) was applied. After normalization (Fig. 12A c), there were no significant differences between groups (CS1: WT=95.6 ± 2.6%, KO=98.9 ± 0.6%, $p>0.05$; CS2: WT= 86.5 ± 9.8%, KO=100 ± 0%, $p>0.05$; CS3: WT= 120.8 ± 16.7%, KO=97.8 ± 1%, $p>0.05$). WT mice showed in fact increased mobility during CS3, reflecting escape behavior likely due to the sensory (shock) experience. Therefore, the value for WT mice was increased after normalization, even though mean mobility decreased during each tone-shock pairing. The freezing analysis (Fig. 12A e, Phases 2, 5, 7) revealed results similar to the activity investigation. Freezing responses differed significantly between groups during CS+US pairings (CS1: WT=28.1 ± 5.7%, KO= 6.3 ± 3.3%, $p<0.05$; CS2: WT=60 ± 5%, KO=1 ± 0.5%, $p<0.05$; CS3: WT=67 ± 4%,

KO=5.9 ± 2.1%, p<0.05), consistently reproducing the results obtained in the previous sets of experiments. Within group, freezing increased significantly only for WT mice during CS2 and CS3 (CS1 vs CS2, p<0.05; CS2 vs CS3, p<0.05), whereas GluR-A KO mice showed no increased freezing throughout the training (CS1 vs CS2, p>0.05; CS2 vs CS3, p<0.05). Even though there was significant increased freezing observed during CS3, the mean values during CSs remained at low levels of freezing for GluR-A KO mice.

ITI analyses: Again, normalization was required because activity not only differed between groups during ITIs (Fig. 12A b, Phases 4, 6, 8; ITI1: WT= 76.8 ± 4.5%, ITI1: KO=99.3 ± 0.4%, p<0.05; ITI2: WT=59.7 ± 3.4%, ITI2: KO=99.6 ± 0.2%; p<0.05; ITI3: WT=42.3 ± 3.7%, ITI3: KO=99.7 ± 0.3%; p<0.05), but already before conditioning (Phase 3; before ITI1: WT=95.4 ± 1%, KO=99.7 ± 0.2%, p<0.05). After normalization (ratio: during ITI/immediately before ITI; Fig. 12A d), mobility was still significantly different between groups (ITI1: WT=80.3 ± 4.2%, KO=99.5 ± 0.5%, p<0.05; ITI2: WT=80.7 ± 7.8%, KO=100.4 ± 0.4%, p<0.05; ITI3: WT=71.9 ± 5.9%, KO=100.1 ± 0.3%, p<0.05), reflecting successful conditioning of WT mice and a lack of CS-induced mobility reduction in GluR-A KO mice. Analysis of freezing responses during ITIs (Fig. 12A e, Phases 4, 6, 8) showed results similar to those of the mobility analysis. GluR-A KO mice did not display any increased freezing responses during ITIs (ITI1: KO=1.9 ± 0.7%, ITI2: KO=1.9 ± 0.8%, p>0.05; ITI3: KO=1.2 ± 0.8%; p>0.05 vs ITI2). WT mice, however, showed a significant increase in freezing levels during ITI3 (ITI1: WT=43.1 ± 7.1%, ITI2: WT=64.4 ± 3.5%, p>0.05; ITI3: WT=79.4 ± 3.1%; p<0.05 vs ITI2), and comparison between groups revealed significant differences in freezing levels throughout the inter CS-US pairing intervals (ITI1: KO vs control, p<0.05; ITI2: KO vs control, p<0.05; ITI3: KO vs control, p<0.05).

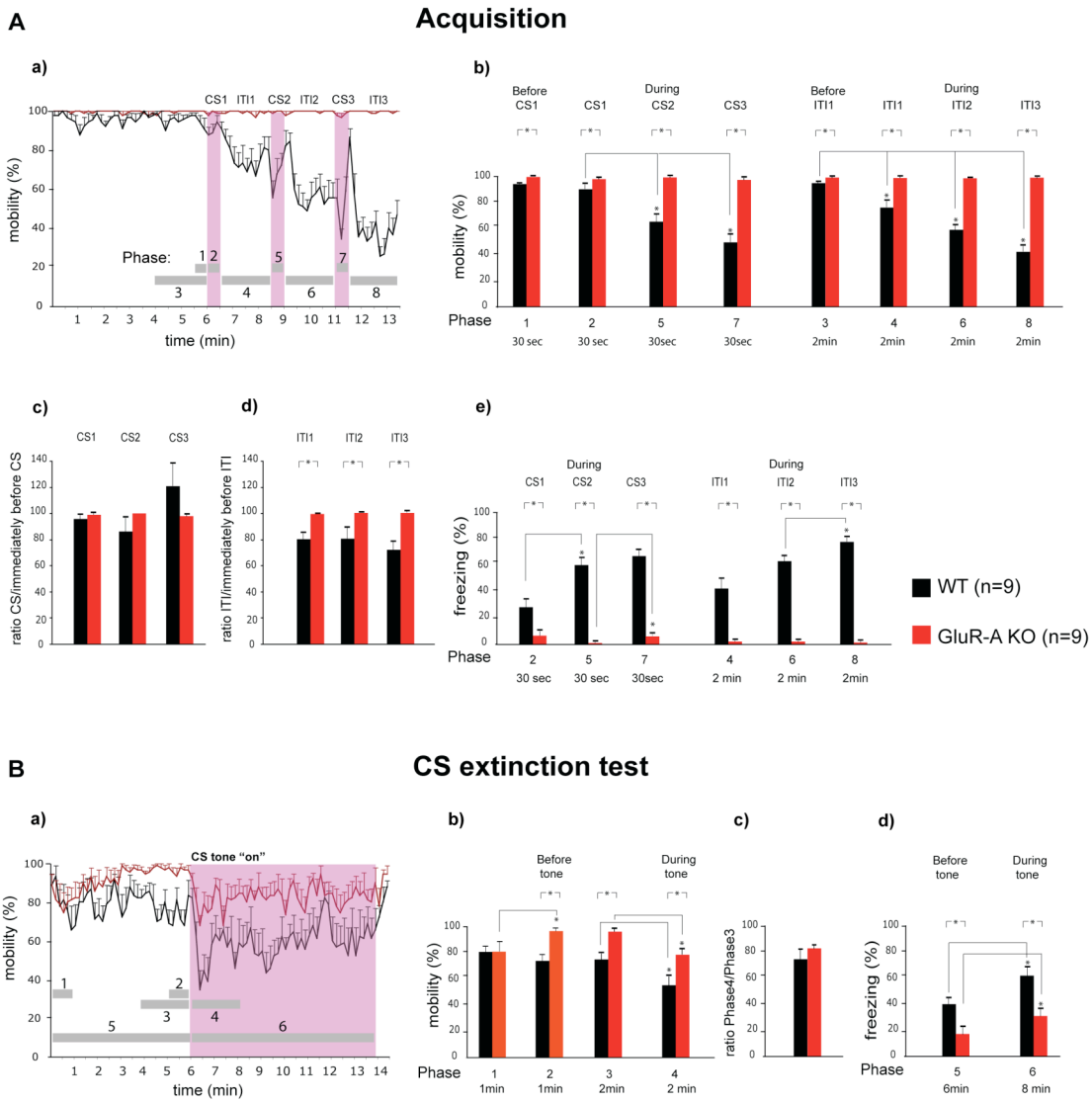

Fig. 12: Summary of the behavioral analysis in the multi-trial fear conditioning paradigm without prior handling and habituation (Cohort 4). GluR-A KO mice showed a strong impairment during acquisition of fear conditioning but displayed successful memory retrieval when tested 24 hrs after conditioning.
A: a) Activity traces for the acquisition session, b) statistical analysis of mobility before, during (CS) and after (ITI) conditioning, c) statistical analysis of normalized mobility during CS (during CS/immediately before CS), d) statistical analysis of normalized mobility during ITI (ratio during ITI/immediately before ITI) and e) statistical analysis of freezing levels during (CS) and after (ITI) conditioning. B: a) Mobility graph for the memory test session, b) statistical analysis of mobility before and during tone presentation, c) statistical analysis of normalized mobility (ratio Phase 4/Phase 3) and d) statisical comparison of freezing responses before and during tone presentation. WT mice (n=9) are shown in black. GluR-A KO mice (n=9) are shown in red. Mean ± SEM. Grey bars in the mobility graphs delineates different Phases.

2.2.1.4.2 CS extinction phase

The observed activity pattern for the memory test session is depicted in Fig. 12B a. Activity before tone onset differed significantly between groups (Fig. 12B b, Phases 1+2; first 60 sec: WT=80.4 ± 3.7%, KO=80.7 ± 7.1%, $p>0.05$; last 60 sec: WT=73.3 ± 4.9%, KO=96.3 ± 2%, $p<0.05$). In contrast to WT mice, GluR-A KO mice displayed significantly increased mobility at the end of

the pre-tone phase (KO: first 60 sec vs last 60, $p<0.05$; WT: first 60 sec vs last 60 sec, $p>0.05$). Following normalization (ratio: Phase 4/Phase 3; Fig. 12B c), there was no significant difference between groups (WT=74.3 ± 7.8%, KO= 82.6 ± 2.8%, $p>0.05$), but again, there was a clear trend that mobility reduction during tone was less in GluR-A KO mice than WT mice. The freezing analysis (Fig. 12B d, Phases 5+6) revealed significantly increased freezing responses upon tone presentation in both groups (before tone: WT=40.2 ± 3.7%, with tone: WT=62 ± 5.2%; $p<0.05$; before tone: KO=17.3 ± 4.9%; with tone: KO=31.1 ± 4.9%, $p<0.05$). However, freezing levels differed significantly between genotypes already before tone onset (before tone: WT=40.2 ± 3.7%, KO=17.3 ± 4.9%, $p<0.05$), and therefore, the average freezing level before tone (Phase 5) was subtracted from the average freezing level with tone (Phase 6). This again revealed that GluR-A KO mice (13.8%) exhibited a trend to freeze after tone presentation less than WT mice (21.8%).

This last experiment showed that without pre-handling the mice and without habituation to the context prior to the acquisition training similar, results to the experiments including handling and habituation could be reproduced. Only the group of mice (cohort 3) which did not receive a habituation session prior to conditioning showed a significant difference in freezing levels during memory testing, whereas in all other investigated groups there was always a trend for GluR-A KO mice to exhibit less freezing during tone presentation than WT mice. It would appear that the pre-handling and habituation experiences had negligible effects on the expression of fear responses in GluR-A KO mice.

Across the four studies described above, the age of the experimental mice varied considerably due to unavailability of enough littermates (see Table 1). To elucidate an age-effect on the acquisition and CS extinction phase during fear conditioning, an analysis of GluR-A KO mice at different ages was performed. Young GluR-A KO mice (2.5 months, n=11) were statistically compared to old GluR-A KO mice (10-12 months, n=10) to see whether the same genotype would reveal at different ages differences in acquisition and retrieval of fear memories. This analysis revealed an absence of age-effects during conditioning and memory testing, as no significant

difference was obtained between groups in any phases of the training (data not shown). This outcome suggested that the results described so far are not confounded by the age of the subjects.

It became clear after analyzing all four experimental groups that GluR-A KO mice were able to respond to the tone presentation 24 hrs after conditioning. This indicates that despite lack of freezing responses to the CS-US pairing during conditioning these mice might have formed a memory for the association between tone (CS) and shock (US).

2.2.2 LA-specific GluR-A KO mice

Due to absence of GluR-A containing AMPA receptors throughout the brain and hence due to impaired synaptic potentiation at multiple synaptic sites, the specific brain region responsible for mediating GluR-A dependent acquisition of fear conditioning cannot be elucidated by analyzing a complete (whole brain) KO line. Therefore we aimed at generating a LA-specific GluR-A gene deletion in the adult brain, since the LA is important for the acquisition and storage of fear memories (LeDoux et al., 1990). The LA specific GluR-A KO mice should now address the importance of GluR-A dependent synaptic potentiation within the distinct site of the LA for the learning of fear responses and its role in the behavioral phenotype seen here in the GluR-A KO mice.

2.2.2.1 IHC analysis of Cre expression pattern in the LA after rAAV-Cre injection

As mentioned before, injection of rAAV-Cre vector particles into the LA of "floxed" (*GluR-A*$^{2lox/2lox}$) mice was employed in attempts to generate LA-specific GluR-A KO mice. Table 2 summarizes the animal groups studied, the age of the mice at the time of surgery, the amounts of virus applied, the recovery time (viral expression time) after surgery and the number of animals with both LA targeted. Only such animals were included in the behavioral evaluation.

Animal groups	Age at time of surgery	Virus volume per injection site and amount of injections per hemisphere	Viral expression time before behavioral analysis	Number of mice with both LA targeted
Group 1 A: Injected with rAAV-Cre B: Not injected	A: 4.5 weeks	<80nl; 1 injection site	9 weeks	A: 6 out of 8 B: 10
Group 2 A: Injected with rAAV-Cre B: Not injected	A: 5.5 weeks	160nl; 2 injection sites	5 weeks	A: 6 out of 8 B: 4
Group 3 A: Injected with rAAV-Cre B: Not injected	A: 6.5 weeks	80nl; 3 injection sites	7 weeks	A: 7 out of 8 B: 8
Group 4 A: Injected with rAAV-Cre B: Injected with rAAV-GFP	A: 4 weeks	320nl; 2 injection sites	4 weeks	A: 2 out of 8 B: 4

Table 2: Summary of the experimental settings.

Subsequent to behavioral analysis, the mice were sacrificed to analyze the specificity and efficiency of Cre expression. This was performed by IHC for Cre recombinase protein. The percentage neurons expressing Cre recombinase within each LA, was assessed by counterstaining against the neuronal marker NeuN. The percentage of colocalization of Cre and NeuN, which reflects the percentage of neurons potentially lacking the GluR-A subunit, within a given area of the infected LA was calculated. The respective positively-infected areas differed between animals. Some areas were higher infected showing in average 67% Cre-positive neurons (Fig. 13A). Other areas were more weakly infected and assessed to be on average 54% positive for Cre expressing neurons (not shown). From these analyses, a value of 50% was taken to be a reasonable estimate of the percentage of Cre-positive neurons within infected regions of the LA displaying Cre expression (i.e. “conversion factor” of 0.5).

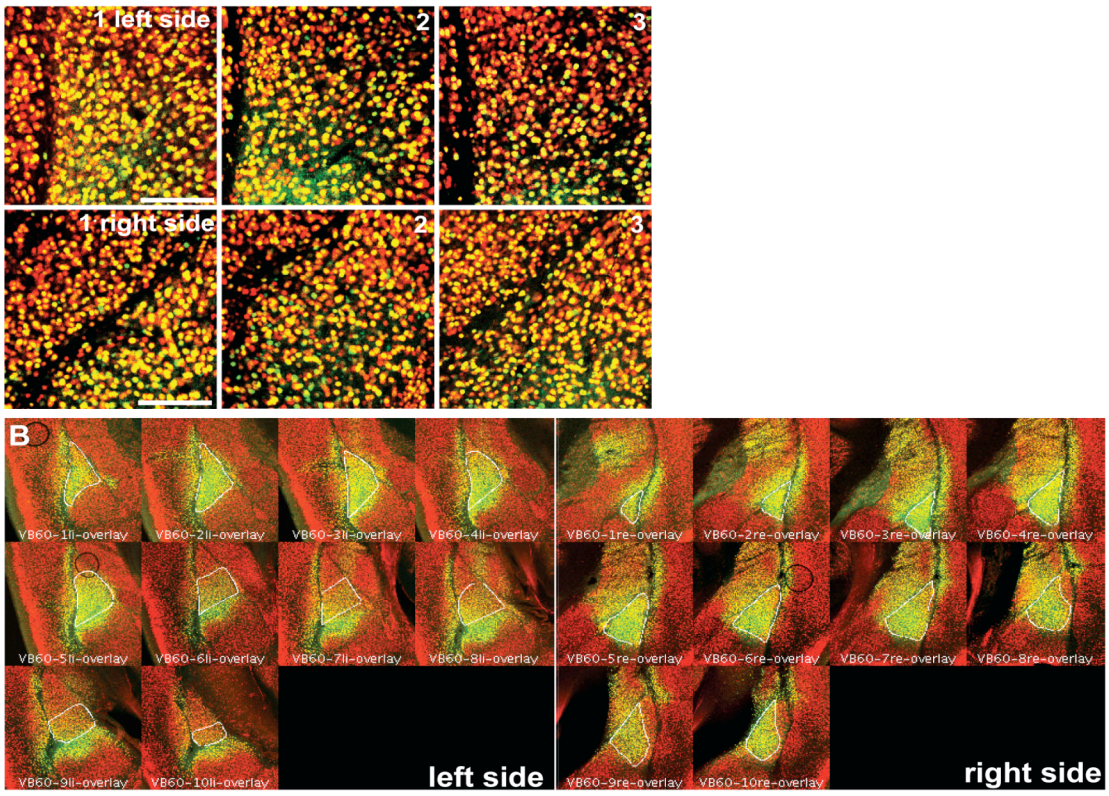

Fig. 13: Example of Cre/NeuN overlay and quantification of relative Cre expressing area in the right and left LA from one animal. In 10-30% of LA neurons Cre recombinase was expressed.
A: Overlay of Cre/NeuN from three consecutive slices (100µm spacing). Cre labeling is shown in green, NeuN labeling is shown in red and colocalization is shown in yellow. Average counting results right side=68% ± 2.19 (SEM) and left side=65% ± 0.33 (SEM). Scalebar: 100µm.
B: Cre expression area compared to the total LA area was 52.5% on the right side and 55.8% on the left side. (ImageJ "area value" (VB60 right): 167568.000; ImageJ "area value" (VB60 left): 178040.000). The Cre-positive areas within the LA (dimensions were visually judged in accordance with the mouse brain atlas) are outlined in white. These Cre-positive areas were compared to a single average LA dimension (ImageJ "area value" total LA (mean of right and left): 318862.5 = 100%) assessed previously (see Methods).

In order to calculate the total percentage Cre positive neurons within the entire LA, the spatial area of the LA showing Cre expression was measured (ImageJ) for some rAAV-Cre injected mice (n=6). By measuring the spatial area of Cre expression in the sections, the percentage of the spatial area of Cre infection within each LA was calculated for these mice. This value is then multiplied with the "conversion factor" to reveal the total fraction of neurons within the LA showing Cre expression. An example of the area quantification in one of the rAAV-Cre injected mice (VB60) is depicted in Fig. 13B and Table 3 shows the results of six mice analyzed in this fashion. Four of the six animals exhibited 10-30% Cre expression in neurons within both (left and right) LA´s.

Mouse number	Area of Cre expression (left)	Neurons expressing Cre (left)	Area of Cre expression (right)	Neurons expressing Cre (right)
VB56	65%	32.5%	52%	26%
VB60	55.8%	27.9%	52.5%	26.25%
VB68	31%	15.5%	27%	13.5%
VB69	35.7%	17.85%	10%	5%
VB70	20.7%	10.35%	12%	6%
VB71	42%	21%	42%	21%

Table 3: Percentage Cre expression in LA neurons evaluated in six rAAV-Cre injected mice. The mice marked in red showed >10% of LA-neurons expressing Cre recombinase.

To qualitatively prove the loss of GluR-A, an IHC analysis was performed on coronal brain sections from rAAV-Cre injected mice. As Cre and GluR-A antibodies commonly used in our laboratory are both produced in rabbit it was not possible to use them simultaneously on the same slice. Thus one slice was stained against the GluR-A subunit and the preceding slice was stained against Cre/NeuN to reveal the area of Cre expression within the LA. Examples from a rAAV-Cre injected mouse are depicted in Fig. 14. It is apparent that there was a clear GluR-A signal loss within the area of Cre expression.

2.2.2.2 Fear conditioning experiments in rAAV-Cre injected mice

Fear conditioning experiments were performed at the earliest four weeks after surgery, which allowed not only for sufficient Cre expression to occur but should ensure appropriate time for the subsequent removal of GluR-A containing AMPA receptors from the soma and synapses. rAAV-Cre injected mice were first tested in the multi-trial fear conditioning paradigm. Only appropriately targeted mice, which showed Cre expression in both LA (right and left), were included in the data analyses presented below.

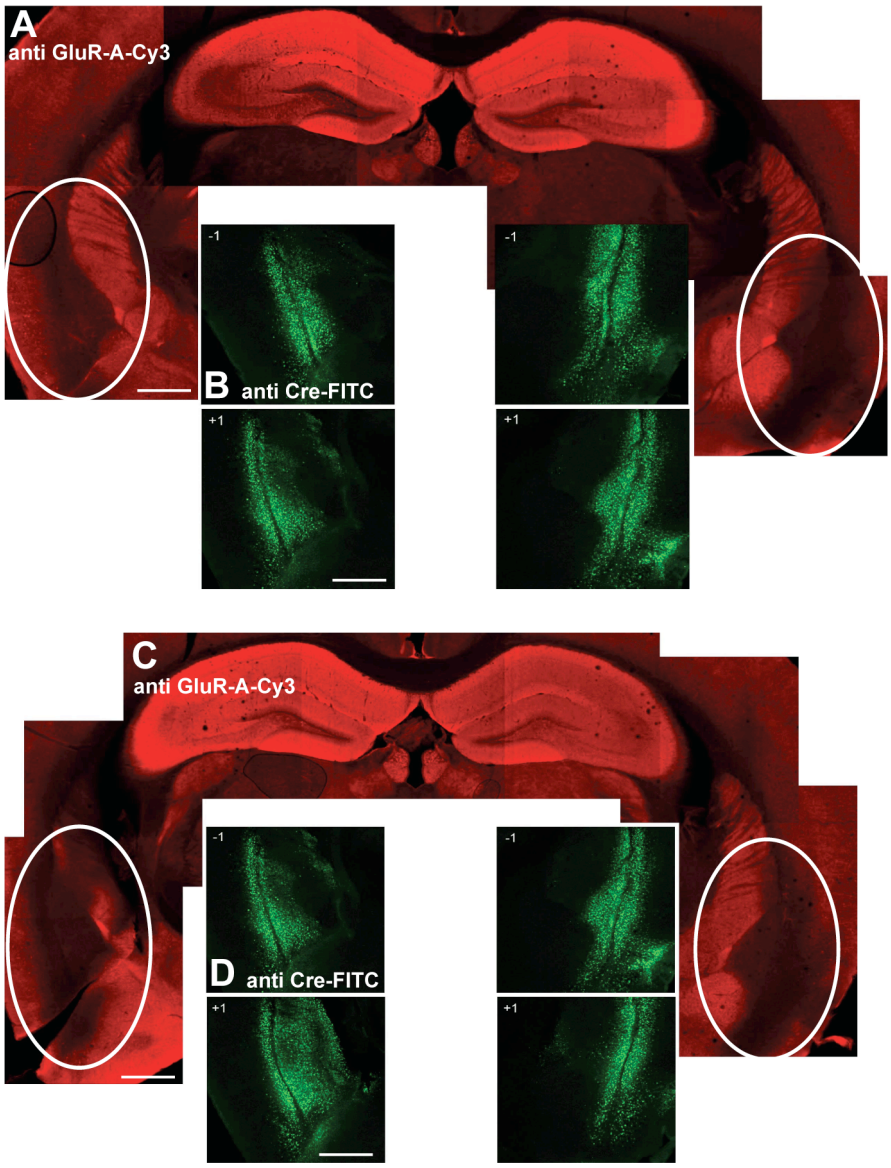

Fig. 14: IHC analysis from one rAAV-Cre injected mice. GluR-A signal loss was detectable in the area of Cre expression.
A, C: Confocal overview images taken from two coronal slices stained against GluR-A (shown in red). Area of GluRA signal loss is outlined in white and resembles the pattern of Cre expression seen in the preceding and following slice.
B, D: Confocal images of Cre expression (shown in green) in the right and left LA in the preceding and following slice to A, C . Scalebar: 1mm.

2.2.2.2.1 Multi-trial fear conditioning paradigm

A group of six *GluR-A*$^{2lox/2lox}$ mice injected with the Cre expressing viral construct (in the following termed LA-KO) was compared to four uninjected control (Ctrl) mice (see Table 2, group 2).

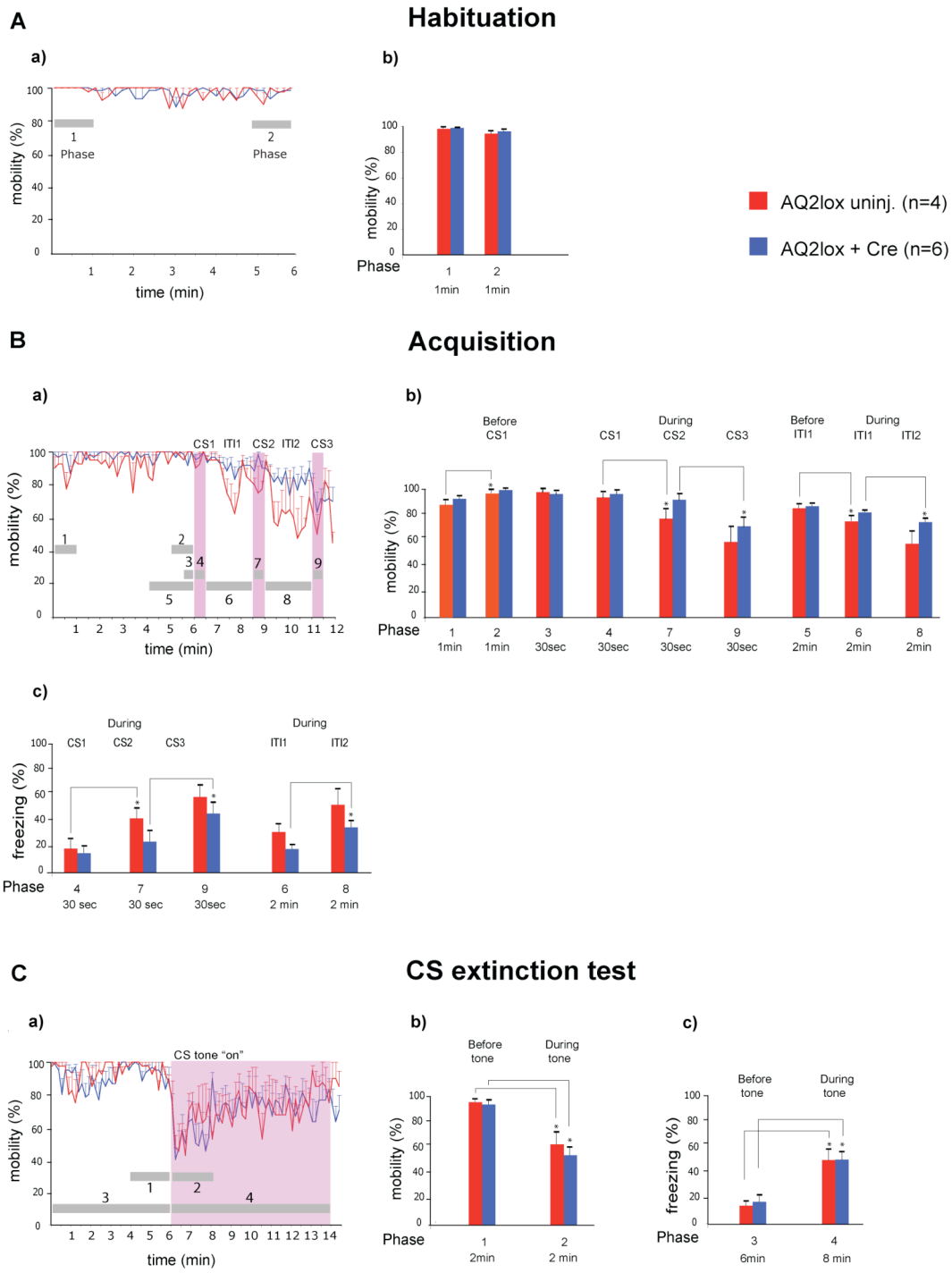

Fig. 15: Behavioral analysis of rAAV-Cre injected mice in the multi-trial fear conditioning experiment. rAAV-Cre injected mice and control mice were able to acquire fear responses during conditioning and showed successful memory retrieval when tested 24 hrs after conditioning.
A: a) Mobility pattern for the habituation session and b) statistical comparison of first min versus last min during the habituation phase. B: a) Activity traces for the acquisition session, b) statistical analysis of mobility before, during (CS) andafter (ITI) conditioning and c) statistical analysis of freezing levels during (CS) and after (ITI) conditioning. C: a) Mobility graph for the memory test session, b) statistical analysis of mobility before and during tone presentation c) and statisical comparison of freezing responses before and during tone presentation. rAAV-Cre injected mice (n=6) are shown in blue. Uninjected mice (n=4) are shown in red. Mean ± SEM. Grey bars in the mobility graphs delineates different Phases.

2.2.2.2.1.1 Habituation phase

The mobility graph for the habituation session is depicted in Fig. 15A a. A comparison of mobility during the first min with activity during the last min during habituation (Fig. 15A b, Phases 1+2) showed that mobility did not change significantly in both groups (first 60 sec: Ctrl=99.6 ± 0.4%, last 60 sec: Ctrl=96.7 ± 2 %, $p>0.05$; first 60 sec: LA-KO=100 ± 0%, last 60 sec: LA-KO=97.2 ± 1.1%, $p>0.05$) and was not significantly different between groups (first 60 sec: LA-KO vs Ctrl, $p>0.05$; last 60 sec: LA-KO vs Ctrl, $p>0.05$), demonstrating similar activity between groups in the habituation phase of training.

2.2.2.2.1.2 Acquisition phase

The mobility pattern during conditioning is shown in Fig. 15B a.

Baseline analysis: Baseline mobility before conditioning (Fig. 15B b, Phases 1+2) was similar between groups (first 60 sec: Ctrl=88.8 ± 3%, LA-KO=95.3 ± 2.6%, $p>0.05$, last 60 sec: Ctrl=98.3 ± 0.7%, LA-KO=97.8 ± 1.3%, $p>0.05$), although the uninjected mice significantly increased their mobility before conditioning (first 60 sec vs last 60 sec, $p<0.05$), whereas the LA specific GluR-A KO mice did not display significantly increased mobility (first 60 sec vs last 60 sec, $p>0.05$).

CS analyses: Mean mobility levels decreased significantly for the uninjected mice during CS2 (Fig. 15B b, Phases 3, 4, 7, 9; before CS1: Ctrl=98.3 ± 1.7%, CS1: Ctrl=94.2 ± 2.8%, $p>0.05$; CS2: Ctrl=77.5 ± 6.3%; $p<0.05$ vs CS1; CS3: Ctrl=59.2 ± 11.1%; $p>0.05$ vs CS3) and decreased significantly for the LA specific GluR-A KO mice during CS3 (before CS1: LA-KO=96.7 ± 1.3%, CS1: LA-KO=97.2 ± 1.6%, $p>0.05$; CS2: LA-KO=92.2 ± 3.7%; $p>0.05$ vs CS1; CS3: LA-KO=71.1 ± 6.2%; $p<0.05$ vs CS2). There were no significant differences between groups (before CS1: LA-KO vs Ctrl, $p>0.05$; CS1: LA-KO vs Ctrl, $p>0.05$; CS2: LA-KO vs Ctrl, $p>0.05$; CS3: LA-KO vs Ctrl, $p>0.05$), demonstrating that both groups similarly reduced mobility during acquisition of fear conditioning. Freezing, conversely, increased significantly during CS2 (Fig. 15B c, Phases 4, 7, 9) for the uninjected group (CS1: Ctrl=18.3 ± 6.9%, CS2: Ctrl=41.7 ± 6.9%, $p<0.05$; CS3: Ctrl=58.3 ± 8%; $p>0.05$ vs CS2) and

during CS3 for the LA specific GluR-A KO mice (CS1: LA-KO =15 ± 4.5%, CS2: LA-KO=23.9 ± 7.7%, $p>0.05$; CS3: LA-KO=45.6 ± 7.8%; $p<0.05$ vs CS2), similar to the change in the mobility across the CS-US pairings. There were no significant differences in freezing between groups (before CS1: LA-KO vs Ctrl, $p>0.05$; CS1: LA-KO vs Ctrl, $p>0.05$; CS2: LA-KO vs Ctrl, $p>0.05$; CS3: LA-KO vs Ctrl, $p>0.05$), demonstrating that both groups displayed increased freezing responses during CS.

ITI analyses: Comparison of the average mobility during ITIs (Fig. 15B b, Phases 5, 6, 8) revealed a significant decrease for the uninjected group during ITI1 (before ITI1: Ctrl=95.8 ± 2.3%, ITI1: Ctrl=84.2 ± 3.9%, $p<0.05$; ITI2: Ctrl=64.4 ± 10.5%; $p>0.05$ vs ITI1) and a significant reduction in activity for the LA specific GluR-A KO mice during ITI2 (before ITI1: LA-KO=97.6 ± 1.1%, ITI1: LA-KO=91.9 ± 1.4%, $p>0.05$; ITI2: LA-KO=83.5 ± 2.5%; $p<0.05$ vs ITI1). There were no significant differences between groups (before ITI1: LA-KO vs Ctrl, $p>0.05$; ITI1: LA-KO vs Ctrl, $p>0.05$; ITI2: LA-KO vs Ctrl, $p>0.05$). Freezing during ITIs (Fig. 15B c, Phases 6, 8), on the contrary, increased significantly only for the LA specific GluR-A KO mice during ITI2 (ITI1: LA-KO=18.6 ± 2.7%, ITI2: LA-KO=35.6 ± 4.5%, $p<0.05$; ITI1: Ctrl=31.9 ± 5.4%, ITI2: Ctrl=53.3 ± 11.6%, $p>0.05$). But there were also no significant differences in freezing levels between groups (ITI1: LA-KO vs Ctrl, $p>0.05$; ITI2: LA-KO vs Ctrl, $p>0.05$), demonstrating that both groups showed conditioning-induced fear responses, reflecting successful conditioning.

2.2.2.2.1.3 CS extinction phase

The memory of the tone was tested 24 hrs after conditioning, and the mobility graph for this session is depicted in Fig. 15C a. Baseline mobility before tone onset differed not significantly between groups (data not shown). Mobility levels (Fig. 15C b, Phases 1+2) were similar between groups (before tone onset: LA-KO vs Ctrl, $p>0.05$; after tone onset: LA-KO vs Ctrl, $p>0.05$) and decreased significantly during tone presentation for both groups (before tone onset: Ctrl=95.4 ± 1.4%, after tone onset: Ctrl=62.9 ± 8.5%, $p<0.05$; before tone onset: LA-KO=93.8 ± 2.7%, after tone onset: LA-KO=54.4 ± 5.5%, $p<0.05$). Equally, freezing responses (Fig. 15C c, Phases 3+4) increased

significantly for both groups after tone onset (before tone: Ctrl=14.4 ± 2.9%, with tone: Ctrl=49.7 ± 7.8%, $p<0.05$; before tone: LA-KO=17.4 ± 4.4%, with tone: LA-KO=50.2 ± 5.6%, $p<0.05$) and there were no significant differences between groups (before tone: LA-KO vs Ctrl, $p>0.05$; with tone: LA-KO vs Ctrl, $p>0.05$). This examination showed that both groups retained a memory of the CS.

The same results were obtained with another cohort (see Table 2, group 1) of LA specific GluR-A KO mice, which were also tested in the multi-trial paradigm (rAAV-Cre injected mice (n=6), uninjected mice (n=10); data not shown). Again, there were no statistical differences between the LA specific GluR-A KO mice and the uninjected mice. Both groups displayed conditioning induced mobility reduction and increased freezing during the acquisition phase of fear conditioning. They also showed successful cued memory retrieval 24 hrs later.

The absence of detectable memory impairment in the LA specific GluR-A KO mice could be explained, on the one hand, by the fact that the Cre expression within the LA has not been sufficient (see 2.2.2.1 for IHC analysis). Alternatively, it could be argued that the amygdaloid circuitry was so strongly potentiated ("saturated plasticity") due to multiple tone-shock pairings that a small impairment in learning would not affect memory formation and could not be detected. Therefore, using the less intense one-pairing protocol might lower the level of fear-induced activity in the amygdala.

2.2.2.2.2 One-trial fear conditioning paradigm

To test if the one-trial fear conditioning paradigm would increase the capacity to detect an effect on learning with only a minor portion of neurons infected, a cohort of seven *GluR-A*$^{2lox/2lox}$ mice injected with the Cre expressing viral construct was compared to eight uninjected mice in the one-trial paradigm (see Table 2, group 3).

2.2.2.2.2.1 Habituation phase

The mobility pattern during this session is depicted in Fig. 16A a. Only the LA specific GluR-A KO mice showed a significant reduction in mobility at the end

of the habituation session (Fig. 16A b, Phases 1+2; first 60 sec: LA-KO=100 ± 0%, last 60 sec: LA-KO=95.2 ± 0.8%, $p<0.05$; first 60 sec: Ctrl=99.6 ± 0.3%, last 60 sec: Ctrl=97.9 ± 0.7%, $p>0.05$), indicating that the LA specific GluR-A KO mice had habituated to the conditioning chamber. Therefore, at the end of the habituation phase, mobility differed significantly between groups (first 60 sec: LA-KO vs Ctrl, $p>0.05$; last 60 sec: LA-KO vs Ctrl, $p<0.05$).

2.2.2.2.2.2 Acquisition phase

The observed activity for this phase is depicted in Fig. 16B a.

Baseline analysis: In this phase baseline mobility before conditioning did not differ significantly between groups (Fig. 16B b, Phases 1+2; first 60 sec: Ctrl=83.1 ± 7.2%, LA-KO=87.6 ± 2.4% $p>0.05$; last 60 sec: Ctrl =95.2 ± 2.3%, LA-KO=98.1 ± 0.9%, $p>0.05$). Increased mobility before conditioning was only significant for the LA specific GluR-A KO mice (LA-KO: first 60 sec vs last 60 sec, $p<0.05$; Ctrl: first 60 sec vs last 60 sec, $p>0.05$).

CS1 analysis: As depicted in Fig. 16B b (Phases 3+4) no group showed significant reduction in activity during CS1 (before CS1: Ctrl=95 ± 3%, CS1: Ctrl=88.8 ± 3.8%, $p>0.05$; before CS1: LA-KO=97.9 ± 1%, CS1: LA-KO=96.4 ± 1.8%, $p>0.05$), and mobility was similar between groups (before CS1: LA-KO vs Ctrl, $p>0.05$; CS1: LA-KO vs Ctrl, $p>0.05$). The freezing analysis (Fig. 16B c, Phase 4), on the contrary, revealed a significant difference between groups during CS1 (CS1: Ctrl=26.9 ± 6.2%, LA-KO= 10.7 ± 4%, $p<0.05$), which suggested that the LA specific GluR-A KO mice displayed less CS-induced freezing during the acquisition phase of fear conditioning.

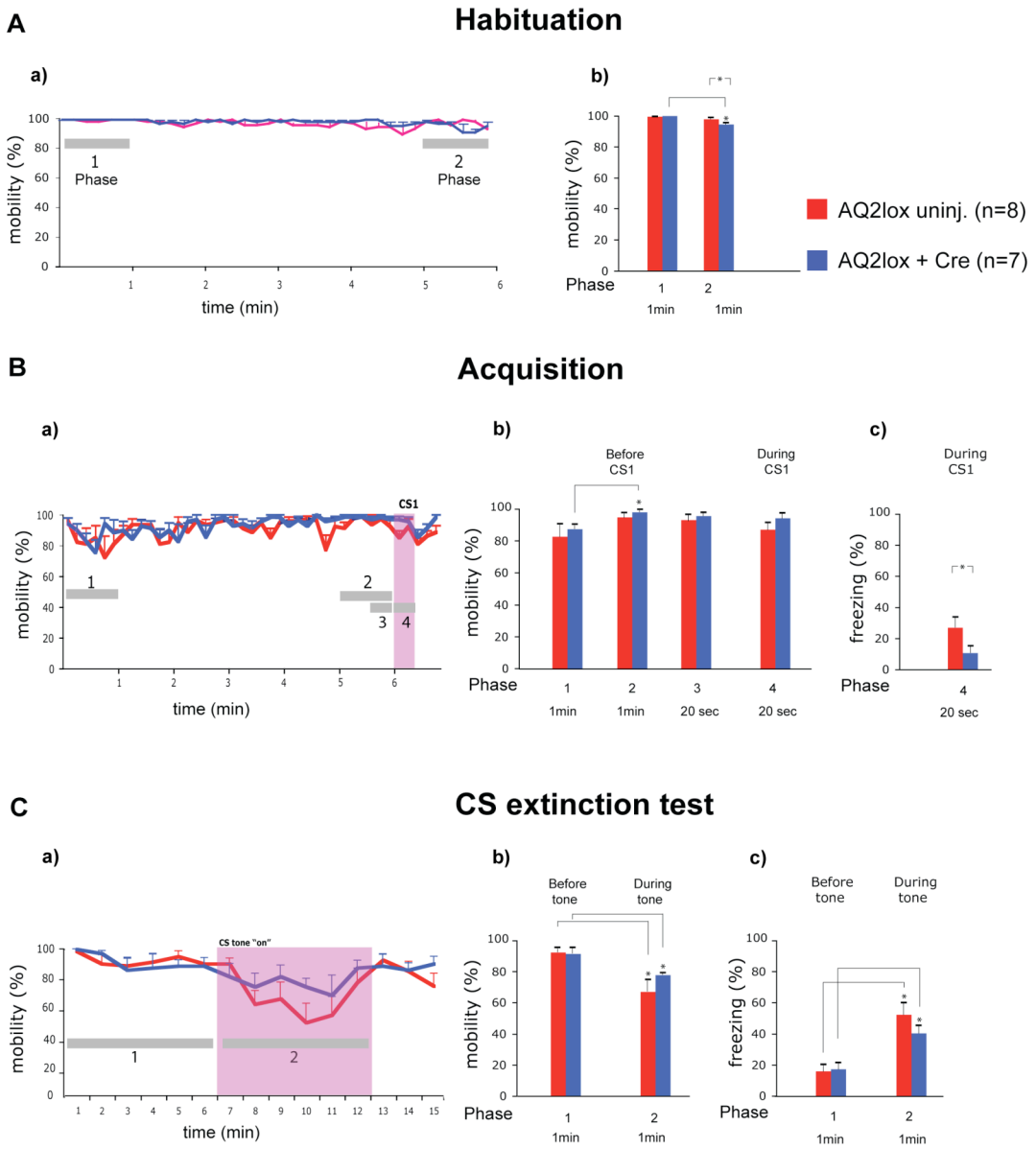

Fig. 16: Behavioral analysis of rAAV-Cre injected mice in the one-trial fear conditioning experiment. rAAV-Cre injected mice and control mice were able to acquire fear responses during conditioning and showed successful memory retrieval when tested 24 hrs after conditioning.
A: a) Mobility pattern for the habituation session and b) statistical comparison of first min versus last min during the habituation phase. B: a) Activity traces for the acquisition session, b) statistical analysis of mobility before, during (CS) and after (ITI) conditioning c) and statistical analysis of freezing levels during (CS) and after (ITI) conditioning. C: a) Mobility graph for the memory test session, b) statistical analysis of mobility before and during tone presentation c) and statisical comparison of freezing responses before and during tone presentation. rAAV-Cre injected mice (n=7) are shown in blue. Uninjected mice (n=8) are shown in red. Mean ± SEM. Grey bars in the mobility graphs delineates different Phases.

2.2.2.2.2.3 CS extinction phase

The mobility pattern during this test session is depicted in Fig. 16C a. As was in the acquisition session, baseline activity before tone onset was not significantly different between groups (not shown). After tone onset both

groups decreased their mobility significantly (Fig. 16C b, Phases 1+2; before tone onset: Ctrl=92.3 ± 2.1%, after tone onset: Ctrl=66.9 ± 6.7%, $p<0.05$; before tone onset: LA-KO=91.2 ± 3.4%, after tone onset: LA-KO=77.9 ± 0.4%, $p<0.05$), and there were no significant differences in mobility between groups (before tone onset: LA-KO vs Ctrl, $p>0.05$; after tone onset: LA-KO vs Ctrl, $p>0.05$). However, the LA specific GluR-A KO mice showed a trend to exhibit less mobility reduction than the uninjected mice. An analysis of freezing responses before and after tone onset (Fig. 16C c, Phases 1+2) revealed similar freezing behavior between groups (before tone: Ctrl=16.5 ± 3.7%, LA-KO=16.9 ± 4.6%, $p>0.05$; with tone: Ctrl=51.9 ± 7.2%, LA-KO=40.5 ± 4.5%, $p>0.05$). Both groups increased freezing significantly upon tone presentation (Ctrl: before tone vs with tone, $p<0.05$; LA-KO: before tone vs with tone, $p<0.05$). Subtracting the average freezing before tone from the average freezing with tone demonstrated that the LA specific GluR-A KO mice (23.6%) exhibited less freezing compared to the uninjected mice (35.4%).

In another cohort of conditional GluR-A mice injected with the Cre expressing viral construct (see Table 2, group 4), the one-trial fear conditioning experiment was repeated and similar results to those presented above were obtained except that no differences were observed in freezing levels during CS1 (data not shown). There were also no significant differences between groups in the memory test session. Both groups showed increased freezing responses and decreased mobility levels upon tone presentation.

In the four cohorts of LA specific GluR-A KO mice analyzed in the two conditioning protocols there was no fear conditioning impairment detectable. The LA specific GluR-A KO mice displayed an ability to acquire fear responses during the acquisition phase of fear conditioning and showed memory of the CS, therefore displaying fear responses during tone presentation. Table 4 summarizes the results obtained with the different LA specific GluR-A KO mice.

Animal groups	Training protocol	Handling	Habituation	Acquisition	CS extinction	Percentage LA-neurons expressing Cre
Group 1 A: Injected with rAAV-Cre B: Not injected	3 pairing (0.4mA/2sec)	√	√	WT: **+** KO: **+**	WT: **+** KO: **+**	Not analyzed
Group 2 A: Injected with rAAV-Cre B: Not injected	3 pairing (0.4mA/2sec)	√	√	WT: **+** KO: **+ (but trend to exhibit less freezing)**	WT: **+** KO: **+**	2 mice analyzed: 2 mice > 10-30% LA neurons
Group 3 A: Injected with rAAV-Cre B: Not injected	1 pairing (0.5mA/1sec)	√	√	WT: **+** KO: **+*/-****	WT: **+** KO: **+ (but trend to exhibit less freezing)**	4 mice analyzed: 2 mice > 10-30% LA neurons
Group 14 A: Injected with rAAV-Cre B: Injected with rAAV-GFP	1 pairing (0.5mA/1sec)	√	√	WT: **+** KO: **+**	WT: **+** KO: **+**	Not analyzed

Table 4: Summary of the fear conditioning results obtained from LA-specifc GluR-A KO mice. Two groups were tested in the multi-trial fear conditioning experiment and another two groups of mice were tested in the one-trial fear conditioning paradigm. All protocols included a handling and habituation session prior conditioning. (**-** = no learning, no memory retrieval; **+** = learning, successful memory retrieval).*Regarding the mobility analysis; **Regarding the freezing analysis.

Even though a clear GluR-A signal loss was seen in the area of Cre expression within the LA of the rAAV-Cre injected mice (2.2.2.1) and even though the semi-quantitative analysis revealed that in some mice roughly 10-30% of LA neurons expressed Cre recombinase (see Table 3), there was no memory impairment detectable in the groups analyzed so far.

Taken together, the data presented in this study illustrate methods to alter gene function in the adult brain in a spatially restricted manner. The

preliminary results provide the key findings for further improvements in generating gene knockouts of molecules important for synaptic plasticity within the entire amygdala to study the molecular basis of fear learning and memory formation.

3. Discussion

The main purpose of this thesis was to analyze the consequences of LA-specific GluR-A gene loss on behavioral outcome during auditory fear conditioning. This should lead to a more detailed understanding of GluR-A mediated synaptic plasticity during fear conditioning within the LA, a region of the brain required for the acquisition of fear memories. GluR-A gene loss is preferably achieved when mice have reached adulthood, since at that age analysis of GluR-A function should not be confounded by possible developmental compensatory mechanisms. Techniques involving conditional gene knockout have the potential to achieve temporally and spatially controlled gene deletion (Nagy, 2000). Spatial restriction can be achieved by stereotactic targeting of viral vectors to certain brain areas of adult mice or by the generation of transgenic mice with tissue-specific gene expression.

In this thesis, both approaches were employed in attempts to attain LA-specific GluR-A gene ablation.

3.1 Generation of an amygdala-specific BAC transgene

In a first approach, transgenic mouse lines, potentially exhibiting amygdala-specific expression were generated. The gene *Lypdc1* was chosen for the generation of transgenic mice, since its published expression according to the SymAtlas database was high and nearly exclusively within the amygdala. ISH analysis verified this observation, since *Lypdc1* expression was mainly restricted to the BLA, with additional weak signals within the CA1 and DG region of the hippocampus. Based on these findings, the subsequent homologous recombination strategy to generate a BAC transgene bearing a modified *Lypdc1* gene locus, expressing the reporter EGFP gene, was designed and successfully completed. However, IHC analysis of the resulting transgenic founder mice showed that EGFP reporter gene expression was detectable within brain areas additional to the amygdala and that, in fact, in some founders expression within the amygdala was absent. These results were in contrast to the ISH findings and to the published *Lypdc1* expression pattern. Strikingly, a prominent expression within the striatum, as observed in some of the founders (e.g. F55), was not seen in the ISH analysis, although the posterior parts of the striatum/caudate putamen were represented on the

particular coronal sections investigated. By the time the founders were analyzed, two additional independent databases published expression patterns of *Lypdc1*. The GENSAT database (www.gensat.org) published data of BAC transgenic mice exhibiting *Lypdc1-driven* EGFP expression and the "Allen Brain Atlas" database (www.brain-map.org) published ISH results of *Lypdc1* expression in WT mice. The *Lypdc1*-driven EGFP expression pattern derived from GENSAT confirmed that *Lypdc1* expression was not restricted to the amygdala, but was found throughout different areas of the brain. Furthermore, as was seen in the founder analysis here, different transgenic lines showed variations in expression strength and pattern. The ISH results from "Allen Brain Atlas" showed a widespread expression pattern of *Lypdc1* throughout the brain. Expression was found in the OB, in midbrain areas such as the striatum/caudate putamen, the hippocampus, the amygdala, the cortex, the cerebellum and in other structures (Fig. 17 A, B).

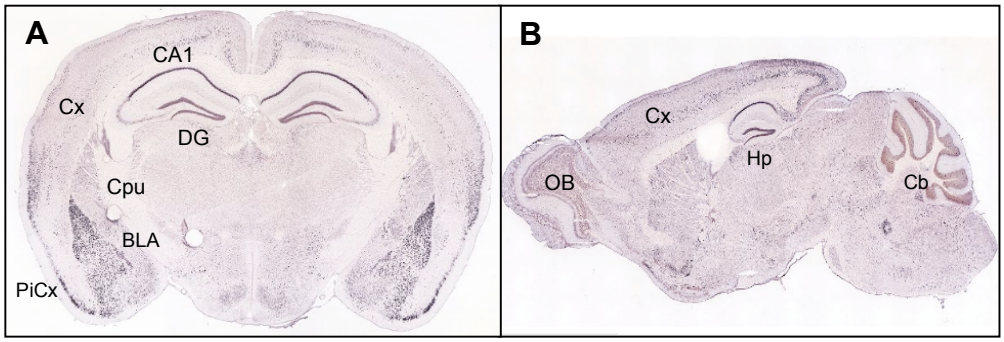

Fig. 17: ISH results of *Lypdc1* expression derived from the "Allen Brain Atlas". The expression pattern is widespread throughout the brain.
A: Coronal section of the mouse brain showing *Lypdc1* expression pattern in CA1 and DG region of the hippocampus, cortex (Cx), piriform cortex (PiCx), caudate putamen (Cpu), basolateral amygdala (BLA) and other areas.
B: Sagittal section of the mouse brain showing *Lypdc1* expression pattern in olfactory bulb (OB), CA1 and DG region of the hippocampus (Hp), cortex (Cx), cerebellum (Cb) and other areas.

These findings thus additionally confirmed the expression results observed in the BAC transgenic mice. These different ISH outcomes may be explained by the use of different detection probes. In the analysis here, short radioactively labeled (~50bp) DNA based oligoprobes were used, whereas the "Allen Brain Atlas" investigators used non-radioactively labeled RNA based probes, with longer sequences. The advantage of non-radioactively labeled probes is that they allow for better visualization of cellular morphology.

Additionally, increasing sequence length of the probe may facilitate the detection of the authentic expression pattern.

Altogether, these results clearly demonstrated that it was not worthwhile modifying this particular gene locus (*Lypdc1*) to drive molecular tools (such as Cre recombinase) for the ensuing generation of amygdala specific manipulations.

Thus, as an alternative, a virus-mediated gene KO technique for deletion of the GluR-A gene within the LA of adult mice was utilized with the aim of studying the consequences of GluR-A gene loss in auditory fear conditioning. rAAV vectors, expressing Cre recombinase under the neuron specific human synapsin promoter, which mediates expression in excitatory as well as inhibitory neurons, but not in other brain cells (like astrocytes), were generated and injected into the LA of conditional GluR-A (*GluR-A*$^{2lox/2lox}$) mice. The expression times after surgery varied between groups, but at the earliest mice were subjected to fear conditioning experiments four weeks after the injection. This should ensure sufficient time for Cre expression, for the subsequent excision of the “floxed” alleles mediated by Cre recombinase, as well as for the removal of the remaining GluR-A containing AMPA receptor proteins from the soma and synapses.

3.2 Fear conditioning experiments in GluR-A KO mice

As an essential first step to analyze the consequences of GluR-A gene loss, validated fear conditioning protocols were established here. Two fear conditioning paradigms were employed and the behavior of WT mice was compared to that of global GluR-A KO mice, which have previously been reported to be impaired in fear conditioning experiments (Humeau et al., 2007). In total, 4 cohorts of mice, containing WT and GluR-A KO animals, were analyzed in the different fear conditioning paradigms. Table 5 summarizes the results.

Animal groups	Training protocol	Age in months	Number of animals	Handling	Habituation	Acquisition	CS extinction
Cohort 1	1 pairing (0.5mA/1 sec)	WT: 2 - 3 KO: 2 – 4.5	WT: 6 KO: 5	√	√	WT: **+** KO: **-**	WT: **+** KO: **+** (trend less freezing)
Cohort 2	3 pairing (0.4mA/2 sec)	WT: 1.5 -2.5 KO: 2 - 12	WT: 12 KO: 21	√	√	WT: **+** KO: **-**	WT: **+** KO: **+** (trend less freezing)
Cohort 3	3 pairing (0.4mA/2 sec)	Both: 2.5	WT: 6 KO: 6	√	X	WT: **+** KO: **-**	WT: **+** KO: **+*/-****
Cohort 4	3 pairing (0.4mA/2 sec)	WT: 1.5 – 5.5 KO: 5.5-7.5	WT: 9 KO: 9	X	X	WT: **+** KO: **-**	WT: **+** KO: **+** (trend less freezing)

Table 5: Summary of fear conditioning results obtained with the global GluR-A KO mouse line. (**-** = no learning, no memory retrieval; **+** = learning, successful memory retrieval).*Regarding the mobility analysis; **Regarding the freezing analysis.

In summary, all four behavioral experiments revealed a strong impairment of GluR-A KO mice in the acquisition and expression of fear responses during conditioning (acquisition phase). This was independent of whether animals received handling or habituation since the behavioral results showed that these “pre-exposure” experiences, prior to conditioning, had negligible effects on the expression of conditioned responses during the acquisition phase. However, in cohort 3, freezing responses (as opposed to the mobility analysis) differed between KO and WT mice during memory testing. However, since this finding was not reproduced in cohort 4 (the reasons for this are presently unknown), it can be concluded that GluR-A KO mice displayed intact, but slightly reduced memory retrieval.

The observed phenotype in these cohorts stands in slight contrast to the data of Lüthi and his colleagues (Humeau et al., 2007). For the acquisition session, the results obtained by Lüthi and his colleagues were entirely reproduced here. Both investigations showed that GluR-A KO mice exhibited absence of freezing behavior during the conditioning period. When fear memory was tested 24 hours later, Humeau et al. (2007) showed that GluR-A KO mice did not exhibit any statistically significant changes in activity and freezing responses throughout the CS presentation compared to before CS onset. On the other hand, as expected, WT mice displayed lower levels of mobility and increased freezing responses upon tone onset (Fig. 19 A, B).

This outcome led the authors to the conclusion that the GluR-A gene deletion results in a failure to acquire and/or retain memory for cued auditory fear conditioning.

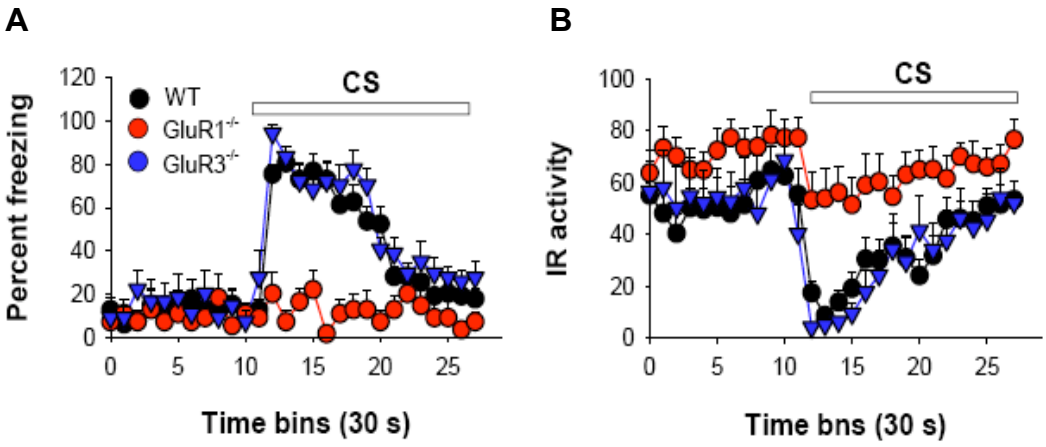

Fig. 19: Memory analysis in GluR-A KO mice after fear conditioning (Humeau et al., 2007). GluR-A KO mice exhibited severe memory impairment in cued fear conditioning.
A: Percentage freezing responses before and during tone (CS) onset (memory test). X-axis: Time in 30 sec bins. Y-axis: Percentage freezing responses.
B: Activity traces before and during CS onset (memory test). X-axis: Time in 30 sec bins. Y-axis: Mean locomotor activity responses.

In the same report Lüthi and his colleagues also obtained electrophysiological data from GluR-A KO mice, which fitted well with the observed behavioral phenotype. LTP was reported to be completely absent at thalamic-to-LA neurons, demonstrating that GluR-A-dependent synaptic plasticity is the main form of LTP underlying the acquisition of fear conditioning.

However, the results obtained in the analysis here revealed that GluR-A KO mice were actually able to acquire some memory trace of the tone, since otherwise they would not have shown decreased mobility and increased freezing responses upon CS presentation. Nevertheless, freezing responses throughout all analyses were lower in GluR-A KO mice compared to WT mice. The different results obtained in the CS extinction test here and by Humeau et al. (2007) might be explained by variations in the settings of the behavioral paradigm. It could be that the context change here was only minor. The walls of the conditioning arena were changed from black to transparent color, and the grids were covered with a PVC plate. However, the dimensions of the

arena were still the same, and the memory test session was conducted with the same fear conditioning apparatus (TSE systems) within the same room in which conditioning took place. It might be worth separating conditioning and memory testing completely. This could be achieved not only by rigorously altering the context, but also by changing rooms and having two fear conditioning systems, one running only for acquisition, and the other for the memory evaluation. It could even be worth changing the experimenters between the two sessions in order to exclude that the animals show generalized fear against context and experimenter. One needs to keep in mind that many factors during learning (conditioning) can have an effect/impact on memory formation, and hence change the behavioral results during memory testing. Another parameter to consider is the frequency of the tone. Here a frequency of 7.5 kHz was used, which was emitted around 80-100 dB. Humeau et al. (2007) used a similar frequency and the same sound intensity. In addition, the habituation session prior to conditioning can also be considered as a reason for different behavioral results in the CS extinction test. Humeau et al. (2007) omitted this phase in their experiments. Other studies have suggested that prior familiarization with the environment, where conditioning subsequently took place, altered the expression and retrieval of conditioned responses (Perez-Villalba et al., 2005; Perez-Villalba et al., 2007). However, the analysis here could not support this hypothesis.

Consistently, GluR-A KO mice exhibited impairment during the conditioning period, reflected by the missing immediate CS+US pairing-induced freezing responses. This acquisition impairment, however, is not due to an inability of the GluR-A KO mice to detect and react to the electric foot-shock (US), since both genotypes showed elevated activity levels (escape/flight behavior) shortly following foot-shock onset (here shown for the multi-trial paradigm; Fig. 18). Foot-shock onset was accompanied in nearly all mice with jump and vocalization responses (“screams”), which indicated that the animals had experienced pain. This demonstrated that both genotypes were able to detect the US, and, as both groups showed a mobility decrease upon tone presentation during memory testing, one can conclude that they were able to respond to the CS alone. Humeau et al. (2007) analyzed the sensitivity of GluR-A KO and WT mice in detecting the CS and US in more

detail. By investigating “novel tone inhibition” they could show that both genotypes were similarly able to process the auditory stimulus (CS). They also demonstrated that both groups detected and reacted to the foot-shock (Humeau et al., 2007).

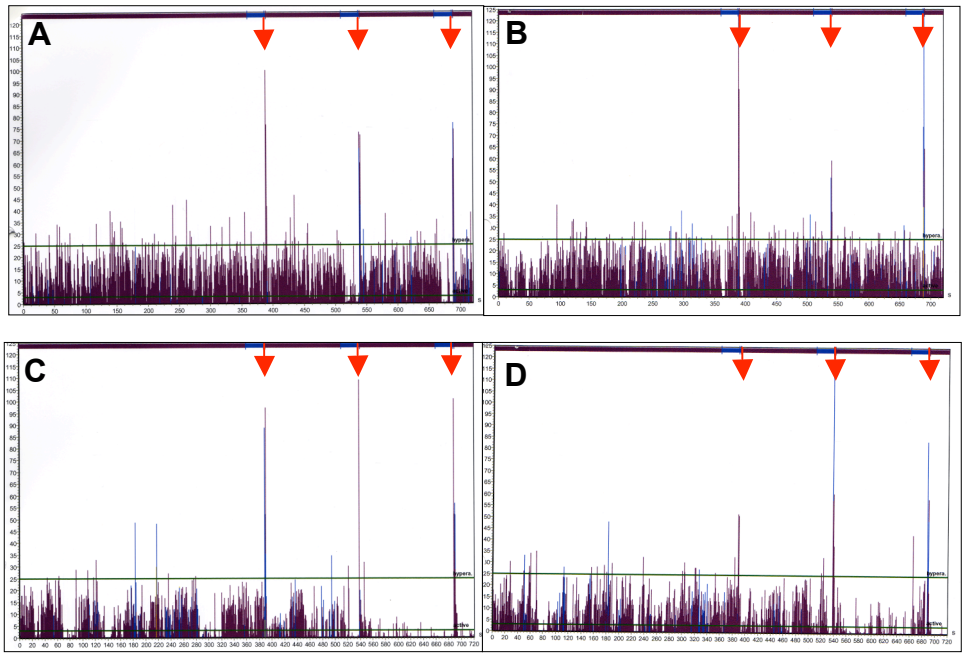

Fig. 18: Individual TSE activity recordings during the acquisition session in the multi-trial paradigm from GluR-A KO mice and WT. Both genotypes displayed increased activity (escape/flight behavior) upon shock onset (red arrows), indicating intact shock sensitivity.
A, B: Examples of the mobility recordings from two GluR-A KO mice. C, D: Examples of the mobility recordings from two WT mice. X-axis: Time in sec. Y-axis: Activity scores in cm/sec.

Despite this prominent learning deficit (i.e. impairment during conditioning), which is not due to an inability to detect the CS and US, in the analysis here, GluR-A KO mice were shown to have acquired some memory trace of the tone. The evidence for this is that GluR-A KO mice would otherwise not have reacted with mobility reduction and increased freezing levels upon CS presentation.

One possibility to explain these observations would be that compensatory mechanisms/strategies occurred, which enabled the GluR-A KO mice to solve the memory task, in spite of pronounced deficits during the acquisition phase. Alternatively, it can be speculated that different plasticity mechanisms could be operative at amygdala connections during fear

conditioning. It seems that GluR-A dependent plasticity is required during the acquisition phase, but that a GluR-A independent mechanism may be operative during memory formation. This would suggest that the short-term association of tone and shock is not necessary for establishing a long-term fear memory trace. This observed behavior is quite similar to the reported phenotype of GluR-A KO mice in hippocampal learning paradigms, in which GluR-A KO mice show a specific spatial working memory impairment but intact spatial reference memory (Reisel et al., 2002). Reisel et al. (2002) attempted to correlate their results with the electrophysiological findings from this mouse line. In GluR-A KO mice early (rapid-onset) LTP is absent (GluR-A dependent) at CA3-to-CA1 hippocampal synapses (Hoffmann et al., 2002) and this could be responsible for the impairment seen in the spatial working memory task. However, these mice have intact late phase LTP (GluR-A independent) and this could account for intact performance in the spatial reference memory task. The spatial working memory task involves a moment-to-moment control of behavior, which is similar to the immediate tone-shock association in the acquisition phase. This information processing has to occur very rapidly and could be explained by processes involving fast GluR-A dependent mechanisms. On the other hand, the long-term memory formation may not need to be formed so quickly and might engage GluR-A independent mechanisms and is therefore intact in GluR-A KO mice.

3.3 Generation of LA-specific GluR-A KO mice and fear conditioning

To address the role of LA-site specific GluR-A containing AMPA receptors during fear conditioning, a Cre expressing viral construct was delivered into the LA of conditional GluR-A mice prior to performing conditioning experiments. This approach aimed at investigating whether the LA is the neural locus, which mediates the GluR-A dependent short-term association of tone and shock, confirmed here to be missing in global GluR-A KO mice. This analysis should also reanalyze the hypotheses established by Rumpel et al. (2005) that GluR-A trafficking within the LA is an important process underlying the acquisition of fear memories, and that disturbing about 10-20% of the LA circuitry is sufficient to produce memory impairment.

3.3.1 IHC analysis to reveal Cre expression within the LA

All animals were sacrificed after behavioral analysis, and Cre expression was assessed by IHC to reveal the targeting efficiency. Only mice in which Cre expression could be found in both LA´s were included in the behavioral data presented here. For some LA-specific GluR-A KO mice, a semi-quantitative analysis was performed to estimate the percentage of neurons expressing Cre recombinase within the total LA. This analysis revealed that in two thirds of the mice analyzed (4 from 6), a similar range of infection, as was seen in Rumpel et al. (2005), could be detected. In these mice, 10-30% of LA neurons expressed Cre recombinase, which likely reflects the percentage of neurons lacking GluR-A. The lack of GluR-A within the Cre expressing LA neurons could have been demonstrated for example by absence of LTP in these cells. Because of technical reasons, this could not be done, but instead anti-GluR-A staining was performed to show the loss of GluR-A at least in a qualitative manner. Indeed, GluR-A signal loss was clearly detectable in the area of Cre expression.

3.3.2 The multi-trial fear conditioning paradigm in LA-specific GluR-A KO mice

During the habituation session, both groups behaved similarly in the mobility analysis. This showed that there were no phenotypical differences between groups during habituation.

In the acquisition session, both groups displayed a gradual decrease in mobility and an increase in freezing responses following the tone-shock pairings. Baseline activity before conditioning was similar between groups. The LA-specific GluR-A KO mice decreased mobility during CS3 as well as during ITI2, and equally increased freezing responses. The uninjected control mice, however, decreased mobility already during CS2 and during ITI1, and conversely increased freezing responses. This suggested that the control mice exhibited significant fear responses already after two tone-shock pairings, whereas the LA-specific GluR-A KO mice required three tone-shock pairings to display significant fear responses. The reduced expression level of GluR-A within the LA could explain that more tone-shock pairings were required to induce conditioned fear responses in these LA-specific GluR-A KO

mice. However, there were in fact no statistically significant differences between groups in mobility and freezing measures, indicating conditioning-induced fear behavior in both groups. Nevertheless, there was a trend that the mean mobility levels of LA-specific GluR-A KO mice were higher and the freezing levels lower compared to the uninjected control mice, supporting the hypothesis that GluR-A mediated plasticity within the LA is necessary for the short-term tone-shock association.

Within the memory test session, mobility of both groups exhibited similar baseline activity. Upon CS presentation, both groups decreased mobility and increased freezing responses, and there were no significant differences between groups, indicating that control as well as LA-specific GluR-A KO mice had formed a memory of the CS.

The results here were in contrast to those published by Rumpel et al. (2005), in which inhibition of GluR-A containing AMPA receptors in as few as 10-20% of LA neurons, led to a detectable difference in freezing levels between groups during CS alone presentation (memory test). The lack of a detectable memory phenotype in the analysis here might be explained by insufficiently widespread infection of LA neurons with the Cre expressing viral construct. Alternatively, the protocol used to induce fear behavior in mice may have been too stringent (three tone-shock pairings) leading to saturated learning, and thus a small impairment in learning, caused by a minor fraction of neurons infected, might not be detectable. In other words, it could be that compensation effects occurred due to overtraining, and therefore, a partial fear memory impairment could not be identified.

To address this possibility, additional experiments using the moderate one-trial fear conditioning paradigm were performed. This permits testing whether a less intense protocol, which still leads to detectable fear responses in control mice, would increase the likelihood in detecting a small memory impairment in the LA-specific GluR-A KO mice.

3.3.3 The one-trial fear conditioning paradigm in LA-specific GluR-A KO mice

In this experiment, baseline activity during the habituation session differed between groups. The LA-specific GluR-A KO mice decreased mobility

towards the last min during habituation. Therefore, there were significant differences between groups at the end of the habituation session, indicating that the LA-specific GluR-A KO mice had habituated to the conditioning environment. Presently, it is not known why the control mice failed to habituate to the environment, and why this phenotype was not apparent in the previous sets of experiments.

During the acquisition session, both groups displayed similar baseline activity before conditioning. In both groups, average mobility during CS1 did not differ to mobility before conditioning, and there were no statistically significant differences between groups. On the contrary, freezing levels during CS1 differed between groups. The mobility analysis would have suggested no conditioning-induced fear behavior, whereas the freezing analysis suggested that the LA-specific GluR-A KO mice exhibited less conditioning-induced freezing responses during the acquisition phase. The freezing investigation supports the idea that GluR-A containing AMPA receptors are required for the short-term tone-shock association underlying the observed defensive behavior during conditioning.

In the memory test session, both groups exhibited comparable baseline mobility. Upon CS presentation, mobility decreased and freezing increased for both groups, and there were no statistically significant differences between groups. Nevertheless, the LA-specific GluR-A KO mice exhibited a trend to freeze less compared to control mice. This would indeed suggest that a memory impairment would be readily detected when employing the one-trial experiment, since only in this experiment was it possible to detect smaller freezing responses in the LA-specific GluR-A KO mice compared to control mice.

However, despite using the moderate one-trial protocol, the LA-specific GluR-A KO mice, which potentially lacked GluR-A containing AMPA receptors within 10-30% of LA neurons, did not exhibit statistically significant altered fear memory acquisition compared to control animals.

If GluR-A is specifically required within the LA for the acquisition of fear memories, the treated mice should not have shown conditioning-induced fear responses during acquisition. Furthermore, they should not have been able to

react upon tone alone presentation, indicating that they had not formed a memory of the conditioned tone. The latter expectation was founded on the study performed by Rumpel et al. (2005). These authors were able to show that upon inhibition of GluR-A trafficking within 10-20% of LA neurons, induced by herpes simplex virus mediated overexpression of the C-terminal domain of the GluR-A subunit ("plasticity block vector"), the treated animals expressed less conditioned fear responses during memory testing compared to controls. This pointed to impaired fear memory formation, when GluR-A containing AMPA receptors were blocked in as few as 10-20% of LA neurons prior to fear conditioning. However, one major drawback of their study was that the C-terminal domain contains various phosphorylation sites and protein docking sites so that its overexpression in neurons may potentially interfere with other cellular processes. Hence, the resulting phenotype might not only be due to a specific GluR-A receptor trafficking blockade. This might explain why a phenotype was observed despite manipulation of only 20% of the circuitry. Interestingly, in their experiments, the treated rats apparently showed normal freezing levels during conditioning, from which one could speculate that blocking AMPA receptor trafficking has no effect on the expression of conditioned fear responses during acquisition. One could also speculate that 10-20% of infected LA neurons would not be sufficient to induce the prominent acquisition impairment seen in the global GluR-A KO mouse line. However, this would not explain why this infection efficiency was sufficient to induce a long-term fear memory impairment. Alternatively, one could speculate that lack of GluR-A dependent plasticity within the LA might not be the cause of the acquisition phenotype seen in the global GluR-A KO. In this model the question arises, which neural locus is mediating GluR-A dependent acquisition of fear conditioning (amygdala versus hippocampus).

A striking finding is that the global GluR-A KO mice were not able to learn the tone-shock pairings, as indicated by absence of immediate tone-shock-induced fear reactions during the acquisition phase. Quite astonishingly, however, is the finding that these mice were nevertheless able to form a memory. Without having 100% infection efficiency, it is hard to conclude that GluR-A containing AMPA receptors within LA neurons would not be required for the acquisition of fear conditioning. Such a high infection

rate is virtually impossible to achieve by viral means, since one would have to inject a very high number of viral particles (with the risk of inducing toxicity). This would certainly lead to areas outwith the amygdala being affected due to diffusion of the virus. Thus, it is still an open question which behavioral phenotype during auditory fear conditioning would be observed in mice lacking GluR-A containing AMPA receptors in principal neurons within their entire LA. One also needs to keep in mind that global GluR-A KO mice are lacking GluR-A containing AMPA receptors not only in all neurons but in all other cells including astrocytes and glial cells. Thus, the observed behavioral phenotype might be explained by an altered integrity of all of these cells leading to their failure to orchestrate conditioned fear acquisition. To elucidate in detail which cells contribute to what extent to the examined phenotype, additional experiments would have to be performed using cell-type specific promoters to perturb GluR-A mediated plasticity in a cell-type specific manner.

A principal mechanism by which a gene loss can be overcome is compensation. A study performed by Han et al. (2007) showed that compensation mechanisms occur within the LA of adult mice. The authors showed that disturbing 20% of the LA circuitry was not sufficient to impair fear conditioning. Han et al. (2007) virally overexpressed a dominant-negative CREB (cAMP responsive element binding protein) mutant in 20% of LA neurons in WT mice, and demonstrated that the treated animals were capable to form a memory of the CS (Han et al., 2007). The authors demonstrated that the remaining, uninfected, LA neurons were able to compensate for this 20% gene loss within the LA circuitry. This is an intriguing finding, indicating that compensation is indeed a mechanism that not only occurs during development, but also in adult systems. The memory trace, as indicated by Arc positive neurons, was clearly detectable after fear conditioning in these animals, but did not co-localize with the GFP-fused CREB mutant, indicating that the “CREB mutant” infected LA neurons had not participated or had not been recruited in the memory trace. Interestingly, in all experiments performed by Han et al. (2007), about 20% of LA neurons were Arc positive and this was independent of the fear conditioning protocol used for inducing conditioned fear in mice. This suggested that in general roughly a third of the LA circuitry is recruited during memory formation. This notion was also

pointed out in Malinow´s publication. There the authors measured increased rectification in a third of LA neurons after fear conditioning (Rumpel et al., 2005). Based on the findings that only a third of the LA is participating in memory formation and, additionally, the assumption that compensation can occur, it is even less clear how Rumpel et al. could induce a memory impairment when infecting only 10-20% of LA neurons with the “plasticity block vector”.

It is therefore likely that in the LA-specific GluR-A KO mice generated here, the remaining uninfected circuitry was sufficient to mediate fear acquisition and memory formation. One would need to achieve 100% GluR-A KO within the entire LA and would need to demonstrate normal fear behavior in these mice during fear conditioning to conclude that GluR-A mediated plasticity would not be required in this learning paradigm. Therefore, for effective behavioral studies in mice, the rAAV mediated Cre delivery has to be optimized to achieve more efficient Cre targeting within the LA.

4. Methods

4.1 General Molecular Biology Methods and Techniques

Standard procedures including nucleic acid cloning, culturing of bacteria, transformation procedures of competent *E.coli* cells, transfection procedures of HEK293 cells, gel electrophoresis techniques and PCR techniques, were derived from previously published protocols (Ausubel et al., 1989; Sambrook et al., 1989; Joyner, 1993)

4.1.1 Isolation of Nucleic Acids

4.1.1.1 Precipitation of nucleic acids

DNA solutions were adjusted to 3 M sodium acetate, pH 5.2. The solution was mixed with 2.5x volume of absolute ethanol and precipitated for 20 min at room temperaturte (RT). The DNA was recovered by centrifugation at 13.000xg for 15-20 min at 4°C. The pellet was washed with 70% ethanol, centrifuged again, air dried (for sequencing supernatant was taken off with pipette to prevent high salt contamination) and resuspended in dH_20; Tris-Cl, pH 8.0 or TE (Tris-EDTA) depending on amount of precipitated DNA.

4.1.1.2 Purification of DNA by QIAquick Gel Extraction Kit

Purification of DNA in the size range of 0.5-10 kb from agarose was carried out according to the manufacturers´ (Qiagen) instructions. Briefly, the desired sized DNA fragments were cut out of the gel and were melted in buffer. Then the plasmid DNA was added to a column containing a raisin where the plasmid DNA will bind to in the appropriate pH and salt concentration. After several centrifugations and washing steps the DNA was eluted from the column with either TE, Tris-Cl, pH 8.5 or dH_2O. A semi-quantitative analysis was performed after purification to assess the amount of DNA. Aliquots of 1 µl and 2 µl of vector and/or insert were run on a gel next to standard marker DNA where the concentration of each band size is known. The concentration of unknown vector and/or insert DNA was visually estimated.

4.1.1.3 Small-scale plasmid DNA preparation

The QIAprep Spin Miniprep Kit was used to purify plasmids according to the manufacturers instruction. Briefly, the cells were pelleted, resuspended and

lysed with detergent containing buffer. After neutralising the reaction the solution was spun to precipitate developed cell debris and genomic DNA. Plasmid DNA remains in the supernatant. The supernatant was added to a column, which contains a raisin where the DNA will bind within a slightly acid pH. After washing the column several times, the DNA was eluted from the raisin with dH_20. DNA prepared with this Kit can directly be used for sequencing, as it is very clean.

4.1.1.4 Large-scale plasmid DNA preparation

Large scale plasmid DNA preparation was carried out using QIAGEN Midi and Maxi Kit according to the manufacturers instructions. The cells were pelleted, then lysed, neutralised and spun to remove the cell debris and genomic DNA. Then the plasmid DNA was added to a column containing a raisin where the DNA will bind to in the appropriate pH and salt concentration, to further clean it up with subsequent washing steps. Finally, the DNA was eluted using a more basic pH and lower salt concentration.

4.1.1.5 Purification of DNA after PCR amplification

The QIAquick PCR purification Kit was used to purify PCR fragments according to the manufacturers instruction. The amplified fragment was diluted in special buffer and subsequently applied on a column containing a raisin, which allows band fragments ranging from 100 bp-10 kb to bind to after centrifugation. After several washing steps the DNA was eluted from the column with Tris-Cl, pH 8.5 or dH_2O.

4.1.1.6 DNA Sequencing

The sequencing reaction was carried out using the chain termination method (Sanger et al., 1979). This technique uses sequence-specific termination of a DNA synthesis reaction using modified nucleotide substrates. 10-20 ng/10 bp of PCR-product was mixed with 4 µl Dye terminator (ABI) and 0.5 µl primer (10 µM) and brought to a final volume of 10 µl with water. Following the sequencing reaction, the DNA was precipitated (see 4.1.2.1) and then loaded on an automatic sequencing machine (Sequencing machine 377; Applied Biosystems).

4.1.1.7 Preparation of oligonucleotides

The preparation of synthetic primers was performed by Thermo Electron Corporation (Germany). A list of primers used in this study can be found in the appendix.

4.1.2 DNA Cloning

4.1.2.1 Preparation of vector DNA for rAAV-hSyn-Cre generation

The recombinant AAV-6P-SEWB plasmid DNA was linearized with *Hind*III/*Nhe*I to create ends compatible with those of the insert DNA fragment and to release the open reading frame (ORF) of the *green fluorescent protein* (GFP) gene, which was to be replaced by the ORF of the Cre recombinase gene. The reaction was incubated at 37°C for 1 hour in 1x Y+ buffers. The linearization of the plasmid vector DNA was assessed by gel electrophoresis and the backbone was purified using QIAquick Gel Extraction Kit.

4.1.2.2 Preparation of the insert DNA for rAAV-hSyn-Cre generation

The double stranded insert DNA fragment to be cloned was generated by PCR. The ORF of Cre was amplified from pRK7.iCre plasmid using primers, which contained sites for *Nhe*I/*Hind*III (3´*Nhe*I; 5´*Hind*III). Prior to cloning, the DNA was purified directly after PCR amplification by QIAquick PCR Purification Kit.

4.1.2.3 DNA ligation

Ligation reactions were performed to catalyse the formation of phosphodiester bonds between adjacent 3´-hydroxyl and 5´-phosphate groups of double stranded DNA. A typical 20 µl reaction was set up as follows: vector and insert DNA were mixed in a molar ratio of approximately 1:3, where the vector concentration was about 25-50 ng/µl. Ligation was carried out in 1x T4 ligation buffer. 5 U/µl of T4 DNA ligase was used for sticky-end ligation. Ligation reactions were incubated for 1-4 hours at RT. Control reactions containing ´plasmid vector DNA only´ and the ´insert DNA only´ were used to assess background ligation levels.

4.1.2.4 Transformation

For rAAV cloning strategies, SURE competent cells (Stratagene) were used to ensure efficient and correct replication of the viral inverse terminal repeats (ITRs). The pelleted DNA (1-2 ng) or 1-10 µl of ligation reaction was added to 50-100 µl aliquots of the competent cells and incubated for 30 min on ice. Then the cells were heated for 30 sec at 42°C. Half a millilitre of 2YT medium was added and the cells were incubated for an hour at 37°C in the incubator or shaker. Finally, the cells were briefly pelleted and resuspended in the right amount of 2YT medium to spread them onto L-agar plates with the appropriate antibiotic concentration and incubated, inverted at 37°C overnight.

4.1.2.5 Preparation of the insert DNA for recombination in *Lypdc1*

GFP was selected as reporter gene for the recombination in the *Lypdc1* containing BAC clone. The ORF of GFP was amplified from pEGFP-N1M-FRT plasmid using KOD Hifi-DNA polymerase and primers (*Lypdc1*.armdown, *Lypdc1*.armup), which had 80 nt homologous arms to *Lypdc1* as overhang. KOD has an extreme high synthesis rate as well as a very tight proofreading function. Those overhang arms were designed to flank the ATG of *Lypdc1* within the first exon, which is used as the first codon during translation. Successful recombination should lead to expression of GFP under the *Lypdc1*-promoter. Once inserted into the mouse genome, it is therefore possible to reveal the expression pattern of the *Lypdc1* gene. Before electroporation of insert DNA into the BAC containing *E.coli* strain, the amplified DNA was digested overnight with *Dpn*I to remove the plasmid input DNA during PCR reaction because *Dpn*I only digests methylated GATC sites within plasmids of bacterial origin.

4.1.2.6 Preparation of electrical competent EL250

For BAC recombination experiments the *E.coli* strain EL250 was used (Liu et al., 2003). This strain has the proteins required for recombination expressed from an integrated defective temperature sensitive λ prophage (42°C for 15 min for induction) and the Flp recombinase, used for excision of the resistance cassette, from an arabinose-inducible promoter (0.1% arabinose for induction). A single bacterial colony from the EL250 strain was picked and

inoculated into 2 ml LB (without antibiotics) and incubated at 32°C overnight in a shaker. The overnight culture was inoculated in a ratio 1:500 - 1:1000 into 200 ml LB and incubated at 32°C until the OD_{600} = 0.5-0.7 was obtained. The cells were pelleted at 5000rpm for 5 min at 4°C (JLA-16.250 Rotor, Beckmann) and supernatant was discarded and the pellet was resuspended in 100 ml ice-cold dH_2O and centrifuged again. The supernatant was discarded and the pellet was resuspended in 50 ml ice-cold dH_2O and centrifuged again. The resulting pellet was again resuspended in 25 ml of ice-cold dH_2O and centrifuged again. The pellet was then resuspended in 30 ml ice-cold 10% glycerol, centrifuged again and finally the cells were resuspended in 500 µl ice-cold 10% glycerol and directly used as 50 µl aliquots for electroporation. Competent cells prepared with this method yielded 10^6-10^9 transformed colonies/µg supercoiled plasmid DNA as assessed with pBluescript vector.

4.1.2.7 Electroporation of DNA into EL250 strain

DNA, freshly made BAC DNA (100 ng), plasmid DNA (1-2 ng) or insert DNA (100-400 ng), was mixed and incubated together with 50 µl of the electrical competent cells for 2 min on ice before used for electroporation. Electroporation was performed using BTX Electro Cell Manipulator 600 under the following conditions: 50 µF, 2.5 kV and a time constant of 5.0-5.4 ms. Immediately after electroporation, 1 ml pre-warmed SOC medium was added and the cells were incubated for 1.5 h at 32°C. Cells were spread on plates with the appropriate antibiotics (for BAC DNA: chloramphenicol; for plasmid DNA: ampicilline and for insert DNA: kanamycin) and incubated overnight at 32°C.

4.1.2.8 Recombination in EL250

A single bacterial colony from the EL250 strain containing the BAC was picked and inoculated into 2 ml LB and incubated at 32°C overnight. Next day, 2.5 ml overnight culture were transferred to 250 ml LB and incubated until OD_{600} = 0.5 was reached. The culture was stored at 42°C (15 – 20 min) for the induction of the recombinant proteins, which are under the control of a heat inducible promoter. Afterwards the cells were kept on ice for another 15

min before they were prepared for electroporation of the insert DNA into EL250 (see 4.1.2.7). After electroporation, the cells were spread on plates containing kanamycin. Since the insert DNA provides kanamycin resistance, only successful homologous recombination events resulted in resistant colonies and were analyzed for positive recombination events either by PCR or by Southern blotting.

4.1.2.9 Excision of neomycin resistance cassette

Frt sites of the same orientation flank the kanamycin resistance gene within the amplified insert DNA used for homologous recombination. Those Frt sites can be recognized by Flp recombinase, which leads to an excision of the flanked DNA. Flp recombinase can be induced in the positively recombined EL250 clones by application of 0.1% L(+) arabinose for 1 h at 32°C. Afterwards the cells are spread on chloramphenicol plates and resistant clones need to be screened for successful removal of the kanamycin gene by PCR or by Southern blotting.

4.1.2.10 Screening recombined BAC clones by Southern blotting

The NEBlot Phototope and Phototope-Star Detection Kit (NEB) were used for chemiluminescent detection of nucleic acids from Southern blots.

Maxi-prep DNA from several chosen recombined BAC clones were digested for 12 h at 37°C as well as with *Bgl*II (O+ buffer) and with *Afl*II (O+ buffer). The restriction enzymes were chosen to cut within the known DNA sequences (*Afl*II) and to cut only in the genomic sequence outside (*Bgl*II) and the probe was designed to hybridize onto the known DNA fragment (EGFP probe = 340 bp) so that they would generate DNA fragment band of known-size. For separation of digested DNA fragments, a 0.7-1.0% agarose gel was used (running conditions: 25 volts, about 20 hrs; or 90 volts, about 6 hrs; changing buffer every 2 hrs). The gel was put into Denaturing buffer (1 M NaOH) for 30 min and then into the Renaturing buffer for 30 min with gentle shaking. Gel was placed on pre-soaked 3-4 layers of WHATMAN paper (Whatman), which was placed on a 'Bridge' over the 20x SSC pool. The membrane was rinsed first with Mili-pore water (Mili-pore), then with 10x SSC buffer and placed on the gel (avoid air bubbles). The sides were sealed with parafilm. 4-layers of

10x SSC presoaked WHATMAN papers were added on top of the membrane. Another 3 cm-thick dry WHATMAN paper was placed on top before placing 3 cm-thick dry paper towels. A weight of about 500 g was placed on top. The transfer was left for 16-20 hrs overnight. The next morning the membrane was washed in 5x SSC buffer twice for 10 min and then air- dried. The DNA was cross-linked onto the membrane by 2 times UV-light automatic cross-linking (Stratagene) and then pre-hybridized. 20 ml of Quick-Hyb. solution (QIAGEN) was used for pre-hybridization. The membrane was pre-hybridized for 1 hour at 68°C. At the same time, the probe was labeled using NEBlot Phototope Kit according to the manufacturers instructions. Following pre-hybridization, hybridization of the membrane was performed. The labeled probe DNA was heated at 95°C for 5 min in a screw-cap Eppendorf-tube before it was added into the hybridization tube. The membrane was hybridized overnight at 68°C. After hybridization, the membrane was washed twice for 5 min in 2x SSC, 0.1% SDS at RT. Afterwards the membrane was washed twice for 15 min in 0.1x SSC, 0.1% SDS at 68°C with gentle shaking. Finally, chemiluminescent detection was performed using Phototope-Star Detection Kit according to the manufacturer's instructions.

4.1.2.11 Preparation of recombined BAC DNA for pronucleus injection

One BAC clone, which was positive in the Southern blot analysis and showed no sequence errors at the junctions and within the ORF of GFP after sequencing, was used to make a large-scale overnight culture to produce sufficient amounts of DNA. BAC DNA was isolated (see 4.1.1.4) and digested afterwards with 50U *Not*I (1x O+ buffer) including 1x spermidine for 24 h at 37°C to release the BAC backbone. Following digestion, the enzyme was heat inactivated for 20 minutes. The BAC DNA was precipitated and was separated from its backbone via sepharose chromatography (Sephadex Cl4b column) before used for pronucleus injection.

4.1.2.12 Sepharose chromatography

The column was prepared in sterile 5 ml plastic pipettes using Sephadex Cl4b (Amersham). The cotton within the pipette is brought to the tip that the

sephadex solution cannot drop out of the tip after loading. After loading up to 1-2cm of sephadex solution into the pipette the sepharose is equilibrated with 10 ml injection buffer. During this process special attention was paid to always keep sepharose covered with buffer to prevent dehydration. Then 0.5 ml of DNA loading buffer is applied to the column followed by loading the BAC DNA solution. Shortly before the loading buffer enters the sepharose another 10 ml of buffer were loaded onto column. 1 ml fractions were collected and those were analysed by gel electrophoresis to reveal the fractions containing the BAC insert fragment. The fractions containing the BAC insert fragment (and not the backbone) are pooled and purified with the Microcon-50 Dialysis Kit (Millipore). The quality and concentration is assessed by gel electrophoresis and OD quantification.

4.1.2.13 Pronucleus injection

Frank Zimmermann and Sascha Dlugosz performed the pronucleus injection in the transgenic unit of the “Zentrales Tierlabor” (ZTL). For nuclear injections a clean preparation ($OD_{260/280}$ = 1.8) and 1-2 µg/ml of concentrated BAC DNA were provided. The transgenic lines were maintained in the ZTL.

4.1.2.14 Founder analysis by PCR

One primer specific for GFP (VB502) and two primers specific for *Lypdc1* (VB501, VB502wt) were designed to analyze the founders for positive integration events. The expected band size for the BAC transgene is 334 bp and the wildtype gene product has a size of 484 bp.

4.1.2.15 Founder analysis by anti GFP staining

The protocol for immunohistochemical stainings on vibratome sections is described in 4.4.3. To reveal the expression pattern of the reporter gene within the transgenic founder mice, which were positively genotyped, 5 coronal sections per animal were stained against GFP.

4.1.2.16 Genotyping of mouse lines by tail PCR

Mouse-tails from transgenic mouse lines were digested with Proteinase K (1 mg/ml) in TENS-buffer at 55°C for 8-12 hours. After precipitation by 1 volume

of isopropanol and washing with 70% ethanol, the genomic DNA was resolved in 100-300 µl distilled water. Genotyping PCRs were setup in 25 µl reactions, containing PCR-buffer (GibcoBRL), 2 mM $MgCl_2$, dNTP-mix (0.2 mM per nucleotide), specific sense- and antisense primers (each 0.4 µM), 0.2-0.5 U Taq-Polymerase, ddH_2O and 1 µl template-DNA-solution (10-100 ng/µl).

4.2 RNA detection

4.2.1 *In situ* hybridization

In situ hybridization on coronal 15 µm brain sections was done according to Wisden et al. (1991), using the following oligonucleotides:

ASexon2oligo: AATTTACGATGAACTCAGGGGATGAGCAATCGTTGTTCAG

ASexon2-3oligo:

GAGACAGGCTGCTGACGATGCACACGACTTCCGGTACATGATCCCAGCA

NR1 positive probe: GAACTGACAGTCCTACTAGCAACCACAGTGTGCTC

Briefly, the cryostat sections were cut from unfixed tissue and then postfixed with 4% PFA and stored in ethanol at 4°C until they were used for ISH. The oligonucleotides (0.3 pmol/µl for 50-55mers) are radiolabeled using terminal deoxyribonucleotide transferase (Roche) and "hot" deoxyadenosinetriphosphate (^{35}S-ATP, 10 pmol). This results in addition of roughly 10-20 AMP residues to the 3´end of the oligonucleotide. A total volume of 25 µl reaction contained 1 µl oligo (0.3 pmol), 5 µl 5x reaction buffer (Roche), 2.5 µl 25 mM $CoCl_2$ (Roche), 2.5 µl ^{35}S-ATP (1300 Ci/mmol, DuPont, NEN, NEG-034H), 1µl TdT rec. (Roche) filled up with DEPC-H_2O to 25 µl and was incubated for 10-15 min at 37°C. The reaction was stopped by adding 25 µl TE buffer and unincorporated nucleotides are removed by applying the reaction to a BioRad Spin column followed by brief centrifugation. 2 µl of the eluate is subjected to liquid scintillation counting to reveal efficacy of labeling (the counts should be in the range of 50.000 dpm/µl – 200.000 dpm/µl). Finally, 1 µl of DTT (dithiothreitol; 1 M stock: 3.09 g in 20 ml dH_2O) was added to the eluate to prevent probes from oxidation. 1-2 µl of labeled probes were diluted in 100 µl/coverslip "minimalist hybridization buffer" (Wisden et al., 1991) and applied to the cryostat sections for incubation at 42°C overnight. The next day, excess probe was washed off with SSC and after dehydrating and drying the sections they were exposed to X-ray film (Kodak).

4.3 Tissue Culture

4.3.1 Transfection of HEK293 cells for virus production

HEK293 cells were cultured in DMEM supplemented with 10% FCS and 50 mg/l penicillin/streptomycin in 5% CO_2 at 37°C. Transfections were performed by calcium phosphate transfection with 10 µg total DNA for 94mm plates. Helper plasmid (pDP1, total amount 5 µg) was mixed together with the rAAV vector (total amount 5 µg) and used for calcium phosphate transfection.

4.4 Biochemical assays

4.4.1 Virus Harvesting and Purification via Iodixanolgradient

Sixty to 72 hours after transfection cells were harvested from the plates after removing the supernatant by using a cell scraper. Cells were resuspended in 10 ml lysis buffer/10 plates (150 mM NaCl, 50 mM Tris pH 8.0) and 500 µl 10% DOC + 2 µl Benzonase (336U/µl) was added after resuspension and incubated for 30 min at 37°C. Then 584 mg NaCl/10ml buffer was added and incubated another 30 min at 56°C. Afterwards the cells were “shock frozen” in ethanol dry-ice bath for approximately 10 min and thawed afterwards in a 37°C waterbath and subsequently spun for 30 min at 4000-7000rpm. Supernatant, containing the virus particles, was removed from the pellet and thaw/frozen once again and spun once again. The sample (supernatant) is carefully loaded on the discontinuous iodixanolgradient (3 ml 54%, 3 ml 40%, 4 ml 25%, 6 ml 15%) and spun for 1.5 hrs at 60000rpm (70 Ti-rotor) at 18°C. The viral particles are mainly found above the 40% fraction and were taken off carefully with a syringe. The viral particle solution was then further concentrated using Amicon concentrators and washed 2-3 times with 1x PBS-MK. After concentrating the solution down to roughly 200 µl, the preparation was aliquoted into 20 µl samples and frozen for long term storage at -70°C.

4.4.2 Comassie staining and Western blotting

After virus purification a total volume of 10 µl of virus solution diluted in 5x WB-sample (Lämli) buffer was loaded on 10% SDS-PAGE gel and run at constant 130 V for 45 min – 1 h. The gel was then stained with Coomassie blue to visualize all proteins separated on the gel. Successful and clean

purification resulted in only 3 bands corresponding to the viral proteins (VP1=87kD; VP2=73kD; VP3=62kD).

For western blotting, depending on the molecular weight of the proteins being detected, 8-10% SDS-PAGE gels were prepared. Protein samples were diluted in 5x Lämli buffer and run at constant 130 V for 45 min – 1 h using WB-Running buffer. The separated proteins were transferred by "wet transfer method" using WB-Blotting buffer onto Hybond-LFP (Amersham) membrane at constant 30 V overnight. Membranes were blocked (10% fat free milk in 1x PBS-T) for 2 hours followed by incubation with primary antibody in the given dilution in PBS-T for 1 h at RT. After washing the membrane several times the secondary antibody was added and incubated for 1 h at RT. Proteins were visualized by chemiluminescence using the ECL detection kit (Amersham).

4.4.3 Immunohistochemistry (IHC)

Animals were anesthetized with isoflurane and perfused intracardially with PBS (approximately 15 ml) followed by 4% PFA/PBS (approximately 15 ml) to fix the tissue. Brains were extracted and post-fixed in 4% PFA/PBS at 4°C overnight. For DAB staining, vibratome cut sections (70-100 µm spacing) were incubated in 0.5% H_2O_2 for 10 min to reduce non-specific background signals followed by incubation in Day1 blocking buffer (Day1 + 4% NGS). For fluorescent staining, vibratome sections were incubated immediately in Day1 blocking buffer. The first antibody was diluted in Day1 buffer + 1% NGS and incubated overnight at RT. Next day, the sections were washed several times with Day2 buffer and then the secondary antibody diluted in Day2 buffer was incubated for 1 hour at RT (in darkness for fluorescent staining). Finally, after several washing steps in Day2 buffer and 1x PBS, the sections were dried and then mounted with Aquamount on coverslips and analyzed using a Zeiss confocal microscope.

4.4.4 Confocal microscopy

Confocal images were obtained using a Zeiss LSM5 PASCAL confocal laser scanning microscope. Images were obtained through excitation of an argon laser (excitation, 488 nm; emission, BP505–530 nm emission filter) for FITC-labeled signals, and a He-Ne laser (excitation, 543 nm; emission filter, LP560

nm) for Cy^3-labeled signals. ImageJ was used to process the confocal images. For the estimation of the Cre infection area in rAAV-Cre injected mice compared to the total area of the LA, the LA dimension was assessed for one WT brain stained against NeuN-Cy^3 (Fig. 20). The determined dimension was taken as average for total LA area in all mice.

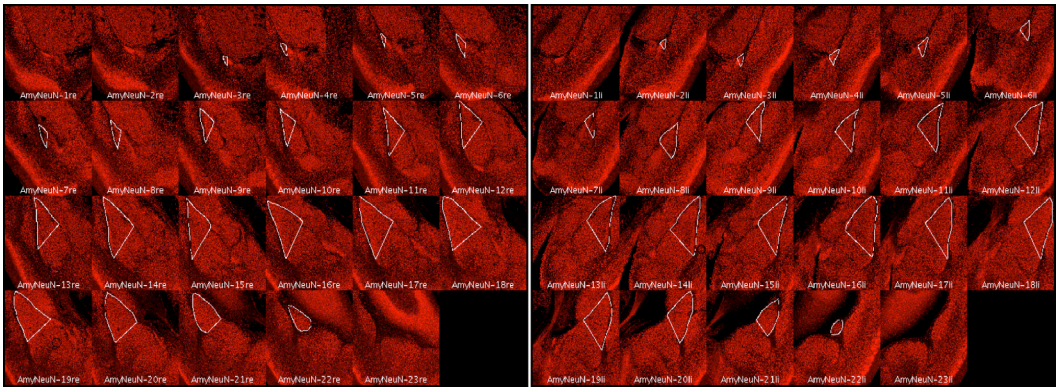

Fig. 20: Area quantification of total LA. Confocal images of WT coronal brain sections stained against NeuN-Cy^3 (red). A total of 23 slices were stained against NeuN, spanning the entire LA. Areas of LA from anterior to posterior (visually judged in accordance to mouse brain atlas) are outlined in white. ImageJ "area" value (right): 309297.0; ImageJ "area" value (left): 328428.0. Mean of left and right: 318862.5 = 100%.

4.5 Stereotaxic injections

4.5.1 Subjects

Young adult (4-6 weeks old) male mice from AQ2lox line (i.e. GluR-$A^{2lox/2lox}$ mice) were injected with the viral constructs of interest (see 4.5.2) under general anesthesia (see 4.5.3). Three to 4 weeks after surgery, during which the rAAV vector reached a steady level of expression and subjects recovered from surgery, the behavioral training was started (see 4.6). All mice were individually caged and maintained on a 12 hours light-dark cycle. All behavioral training was conducted during daytime. Animals had free access to food and water at all times. All animal care and procedures were in accordance with the German animal welfare guidelines specified in the TierSchG.

4.5.2 Viral constructs

pAAV-hSyn-iCre/IRESvenus:

The Cre recombinase is under the control of the human synapsin promoter

followed by an internal ribosomal entry site (IRES) for the independent translation of a second ORF - in this case Venus - from the same transcript. Two proteins are expressed from one mRNA, however it is known that cDNAs downstream of IRES elements are less strong expressed then directly from the promoter itself.

pAAV-6P-SEWB:

GFP is under the control of the human synapsin promoter.

4.5.3 Surgery

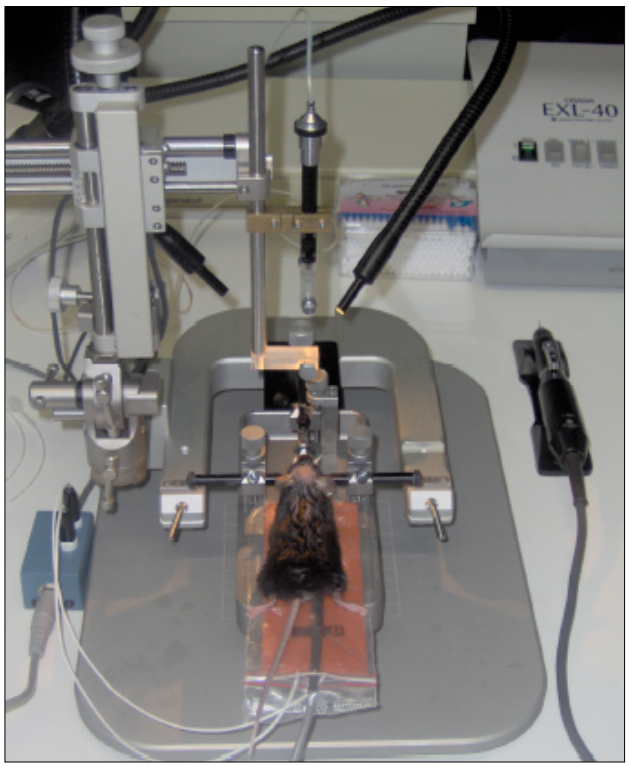

Fig. 21: Stereotactic device used for surgery.

The BENCHMARK stereotaxic instrument (Fig. 21) was used in combination with the LEICA MZ6 stereomicroscope and KL 1500 electronic light guide. The anterioposterior axis (for coronal planes) is referred to as Y-axis, the medio-lateral (for saggital planes) as X-axis and the dorsoventral (for horizontal planes) direction as Z-axis. The injection capillaries were pulled on a P97 horizontal puller using marked micropipettes (5* µl, intraMARK, BlauBrand). The specific settings of the needle puller resulted in elongated tips (Heat 660, VEL = 54). This elongated tip was then trimmed with scissors to approximately 1.2 cm length to obtain a very sharply edged tip with a diameter of 10-40 µm. The 1 µl calibration marks on the pipette were used to estimate the volume of injecting solution, with each section corresponding to ~70-80nl. The mice were anesthetized with i.p. injection of ketamine (100 mg/kg) / xylazine (10 mg/kg). Experimental animals were kept deeply anesthetized by monitoring hindlimb withdrawal, eyelid reflex and respiration rate. A heating block (FHC) was utilized to maintain the animals body temperature. In preparation for the surgery the scalp was

shaved with an electrical trimmer. The eyes of the animal were covered with an eye ointment. The tip of the tongue of animal was kept outside the mouth to avoid accumulation of fluids in pharynx. Then the animal was mounted on the instrument by placing the ear bars into the external auditory meatus. It was made sure that the tip of the ear bar was fit into the socket very well. The incisor bar was placed so that the upper incisors hooked over the front inside edge. It was ensured that the lower incisors are underneath the bar. The snout was pressed down against the bar using the snout holder to make sure that the head is stabilized properly for all surgical procedures. As a first step in the surgery, a midline incision in the scalp was conducted. Enough pressure was applied during cutting to produce a clean cut in one stroke. Then the skin was kept apart laterally using two clips to make enough space on the skull. The skull was cleaned by a scalpel and PBS solution to see the reference point bregma unambiguously. Craniotomies above the desired location (Y=1.5; X=3.3-3.4) were done with a dental drill. Then the injection pipette was mounted on dorso-ventral axis of the stereotaxic instrument and filled with viral solution by dipping the tip into a drop of solution while applying negative pressure with a syringe. Pipette tip was positioned at the bregma and X, Y and Z axes were set to zero. A total of 1-3 injections per hemisphere were made and at each injection spot around 80-320 nl of viral preparation was injected (Z=3.7-3.8). The solution was injected by application of manual pressure with a syringe. After the injections were finished in one hemisphere, the injections in the second hemisphere were done at the same measurements. Finally, the skin was sutured and animals were kept at 37°C to recover from anesthesia. All surgical manipulations were done under optical control using a LEICA MZ6 stereomicroscope.

4.6 Cued fear conditioning

4.6.1 Subjects

Animals used in the fear conditioning paradigm were either from the A1lox line (complete GluRA knockouts, Zamanillo et al., 1999) or were generated to lack GluRA specifically in the lateral amygdala by stereotaxic injection of a Cre expressing vector into GluRA floxed (GluR-$A^{2lox/2lox}$ mice) (see above). Animals injected with a GFP expressing viral construct or uninjected mice

served as controls. In the case for the A1lox group, the mice were either homozygous for the GluR-A deletion or wildtype mice, which served as controls. The experimenter was blinded to the genotype of the animals until the end of training.

4.6.2 General mice handling prior to behavioral testing

Mice were taken out of their cage by the tail and placed on the experimenter's arm wearing a lab coat. This was done until the mice were used to the experimenter and to the fact that they were taken out of the cage.

4.6.3 Apparatus

The behavioral procedure was performed using the TSE Fear conditioning system (TSE systems). The system has been developed to study contextual and cued fear conditioning in rodents. The system consists of the following components: 1) a box with animal location sensors, shockable grid and test arena; 2) a box housing with loudspeaker, light and ventilator; 3) a control unit with integrated shocker/scrambler and 4) TSE software for fear conditioning analysis. The base construction includes the animal detection sensors where an animal’s position inside a removable Perspex arena, which can be placed inside the sensor frame (dimension: 25 cm x 25 cm x 35 cm, black (context A) and transparent (context B)), is monitored using infra-red light barriers. Each single light barrier consists of one infra-red transmitter and one receiving senor. The basic sensor level, the so-called X-Y level, is used to determine the horizontal coordinates of the animal and thus its location. With the control unit it is possible to generate a sound for creating the conditional stimulus (CS, 7.5 kHz) and white noise (max. intensity 100 dB). The amplitude of the sound, the frequency as well as the light intensity can be adjusted according to the experimenter’s demands. The shocker/scrambler is a microprocessor controlled current generator in which the amplitude of the current is adjustable in steps of 0.1 mA up to 3 mA. The software controls the test in the box, collects, displays and stores all experimental data and allows for detailed analysis and documentation.

4.6.3 Procedure

Experimental groups were habituated to the conditioning chamber one day prior to conditioning unless specified otherwise. During the habituation phase of the training, animals were placed in the conditioning chamber (black Perspex arena; shock grid accessible = context A) and allowed to freely move around for a period of 8 min. The animal's activity and location within the arena was monitored throughout this session. At the conditioning day (acquisition phase) mice were transferred to the conditioning chamber (black Perspex arena, shock grid accessible/visible = context A) and after an initial acclimatization period of 6 min animals received either three pairings (multi-trial) or one pairing (one-trial) of the auditory conditioning stimulus paired with foot shock (0.4 mA, 2 sec or 0.5 mA, 1 sec, respectively). In case of the three pairing paradigm, the cue was present for 30 sec, which was co-terminated by the foot shock (0.4 mA, 2 sec) and in case of the one pairing paradigm the cue was present for 20 sec, which was co-terminated by the foot shock (0.5 mA, 1 sec). Pairings were separated by 2 min (ITI) and mice were removed from the chamber 30 sec, 2 min or 2.5 min after the last shock presentation (Fig. 22). 24 h after the acquisition phase animals were tested for long-term retention of the fear memory (e.g. CS-induced conditioned responses) in the CS extinction phase of the training. For this test, the chamber was rearranged to create a new contextual configuration, therefore the transparent Perspex arena was used instead of the black one and a PVC plate covered the shock grid. For the multi-trial paradigm, the CS was present for 8 min after an initial 6 min pretone/acclimatization period. For the one trial paradigm, there was a 1 min pretone/acclimatization phase followed by presentation of the CS for another minute. In both paradigms, the animals were taken out of the chamber 30 sec after the CS presentation terminated. During the entire session the animal's position was recorded.

4.6.4 Scoring

During each stage of the experiment, the mouse's tendency to freeze was scored by the integrated TSE software. The TSE system counts a freezing event if the animal has not been moving for > 1 sec. The total freezing duration in each individual sub-phase (during CS and during ITI) was

recorded and from this data the percentage freezing during those different stages was calculated.

Multi-trial paradigm:

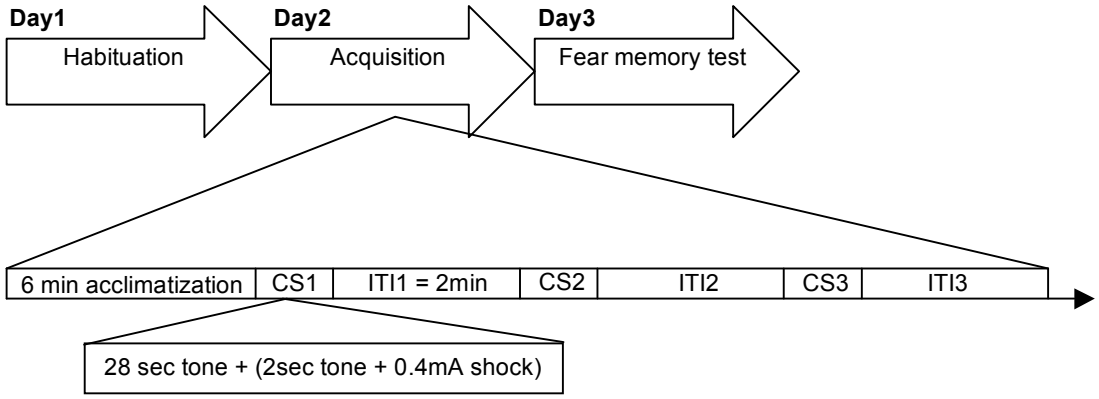

One-trial paradigm:

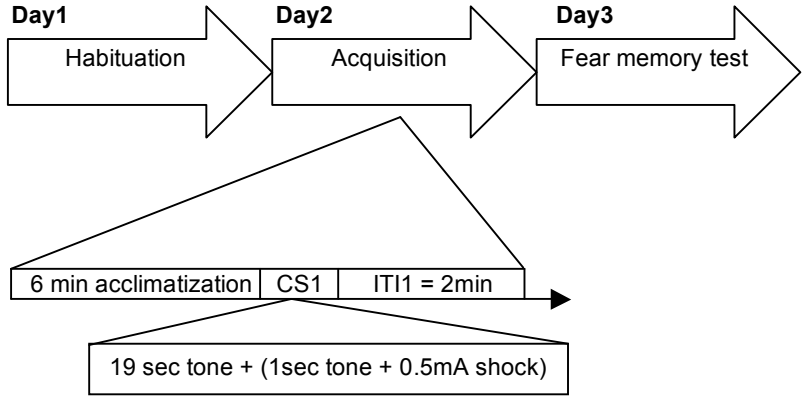

Fig. 22: Schematic representation of fear conditioning paradigms.

4.6.5 Data analysis

The data processing was performed in Matlab 7.0 (Mathwork) to generate a continuous time line for the data collected with the TSE system. An animal was immobile when it moved less then 1 cm/sec. The mobility scores were averaged and displayed in 10 sec/bins. Data were represented as mean ± SEM. Student's *t* test was employed to compare the differences between genotypes. For the statistical analysis a p-value less than 0.05 was considered to be statistically significant. To test for different quantification

methods an analysis was done with one group of experiments to compare the above-mentioned threshold data quantification method with non-thresholded quantification of mobility. There were no significant differences between these quantification methods (Fig. 23) and therefore the prior method was used for all behavioral data processing.

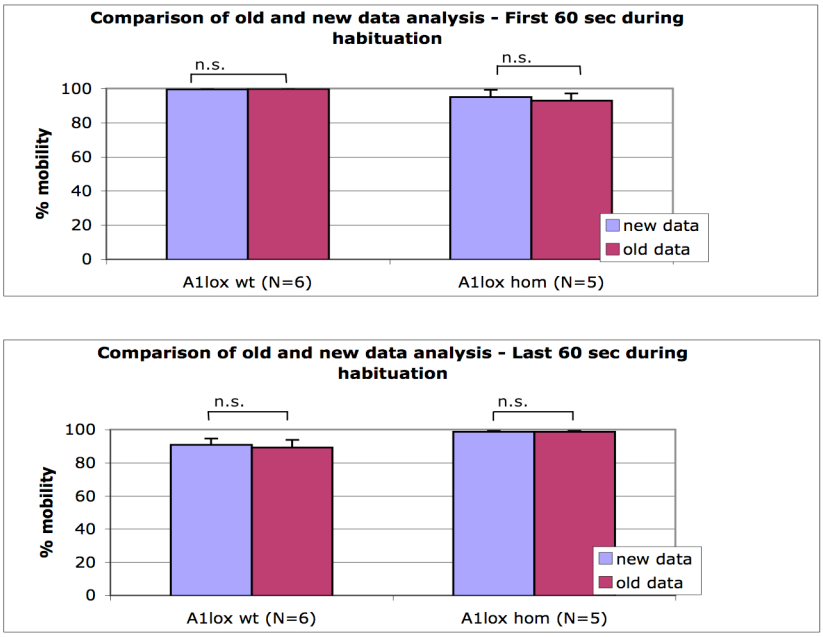

Fig. 23: The mobility scores do not depend on the way data analysis is performed.
The average mobility for the first 60 sec (A) and last 60 sec (B) during the habituation phase is shown for both quantification methods. There was no significant difference between different methods of data analysis (A: $WT_{(new)}$=90.8 ± 3.9%, $WT_{(old)}$=89.2 ± 4.5%, p>0.05; $KO_{(new)}$=98.7 ± 0.6, $KO_{(old)}$=98.7 ± 0.6, p>0.05). Old data quantification (interpolation method with threshold for immobility <1cm/sec) was used for all behavioral data analysis.

5. Materials

5.1 Special reagents

Agarose	Invitrogen
L(+) arabinose	Sigma
APS	Sigma
Aquamount	Polysciences
5-Brom-4-Chlor-3-Indolyl-β-D-Galactopyranosid (X-Gal)	Gerbu
Bromphenolblue	IBI
Precision Plus Protein Standard	Bio Rad
Bovine serum albumin (BSA)	Sigma
3,3`-Diaminobenzidin (DAB)	Fluka
DMSO	Sigma
EDTA	Merck
Ethanol	Roth
Ethidium bromide	Serva
Glycerol	Merck
Isofluran	Baxter
Isopropanol	Fluka
Ketamine	Inversa
Licain (Lidocaine)	Delta Select
ß-Mercaptoethanol	Sigma
Normal goat serum	Vector
Penicillin/Streptomycin	Gibco
Polyacrylamide	Bio Rad
Paraformaldehyd, 37 %	Merck
Potassiumferrocyanid (K_6 Fe $(CN)_6$)	Sigma
Potassiumferricyanid (K_3 Fe $(CN)_6$)	Sigma
Phenol / Chloroform	Roth/Merck
Quick-Hyb-Solution	Stratagene
Random Primed DNA Labeling Kit	Roche
Sodium dodecylsulfate (SDS)	Serva
Sodium acetate	Merck
Salmon sperm DNA	Roche
Triton X-100	Merck

TEMED	Bio Rad
Trizma	Sigma
Hydroxy peroxide, 30%	Roth
Xylazine	Bayer

5.2 Antibiotics

Kanamycine	Sigma
Tetracycline	Sigma
Ampicilline	Sigma
Chloramphenicol	Roche

5.3 Enzymes

Benzonase	Sigma
E.coli DNA-Polymerase I (Klenow-Fragment)	Roche
Proteinase K	Roche
Restrictionendonucleases	MBI/NEB
T4-DNA-Ligase	Roche
Taq-DNA-Polymerase	Gibco BRL
KOD Hifi Polymerase	Novagen

5.4 Antibodies (dilutions for IHC)

Anti-GFP (rabbit) (1:5000-8000)	Clontech
Anti-NeuN (mouse) (1:1000)	Chemicon
Anti-Cre (rabbit) (1:3000)	Convance
Anti-GluRA (rabbit) (1:200)	Chemicon
Anti VP1/2/3 (1:250-500)	Progen
Secondary antibodies	
Cy3-conjugated (1:200)	Dianova
FITC-conjugated (1:200)	Dianova
Peroxidase-conjugated (1:600)	Dianova

5.5 Nucleotides

Desoxyribonucleotides (dNTPs)	MBI
αS^{35}dATP	Roche

5.6 Mouselines

AQ2lox	Gria1 exon11 flanked by loxP
A1lox	Gria1 exon11 deletion

5.7 *E.coli* strains

Top 10	Invitrogen
SURE cells	Stratagene
EL250	Research – Genetics

5.8 Technical devices

Biospin 6 column	Biorad
Coverslips (24x50 mm)	Roth
Whatman paper 3MM	Whatman
Microscope slides (76x26 mm)	Menzel-Gläser
Hybond-LFP	Amersham
Safe-lock tubes, 1,5 ml, 2 ml	Eppendorf
MicroAmp tubes 200 µl	Perkin Elmer
Falcon tubes, 50 ml, 400 ml	Nalgene
Uvette	Eppendorf
Amicon Ultracel 100K	Millipore

5.9 Special devices

Optima LE 80 K Ultracentrifuge	Beckman
Biophotometer	Eppendorf
Biofuge fresco Centrifuge	Hereaus
Concentrator 5301 (SpeedVac)	Eppendorf
Labofuge 400L Centrifuge	Hereaus
PCR Thermocycler GeneAmp PCR-System 9600	Perkin Elmer
Vibratom VT1000S	Leica
UV-Spectrophotometer Ultrospec 3000	Pharmacia
Heating Pad	FHC
DC Temperature Control Unit	FHC
Termistor Probe	FHC

Benchmark stereotaxic instrument	myNeurolab
Leica MZ6 stereo microscope	Leica
KL 1500 eletronic light guide	SCHOTT
Osada EXL-40	Osada
Micropipette Puller P-97	Sutter Instr.
Zeiss Axiovert 200M	Zeiss
TSE fear conditioning system	TSE systems

5.10 Special software

Adobe Photoshop CS2	Adobe Systems
DNS Strider 1.3	CEA
Gene Construction Kit, Version 2.5.5	Textco
Microsoft Word X for Mac	Microsoft Corp.
Microsoft Excel for Mac	Microsoft Corp.
Microsoft Powerpoint for Mac	Microsoft Corp.
Seqman	DNASTAR
Editseq	DNASTAR
ImageJ	NIH, USA

5.11 Primers

For Cre amplification from pRK7.iCre plasmid:

3`*Hind*III: tgccaagaagctttcagtttcagtccccatcctcg

5`*Nhe*I: acattgctagcgtccaccatggtgcccaagaag

For amplification of the modification cassette from pEGFP-N1M-FRT plasmid for targeting into *Lypdc1*-BAC clone:

Lypdc1.armdown: gcactggggctgagagcagggacgcttggcgagatagcaggagcgtgtct ggccaggcagctggcctcttcatcttcttagagtaacctgaggctatggc agggcctgaagttcc

Lypdc1.armup: tcgccgcggccagaacagcctccgctgcggtcgtggtctctgatgctctt gcccgctcccggccctgccgatccgggaggatggtgagcaagggcgagga gctgttcacc

For plasmid sequencing:

VGPF1: cttsacytcrgcgcgggtcttgtag
VGFP2: gmgaycacatggtcctgctggag
iCre mid: cattgcctacaacaccctgctg
iCRe mid.rev: cagcafggtgttgtaggcaatg

For amplification of the EGFP probe for Southern blot:

VGPF1: cttsacytcrgcgcgggtcttgtag
pEGFP-SEq-5s: atggtgagcaagggcgaggagc

For genotyping of BAC founders:

VB501: cagggagcgcgaatccaaggagc
VB502: cctcgccggacacgctgaacttgt
VB502wt: ctcggctctcctgcagcgcggga

For genotyping 1) AQ2lox and 2) A1lox mice line:

1) MH60: cactcacagcaatgaagcaggac
3´intro3: ctgcctgggtaaagtgacttgg
2) 1005: aatgcctagtactatagtgcacg
3´intro3: ctgcctgggtaaagtgacttgg
2x1Lox-pz: cactcacagcaatgaagcag

5.12 Solutions

1x PBS: 137 mM NaCl
2.7 mM KCl
1.4 mM KH_2PO4
4.3 mM Na_2HPO_4, pH 7.4

1x PBS-T: 1x PBS, 0.05% Tween

1x PBS-MK: 1x PBS, 1 mM $MgCl_2$
2.5 mM KCl

Proteinase K buffer (TENS -): 100 mM Tris/HCl pH 8.0
5 mM EDTA
200 mM NaCl

	0.5% SDS + Proteinase K (final conc.: 100 µg/ml) added shortly before use
100x TE:	1 M Tris/HCl pH 7.6, 10 mM EDTA
10x DNA loading buffer:	30% Glycerol 0.25% Bromphenolbleu 0.25% Xylencyanol 25 mM EDTA
1x TAE buffer:	40 mM Tris 5 mM Sodium acetate 2 mM EDTA pH 8.3
20x SSC	3 M NaCl 300 mM Sodium acetate adjust with NaOH to pH 7
Denaturing solution:	1.5 M NaCl 0.5 M NaOH
Renaturing solution:	1.5 M NaCl 1.5 M Tris/HCl pH 7.5
Day 1 buffer:	1% BSA 0.3-0.5% Triton X-100 in 1x PBS
DAB staining solution:	0.04% DAB 20 mM Tris pH 7.6 $7.5x10^{-3}$% H_2O_2

Day 2 buffer:	Day1 buffer diluted 1:3 in 1x PBS
WB-Running buffer (10x):	250 mM Trizma 1.92 M Glycine 1% SDS add to 1l with dH_2O pH 8.3
WB-Blotting buffer (1x):	25 mM Trizma, 192 mM Glycin 10% (v/v) Methanol
WB-Sample (Lämli) buffer (5x):	500 mM DTT 10% (w/v) SDS 50% (v/v) Glycerol, 250 mM Tris/HCl pH 6.8, 0.5% Bromphenolblue, add 10% (v/v) 2-Mercaptoethanol just before use
Coomassie staining solution:	2.5% (w/v) Coomassie-Brilliant-Blue 4% (v/v) Methanol 45% (v/v) dH_2O 10% (v/v) Acetic acid
Coomassie destaining solution:	7.5% Glacial Acetic acid 5% Methanol add to 1l dH_2O
4% Paraformaldehyde:	200 g Paraformaldehyde 2.5l dH_2O add 10 M NaOH (until solution becomes clear)

	add 2x PBS 1:1, pH 7.3 (adjusted with HCl)
LB medium:	1% (w/v) Bacto-Trypton, 0.5% (w/v) Yeast extract 1% NaCl
2YT medium:	2.6% (w/v) Bacto-Trypton 1.6% (w/v) Yeast extract 0.8% (w/v) NaCl add to 3l dH_2O, pH 7.5 (adjust with 2 M NaOH)
Pronucleus Injection buffer:	10 mM Tris/HCl 0.1 mM EDTA 100 mM NaCl 3x sterile-filtered

6. Abbreviations

α	alpha
AMPA	α–amino-3-hydroxy-5-methyl-4-isoxazoleproionate
rAAV	recombinant adeno-associated virus
BAC	bacterial artificial chromosome
BNST	bed nucleus stria terminalis
BLA	basolateral amygdala
BSA	bovine serum albumin
bp	base pair
CA1	cornu ammonis 1
CeA	central amygdala
Cb	cerebellum
CNS	central nervous system
Cpu	caudate putamen
CR	conditioned response
CS	conditioned stimulus
C-terminal	carboxyl (COOH)-terminal
Cy^3	cyanine dye 3
Cx	cortex
Da	Dalton
DAB	3,3` diaminobenzidine
DG	dentate gyrus
DMEM	Dulbecco´s Modified Eagle medium
DMSO	dimethyl sulfoxide
DNA	desoxyribonucleic acid

DPI	days post infection/injection
ds	double stranded
mGluRs	metabotropic glutamate receptors
NMDA	N-methyl-D-aspartic acid
dNTPs	desoxynucleosid triphosphate
EDTA	ethylenediaminetetraacetic acid
EGFP	enhanced green fluorescent protein
et al.	and others
FCS	fetal calf serum
FITC	fluorescin isothiocyanate
g	gram
GABA	gamma-aminobutyric acid
h	hour
Hp	hippocampus
iGluRs	ionotropic glutamate receptors
IHC	immunohistochemistry
ISH	*in situ* hybridization
ICM	intercalated cell mass
ITI	intertrial interval
k	kilo
kD	kilo Dalton
KO	knockout
LA	lateral amygdala
LTP	long-term potentiation
m	milli

mA	milliampere
mGluRs	metabotropic glutamate receptors
M	molar
min	minute
mRNA	messenger ribonucleic acid
nl	nano litre
NMDA	N-methyl-D-aspartate
OB	olfactory bulb
P	postnatal day
PAGE	polyacrylamide gel electrophoresis
PBS	phosphate buffer saline
PBS-T	PBS-Tween
PCR	polymerase chain reaction
PFA	paraformaldehyde
pH	potentia hydroxy
PiCx	piriform cortex
RNA	ribonucleic acid
RPM	rounds per minute
RT	room temperature
sec	second
SEM	standard error of mean
SDS	sodium dodecyl sulfate
TE	Tris/EDTA buffer
U	unit
US	unconditioned stimulus

V	volt
VGCCs	voltage gated Ca^{2+} channels
VP	viral protein
µ (m, l)	micro (metre, litre)
WT	wild type

7. References

Amorapanth P, LeDoux JE, Nader K (2000) Different lateral amygdala outputs mediate reactions and actions elicited by a fear-arousing stimulus. Nat Neurosci 3:74-79.

Bauer EP, Schafe GE, LeDoux JE (2002) NMDA receptors and L-type voltage-gated calcium channels contribute to long-term potentiation and different components of fear memory formation in the lateral amygdala. J Neurosci 22:5239-5249.

Blair HT, Schafe GE, Bauer EP, Rodrigues SM, LeDoux JE (2001) Synaptic plasticity in the lateral amygdala: a cellular hypothesis of fear conditioning. Learn Mem 8:229-242.

Blair HT, Sotres-Bayon F, Moita MA, Ledoux JE (2005) The lateral amygdala processes the value of conditioned and unconditioned aversive stimuli. Neuroscience 133:561-569.

Bliss TV, Collingridge GL (1993) A synaptic model of memory: long-term potentiation in the hippocampus. Nature 361:31-39.

Campeau S, Davis M (1995) Involvement of subcortical and cortical afferents to the lateral nucleus of the amygdala in fear conditioning measured with fear-potentiated startle in rats trained concurrently with auditory and visual conditioned stimuli. J Neurosci 15:2312-2327.

Campeau S, Davis M (1995) Involvement of the central nucleus and basolateral complex of the amygdala in fear conditioning measured with fear-potentiated startle in rats trained concurrently with auditory and visual conditioned stimuli. J Neurosci 15:2301-2311.

Campeau S, Miserendino MJ, Davis M (1992) Intra-amygdala infusion of the N-methyl-D-aspartate receptor antagonist AP5 blocks acquisition but not expression of fear-potentiated startle to an auditory conditioned stimulus. Behav Neurosci 106:569-574.

Cannan WB (1927) The James-Lange theory of emotion: a critical examination and an alternative theory. Am J Physiol 39: 106-124.

Chapman WP, Schroeder HR, Geyer G, Brazier MA, Fager C, Poppen JL, Solomon HC, Yakovlev PI (1954) Physiological evidence concerning importance of the amygdaloid nuclear region in the integration of circulatory function and emotion in man. Science 120:949-950.

Collins DR, Pare D (2000) Differential fear conditioning induces reciprocal changes in the sensory responses of lateral amygdala neurons to the CS(+) and CS(-). Learn Mem 7:97-103.

Darwin C (1872) The expression of the emotions in man and animals. Chicago, IL: Uni. Of Chicago Press.

Davis M (1993) Pharmacological analysis of fear-potentiated startle. Braz J Med Biol Res 26:235-260.

Du B, Wu P, Boldt-Houle DM, Terwilliger EF (1996) Efficient transduction of human neurons with an adeno-associated virus vector. Gene Ther 3:254-261.

Duan D, Sharma P, Yang J, Yue Y, Dudus L, Zhang Y, Fisher KJ, Engelhardt JF (1998) Circular intermediates of recombinant adeno-associated virus have defined structural characteristics responsible for long-term episomal persistence in muscle tissue. J Virol 72:8568-8577.

During MJ, Young D, Baer K, Lawlor P, Klugmann M (2003) Development and optimization of adeno-associated virus vector transfer into the central nervous system. Methods Mol Med 76:221-236.

Esteban JA, Shi SH, Wilson C, Nuriya M, Huganir RL, Malinow R (2003) PKA phosphorylation of AMPA receptor subunits controls synaptic trafficking underlying plasticity. Nat Neurosci 6:136-143.

Fanselow MS, Kim JJ (1994) Acquisition of contextual Pavlovian fear conditioning is blocked by application of an NMDA receptor antagonist D,L-2-amino-5-phosphonovaleric acid to the basolateral amygdala. Behav Neurosci 108:210-212.

Fanselow MS, LeDoux JE (1999) Why we think plasticity underlying Pavlovian fear conditioning occurs in the basolateral amygdala. Neuron 23:229-232.

Farb CR, Ledoux JE (1999) Afferents from rat temporal cortex synapse on lateral amygdala neurons that express NMDA and AMPA receptors. Synapse 33:218-229.

Farb CR, LeDoux JE (1997) NMDA and AMPA receptors in the lateral nucleus of the amygdala are postsynaptic to auditory thalamic afferents. Synapse 27:106-121.

Feindel W, Gloor P (1954) Comparison of electrographic effects of stimulation

of the amygdala and brain stem reticular formation in cats. Electroencephalogr Clin Neurophysiol 6:389-402.

Fendt M, Schmid S (2002) Metabotropic glutamate receptors are involved in amygdaloid plasticity. Eur J Neurosci 15:1535-1541.

Gong S, Zheng C, Doughty ML, Losos K, Didkovsky N, Schambra UB, Nowak NJ, Joyner A, Leblanc G, Hatten ME, Heintz N (2003) A gene expression atlas of the central nervous system based on bacterial artificial chromosomes. Nature 425:917-925.

Goosens KA, Maren S (2001) Contextual and auditory fear conditioning are mediated by the lateral, basal, and central amygdaloid nuclei in rats. Learn Mem 8:148-155.

Goosens KA, Maren S (2004) NMDA receptors are essential for the acquisition, but not expression, of conditional fear and associative spike firing in the lateral amygdala. Eur J Neurosci 20:537-548.

Han JH, Kushner SA, Yiu AP, Cole CJ, Matynia A, Brown RA, Neve RL, Guzowski JF, Silva AJ, Josselyn SA (2007) Neuronal competition and selection during memory formation. Science 316:457-460.

Hoffmann D, Sprengel R, Sakmann B (2002) Molecular dissection of associative plasticity in CA1 pyramidal neurons. Proc Natl Acad Sci USA 99:7740-7745.

Hernandez YJ, Wang J, Kearns WG, Loiler S, Poirier A, Flotte TR (1999) Latent adeno-associated virus infection elicits humoral but not cell-mediated immune responses in a nonhuman primate model. J Virol 73:8549-8558.

Huang YY, Kandel ER (1998) Postsynaptic induction and PKA-dependent expression of LTP in the lateral amygdala. Neuron 21:169-178.

Humeau Y, Herry C, Kemp N, Shaban H, Fourcaudot E, Bissiere S, Luthi A (2005) Dendritic spine heterogeneity determines afferent-specific Hebbian plasticity in the amygdala. Neuron 45:119-131.

Humeau Y, Luthi A (2007) Dendritic calcium spikes induce bi-directional synaptic plasticity in the lateral amygdala. Neuropharmacology 52:234-243.

Humeau Y, Reisel D, Johnson AW, Borchardt T, Jensen V, Gebhardt C, Bosch V, Gass P, Bannerman DM, Good MA, Hvalby O, Sprengel R,

Luthi A (2007) A pathway-specific function for different AMPA receptor subunits in amygdala long-term potentiation and fear conditioning. J Neurosci 27:10947-10956.

James W (1884) What is an emotion? Mind 9: 188-205.

Jooss K, Yang Y, Fisher KJ, Wilson JM (1998) Transduction of dendritic cells by DNA viral vectors directs the immune response to transgene products in muscle fibers. J Virol 72:4212-4223.

Kim JJ, Rison RA, Fanselow MS (1993) Effects of amygdala, hippocampus, and periaqueductal gray lesions on short- and long-term contextual fear. Behav Neurosci 107:1093-1098.

Kim M, Campeau S, Falls WA, Davis M (1993) Infusion of the non-NMDA receptor antagonist CNQX into the amygdala blocks the expression of fear-potentiated startle. Behav Neural Biol 59:5-8.

Kim M, Davis M (1993) Lack of a temporal gradient of retrograde amnesia in rats with amygdala lesions assessed with the fear-potentiated startle paradigm. Behav Neurosci 107:1088-1092.

Kim M, Davis M (1993) Electrolytic lesions of the amygdala block acquisition and expression of fear-potentiated startle even with extensive training but do not prevent reacquisition. Behav Neurosci 107:580-595.

Klüver H and Bucy PC (1939) Preliminary analysis of temporal lobes in monkeys. Arch Neurol Psychiatry 42: 979-1000.

Klüver H and Bucy PC (1937) „Psychic blindness“ and other symptoms following bilateral temporal lobectomy in rhesus monkeys. Am J Physiol 119: 352-353.

Lang PJ, Davis M, Ohman A (2000) Fear and anxiety: animal models and human cognitive psychophysiology. J Affect Disord 61:137-159.

LeDoux J (2003) The emotional brain, fear, and the amygdala. Cell Mol Neurobiol 23:727-738.

LeDoux JE (2000) Emotion circuits in the brain. Annu Rev Neurosci 23:155-184.

LeDoux JE, Cicchetti P, Xagoraris A, Romanski LM (1990) The lateral amygdaloid nucleus: sensory interface of the amygdala in fear conditioning. J Neurosci 10:1062-1069.

LeDoux JE, Sakaguchi A, Iwata J, Reis DJ (1986) Interruption of projections

from the medial geniculate body to an archi-neostriatal field disrupts the classical conditioning of emotional responses to acoustic stimuli. Neuroscience 17:615-627.

Lee Y, Walker D, Davis M (1996) Lack of a temporal gradient of retrograde amnesia following NMDA-induced lesions of the basolateral amygdala assessed with the fear-potentiated startle paradigm. Behav Neurosci 110:836-839.

Liu P, Jenkins NA, Copeland NG (2003) A highly efficient recombineering-based method for generating conditional knockout mutations. Genome Res 13:476-484.

Mack V, Burnashev N, Kaiser KM, Rozov A, Jensen V, Hvalby O, Seeburg PH, Sakmann B, Sprengel R (2001) Conditional restoration of hippocampal synaptic potentiation in Glur-A-deficient mice. Science 292:2501-2504.

Malenka RC, Nicoll RA (1999) Long-term potentiation--a decade of progress? Science 285:1870-1874.

Malinow R, Malenka RC (2002) AMPA receptor trafficking and synaptic plasticity. Annu Rev Neurosci 25:103-126.

Maren S (1996) Synaptic transmission and plasticity in the amygdala. An emerging physiology of fear conditioning circuits. Mol Neurobiol 13:1-22.

Maren S (2001) Neurobiology of Pavlovian fear conditioning. Annu Rev Neurosci 24:897-931.

Maren S (2001) Is there savings for pavlovian fear conditioning after neurotoxic basolateral amygdala lesions in rats? Neurobiol Learn Mem 76:268-283.

Maren S, Aharonov G, Fanselow MS (1996) Retrograde abolition of conditional fear after excitotoxic lesions in the basolateral amygdala of rats: absence of a temporal gradient. Behav Neurosci 110:718-726.

Maren S, Aharonov G, Stote DL, Fanselow MS (1996) N-methyl-D-aspartate receptors in the basolateral amygdala are required for both acquisition and expression of conditional fear in rats. Behav Neurosci 110:1365-1374.

Maren S, Fanselow MS (1995) Synaptic plasticity in the basolateral amygdala

induced by hippocampal formation stimulation in vivo. J Neurosci 15:7548-7564.

Maren S, Quirk GJ (2004) Neuronal signalling of fear memory. Nat Rev Neurosci 5:844-852.

McCown TJ, Xiao X, Li J, Breese GR, Samulski RJ (1996) Differential and persistent expression patterns of CNS gene transfer by an adeno-associated virus (AAV) vector. Brain Res 713:99-107.

McDonald AJ (1998) Cortical pathways to the mammalian amygdala. Prog Neurobiol 55:257-332.

McKernan MG, Shinnick-Gallagher P (1997) Fear conditioning induces a lasting potentiation of synaptic currents in vitro. Nature 390:607-611.

Miserendino MJ, Sananes CB, Melia KR, Davis M (1990) Blocking of acquisition but not expression of conditioned fear-potentiated startle by NMDA antagonists in the amygdala. Nature 345:716-718.

Misslin R (2003) The defense system of fear: behavior and neurocircuitry. Neurophysiol Clin 33:55-66.

Nader K, Majidishad P, Amorapanth P, LeDoux JE (2001) Damage to the lateral and central, but not other, amygdaloid nuclei prevents the acquisition of auditory fear conditioning. Learn Mem 8:156-163.

Nakai H, Yant SR, Storm TA, Fuess S, Meuse L, Kay MA (2001) Extrachromosomal recombinant adeno-associated virus vector genomes are primarily responsible for stable liver transduction in vivo. J Virol 75:6969-6976.

Nicoll RA, Malenka RC (1999) Expression mechanisms underlying NMDA receptor-dependent long-term potentiation. Ann N Y Acad Sci 868:515-525.

Pare D (2004) Presynaptic induction and expression of NMDA-dependent LTP. Trends Neurosci 27:440-441.

Pare D, Collins DR (2000) Neuronal correlates of fear in the lateral amygdala: multiple extracellular recordings in conscious cats. J Neurosci 20:2701-2710.

Pare D, Quirk GJ, Ledoux JE (2004) New vistas on amygdala networks in conditioned fear. J Neurophysiol 92:1-9.

Pavlov IP (1927) Conditioned reflexes: an investigation of the

physiological of the cerebral cortex. London: Oxford Univ. Press.

Peel AL, Klein RL (2000) Adeno-associated virus vectors: activity and applications in the CNS. J Neurosci Methods 98:95-104.

Perez-Villalba A, Mackintosh NJ, Canales JJ (2007) Influence of massed and distributed context preexposure on contextual fear and Egr-1 expression in the basolateral amygdala. Physiol Behav.

Perez-Villalba A, Teruel-Marti V, Ruiz-Torner A, Olucha-Bordonau F (2005) The effect of long context exposure on cued conditioning and c-fos expression in the rat forebrain. Behav Brain Res 161:263-275.

Pitkanen A, Jolkkonen E, Kemppainen S (2000) Anatomic heterogeneity of the rat amygdaloid complex. Folia Morphol (Warsz) 59:1-23.

Pitkanen A, Pikkarainen M, Nurminen N, Ylinen A (2000) Reciprocal connections between the amygdala and the hippocampal formation, perirhinal cortex, and postrhinal cortex in rat. A review. Ann N Y Acad Sci 911:369-391.

Podsakoff G, Wong KK, Jr., Chatterjee S (1994) Efficient gene transfer into nondividing cells by adeno-associated virus-based vectors. J Virol 68:5656-5666.

Quirk GJ, Armony JL, LeDoux JE (1997) Fear conditioning enhances different temporal components of tone-evoked spike trains in auditory cortex and lateral amygdala. Neuron 19:613-624.

Quirk GJ, Repa C, LeDoux JE (1995) Fear conditioning enhances short-latency auditory responses of lateral amygdala neurons: parallel recordings in the freely behaving rat. Neuron 15:1029-1039.

Radley JJ, Farb CR, He Y, Janssen WG, Rodrigues SM, Johnson LR, Hof PR, LeDoux JE, Morrison JH (2007) Distribution of NMDA and AMPA receptor subunits at thalamo-amygdaloid dendritic spines. Brain Res 1134:87-94.

Reisel D, Bannerman DM, Schmitt WB, Deacon RM, Flint J, Borchardt T, Seeburg PH, Rawlins JN (2002) Spatial memory dissociations in mice lacking GluR1. Nat Neurosci 5:868-873.

Repa JC, Muller J, Apergis J, Desrochers TM, Zhou Y, LeDoux JE (2001) Two different lateral amygdala cell populations contribute to the initiation and storage of memory. Nat Neurosci 4:724-731.

Rodrigues SM, Bauer EP, Farb CR, Schafe GE, LeDoux JE (2002) The group I metabotropic glutamate receptor mGluR5 is required for fear memory formation and long-term potentiation in the lateral amygdala. J Neurosci 22:5219-5229.

Rodrigues SM, Schafe GE, LeDoux JE (2001) Intra-amygdala blockade of the NR2B subunit of the NMDA receptor disrupts the acquisition but not the expression of fear conditioning. J Neurosci 21:6889-6896.

Rogan MT, Staubli UV, LeDoux JE (1997) Fear conditioning induces associative long-term potentiation in the amygdala. Nature 390:604-607.

Romanski LM, Clugnet MC, Bordi F, LeDoux JE (1993) Somatosensory and auditory convergence in the lateral nucleus of the amygdala. Behav Neurosci 107:444-450.

Romanski LM, LeDoux JE (1992) Equipotentiality of thalamo-amygdala and thalamo-cortico-amygdala circuits in auditory fear conditioning. J Neurosci 12:4501-4509.

Romanski LM, LeDoux JE (1992) Bilateral destruction of neocortical and perirhinal projection targets of the acoustic thalamus does not disrupt auditory fear conditioning. Neurosci Lett 142:228-232.

Roozendaal B, Koolhaas JM, Bohus B (1991) Central amygdala lesions affect behavioral and autonomic balance during stress in rats. Physiol Behav 50:777-781.

Roozendaal B, Koolhaas JM, Bohus B (1991) Attenuated cardiovascular, neuroendocrine, and behavioral responses after a single footshock in central amygdaloid lesioned male rats. Physiol Behav 50:771-775.

Rumpel S, LeDoux J, Zador A, Malinow R (2005) Postsynaptic receptor trafficking underlying a form of associative learning. Science 308:83-88.

Sah P, Faber ES, Lopez De Armentia M, Power J (2003) The amygdaloid complex: anatomy and physiology. Physiol Rev 83:803-834.

Samson RD, Pare D (2005) Activity-dependent synaptic plasticity in the central nucleus of the amygdala. J Neurosci 25:1847-1855.

Schafe GE, Nader K, Blair HT, LeDoux JE (2001) Memory consolidation of Pavlovian fear conditioning: a cellular and molecular perspective. Trends Neurosci 24:540-546.

Schmitt WB, Sprengel R, Mack V, Draft RW, Seeburg PH, Deacon RM, Rawlins JN, Bannerman DM (2005) Restoration of spatial working memory by genetic rescue of GluR-A-deficient mice. Nat Neurosci 8:270-272.

Shi C, Davis M (1999) Pain pathways involved in fear conditioning measured with fear-potentiated startle: lesion studies. J Neurosci 19:420-430.

Sigurdsson T, Doyere V, Cain CK, LeDoux JE (2007) Long-term potentiation in the amygdala: a cellular mechanism of fear learning and memory. Neuropharmacology 52:215-227.

Su AI, Wiltshire T, Batalov S, Lapp H, Ching KA, Block D, Zhang J, Soden R, Hayakawa M, Kreiman G, Cooke MP, Walker JR, Hogenesch JB (2004) A gene atlas of the mouse and human protein-encoding transcriptomes. Proc Natl Acad Sci U S A 101:6062-6067.

Swanson LW, Petrovich GD (1998) What is the amygdala? Trends Neurosci 21:323-331.

Tenenbaum L, Chtarto A, Lehtonen E, Velu T, Brotchi J, Levivier M (2004) Recombinant AAV-mediated gene delivery to the central nervous system. J Gene Med 6 Suppl 1:S212-222.

Walker DL, Davis M (2000) Involvement of NMDA receptors within the amygdala in short- versus long-term memory for fear conditioning as assessed with fear-potentiated startle. Behav Neurosci 114:1019-1033.

Walker DL, Davis M (2002) The role of amygdala glutamate receptors in fear learning, fear-potentiated startle, and extinction. Pharmacol Biochem Behav 71:379-392.

Walker DL, Rattiner LM, Davis M (2002) Group II metabotropic glutamate receptors within the amygdala regulate fear as assessed with potentiated startle in rats. Behav Neurosci 116:1075-1083.

Weiskrantz L (1956) Behavioral changes associated with ablation of the amygdaloid complex in monkeys. J Comp Physiol Psychol 49:381-391.

Weisskopf MG, Bauer EP, LeDoux JE (1999) L-type voltage-gated calcium channels mediate NMDA-independent associative long-term potentiation at thalamic input synapses to the amygdala. J Neurosci 19:10512-10519.

Wilensky AE, Schafe GE, Kristensen MP, LeDoux JE (2006) Rethinking the

fear circuit: the central nucleus of the amygdala is required for the acquisition, consolidation, and expression of Pavlovian fear conditioning. J Neurosci 26:12387-12396.

Zamanillo D, Sprengel R, Hvalby O, Jensen V, Burnashev N, Rozov A, Kaiser KM, Koster HJ, Borchardt T, Worley P, Lubke J, Frotscher M, Kelly PH, Sommer B, Andersen P, Seeburg PH, Sakmann B (1999) Importance of AMPA receptors for hippocampal synaptic plasticity but not for spatial learning. Science 284:1805-1811.

Zola-Morgan S, Squire LR, Alvarez-Royo P, Clower RP (1991) Independence of memory functions and emotional behavior: separate contributions of the hippocampal formation and the amygdala. Hippocampus 1:207-220.